DRIVERS OF MICROBIAL METABOLISM, NUTRIENT CYCLING AND GREENHOUSE GAS PRODUCTION IN AGRICULTURAL STREAMBED SEDIMENTS

by

SOPHIE ANNE COMER-WARNER

A thesis submitted to the University of Birmingham

for the degree of DOCTOR OF PHILOSOPHY

School of Geography, Earth and Environmental Science

College of Life and Environmental Sciences

University of Birmingham

March 2018

Abstract

Drivers of carbon and nitrogen cycling, and associated greenhouse gas (GHG) production, were investigated in streambed sediments. Research was conducted to address a lack of availability of adequate porewater sampling technologies and standard protocols, and to determine the effect of temperature, sediment properties and season as primary drivers of nutrient cycling and GHG production in the streambed. A high-resolution sampler of nitrate isotope and concentration data was developed by confirming diffusive equilibrium in thin-film (DET) gel samplers did not cause fractionation of nitrate isotopes. An investigation of commonly used sampling techniques provided information on the most appropriate samplers to use and illustrated that ammonium concentrations vary significantly between sampling techniques. Thermal sensitivity of CO_2 and CH_4 emissions was dependent on sediment type, organic matter and geology, with these factors having a major effect. CO_2 and CH_4 concentrations were higher in sand than gravel sediments, but season had a minor influence. Nitrogen cycling was highest in sand than gravel sediments, resulting in high rates of denitrification and low N_2O concentrations in the sand sediments. Nitrogen cycling and associated N_2O concentrations varied greatly with season in gravel sediments. This indicates that different greenhouse gases may be produced in different areas of the streambed.

Acknowledgments

I would like to thank my partner, Anika Comer-Warner, without whose support and encouragement I could not have achieved so much. From supporting my decision to undertake this PhD, despite it meaning she would have to give up everything to move to a new continent, to encouraging me through the most difficult and trying times, when nothing seemed possible and a PhD never achievable. I am also eternally grateful for her direct help with my research, from joining field campaigns to listening to countless presentations before conferences, providing a great moment when Stefan was impressed Anika knew about denitrification, not too bad for an English major!

I would also like to thank my parents, Dianne and Gary, and my sister, Gemma. Without your belief and support throughout my whole life, I would not have attempted so much, you have provided motivation and self-belief when I needed it most. Your advice, such as this my dad once said, “If you look into the Grand Canyon, what do you see? That river did not make that canyon in a day, it took a long time, a little bit at a time. This is how you need to approach your work”, has always been practical, timely and inspiring.

A special gratitude, of course, goes to my primary supervisors, Professor Stefan Krause and Professor Daren Gooddy, for their practical guidance and knowledgeable insight over the past three and a half years. The research project they developed provided an exciting PhD topic, but they also allowed my project to be flexible, allowing me to suggest ideas and guide my PhD as well. I am forever grateful for their help and support over the course of my PhD. I would also like to thank Paul Romeijn, Dr. Sarah Bennett, Dr. Sami Ullah, Dr, Ben Marchant and Dr. Nick Kettridge, as well as numerous members of our research group, support staff at the University of Birmingham and those who performed isotopic analysis, who have provided invaluable help, support and advice through the course of my PhD.

Table of Contents

List of Figures

List of Tables

List of Abbreviations

~ – Approximately

°C – Degrees Celsius

> – Greater Than

< – Less Than

µg – Microgram

µl – Microlitre

µm – Micrometre

µM – Micromolar

µmol – Micromole

% – Percent

‰ – Permille

Ag_2O – Silver Oxide

AIC – Akaike Information Criterion

ANOVA – Analysis of Variance

Ar – Argon

BGS – British Geological Survey

BIFoR – Birmingham Institute of Forest Research

C – Carbon

CH_4 – Methane

CO_2 – Carbon Dioxide

cm – Centimetre

$\delta^{13}C_{CO2}$ –Isotopic Carbon Ratio of Carbon Dioxide

$\delta^{15}N_{NO3^-}$ –Isotopic Nitrogen Ratio of Nitrate

$\delta^{15}N_{NO3^-+NO2^-}$ –Isotopic Nitrogen Ratio of Nitrate and Nitrite

$\delta^{18}O_{NO3^-}$ –Isotopic Oxygen Ratio of Nitrate

$\delta^{18}O_{NO3^-+NO2^-}$ –Isotopic Oxygen Ratio of Nitrate

DET – Diffusive Equilibrium in Thin-film

DGT – Diffusive Gradient in Thin-film

DO – Dissolved Oxygen

DOC – Dissolved Organic Carbon

Dr. – Doctor

ECD – Electron Capture Detector

FDA – Fluorescein Diacetate

FID – Flame Ionisation Detector

g – Gram

GC – Gas Chromatograph

GHG – Greenhouse Gas

HCl – Hydrochloric Acid

hr – Hour

HZ – Hyporheic Zone

IAEA – International Atomic Energy Agency

IRMS – Isotope Ratio Mass Spectrometry

Kg – Kilogram

Km – Kilometre

KNO_3 – Potassium Nitrate

l - Litre

LOD – Limit of Detection

LSMSF – Life Sciences Mass Spectrometry Facility

m – Metre

M – Molar

mg – Milligram

min – Minute

ml – Milliletre

mm - Millimetre

mM – Millimolar

MMA – Microbial Metabolic Activity

mmol - Millimole

MΩ – Megaohm

N – Nitrogen

N_2 – Nitrogen

N_2O – Nitrous Oxide

NaCl – Sodium Chloride

$NaNO_3$ – Sodium Nitrate

NERC – Natural Environment Research Council

ng – Nanogram

NH_4^+ – Ammonium

NH_4Cl – Ammonium Chloride

NIGL – NERC Isotope Geosciences Laboratories

nm – Nanometer

nM - Nanomolar

nmol - Nanomole

NO_2^- – Nitrite

NO_3^- – Nitrate

O_2 – Oxygen

OM – Organic Matter

Pg – Petagram

pH – Potential of Hydrogen

ppb – Parts per Billion

ppm – Parts per Million

PVC – Polyvinyl Chloride

Q_{10} – Temperature Coefficient

Raz – Resazurin

rpm – Revolutions per Minute

Rru – Resorufin

s – Second

SI – Supporting Information

TCD – Thermal Conductivity Detector

Tg – Terragram

THAM – Tris-hydroxymethyl-aminomethane

URL – Urban River Laboratory

USGS – United States Geological Survey

UV-Vis – Ultraviolet-Visible

yr – Year

Chapter 1: Introduction

1.1 Scientific Rationale

Interest in the biogeochemistry of streams and rivers has been increasing since their recognition as 'active pipelines'[1–4], with 0.8 Pg of carbon, up to 50% of that received by inland waters, released as CO_2 to the atmosphere annually as a result of gas exchange[2,4–6]. Furthermore, streams and rivers play a large role in the nitrogen cycle, and are able to support large conversion rates of nitrate to N_2 gas, predominantly via denitrification[7–10].

GHGs are produced during nutrient cycling, with CO_2 and CH_4 formed as end-products during respiration[11], and N_2O formed as an intermediate product in both denitrification and nitrification[12]. The large rates of carbon and nitrogen turnover observed in streams and rivers, therefore, result in surface waters which are often supersaturated with CO_2, CH_4 and N_2O, with respect to the atmosphere[3,13–17], leading to outgassing[18]. This results in streams and rivers being globally important in carbon and nitrogen emissions, with estimated emissions of 1.8 Pg CO_2-C yr^{-1} [3], 26.8 Tg CH_4-C yr^{-1} [19], and between 0.1 and 0.68 Tg N_2O-N yr^{-1} [20,21], for CO_2, CH_4 and N_2O respectively. The CH_4 and N_2O fluxes are relatively small compared to those of CO_2, however, the CH_4 flux is equivalent to over 25% of the terrestrial carbon sink when considered as C equivalents, CH_4 fluxes may be regionally significant and stream N_2O fluxes account for 10% of total anthropogenic emissions, resulting in sustained interest in their production in inland waters[22,23,21,24].

Agricultural streams and rivers are ubiquitous across large regions of the world, and receive large inputs of nutrients either directly into surface water or through subsurface flow paths[25]. This causes major issues, such as eutrophication, in agricultural catchments resulting in decreases in water quality, oxygen availability and stream habitats[25–28]. Additionally, agricultural streams are characterized by large amounts of fine, OM-rich sediment[19], which promote increases in metabolism and associated carbon dioxide and methane

production[16,17,19,29–31]. This is in contrast to coarse gravel sediments, which may act as a CH_4 sink[32]. Regulating nutrient concentrations in these environments is therefore of upmost importance to the overall health of these ecosystems.

Streambeds, particularly at the sediment-water interface[33–35], are hotspots of biogeochemical reactivity[4,36–38], characterized by increased residence times and substrate availability[39–43]. This results in enhanced rates of carbon turnover, microbial metabolism and nutrient spiraling[4,25,36–39,44,45], leading to the streambed being described as the 'river's liver' and accounting for 40-90% of total stream metabolism[46,47]. Additionally, nutrient attenuation and denitrification are typically elevated in sediments relevant to surface water[48], therefore, sediments have the capacity to improve water quality and ecosystem health[49–51]. Due to associated GHG production, however, streambed sediments may support significant concentrations of all three major GHGs, with CO_2 and CH_4 often greater than in the surface water[52], and potentially significant amounts of N_2O released from these environments[21,14,53]. Despite this, however, research has primarily focused on GHGs in the surface water, and as such, knowledge of streambed GHG production, and nutrient cycling in general, remains insufficiently understood[4,6,31,48].

The limited understanding of biogeochemical processes, despite widespread acceptance of their importance, is partially due to a lack of availability of sufficient monitoring methodologies[25,45,54–56]. The development of techniques capturing high-spatial resolution in the upper few centimetres of the streambed, where the majority of biogeochemistry occurs[33–35], is particularly crucial[45]. Techniques to allow sampling of isotopic, as well as, concentration data, will also enable improved understanding of mechanistic processes to be gained[12,57]. Developing further methodologies and sampling protocols, along with continuing research into streambed biogeochemistry, will allow more efficient management and restoration of agricultural streams, and improve ecosystem health and services[58–61].

1.2 Aims and Objectives of Research

The work presented in this thesis aims to address existing knowledge gaps in streambed carbon and nitrogen cycling, through the development of sampling methodologies and investigation of biogeochemical processes. The research objectives are:

1. To address technical sampling difficulties and a lack of standard sampling protocols so enabling effective analysis of streambed biogeochemical processes, and to facilitate interdisciplinary research in the streambed.

2. To investigate the environmental drivers of streambed carbon and nitrogen cycling, and associated GHG production, focusing on temperature, sediment type and season as key proximal drivers.

1.3 Layout of the Thesis

This thesis is structured so that after the introduction, the next two chapters address research objective (1), presenting the development of a new sampling methodology (Chapter 2) and a comparison of existing sampling technologies (Chapter 3). The following three chapters address research objective (2), through the use of laboratory incubation experiments to investigate streambed carbon emissions (Chapter 4), and through *in-situ* porewater observations of carbon (Chapter 5) and nitrogen (Chapter 6) cycling within the sediment of an agricultural stream.

Chapter 2

Opening Opportunities for High-Resolution Isotope Analysis - Quantification of $\delta^{15}N_{NO3^-}$ and $\delta^{18}O_{NO3^-}$ in Diffusive Equilibrium in Thin–Film Passive Samplers.

This chapter aims to develop a novel methodology for high-spatial resolution sampling of porewater nitrate concentration and isotopic data. This will enable more detailed process information to be investigated than available through concentration data alone, specifically focusing on the key biogeochemical interactions occurring at the sediment-water interface. A

laboratory experiment was performed to determine whether nitrate sampling via DET gels causes fractionation of $\delta^{15}N_{NO3^-}$ and $\delta^{18}O_{NO3^-}$. Subsequently, an initial field application was conducted to illustrate the insight available through the developed methodology. Analysis of nitrate isotope samples using the silver nitrate method was performed by staff at the stable isotope facility at the British Geological Survey and analysis of samples using the denitrifier method was performed by staff at the analytical facilities, University of East Anglia. This chapter is published in Analytical Chemistry (DOI: 10.1021/acs.analchem.700028).

Chapter 3

A comparison of available field methodologies for nutrient sampling in streambed porewaters.

This chapter aims to investigate and compare common technologies used to sample porewaters for the investigation of streambed biogeochemistry. Whether varying techniques produce different nutrient profiles, and the advantages and limitations of common methodologies will be reviewed, to allow specific research questions to be more effectively addressed. A field study of three commonly used sampling techniques was performed by co-authors and the resulting nutrient concentrations and profiles compared. A literature review of the available biogeochemical sampling techniques was then undertaken, focusing on sampling details, resolution, advantages and limitations. This work was collaborative with the candidate performing the laboratory analysis of the DET gel data, the laboratory comparison experiments, all data and statistical analysis, and manuscript preparation. Sample collection from the Hammer stream and laboratory analysis of nutrient concentrations from USGS Minipoint and multilevel minipiezometer samples was performed by co-authors.

Chapter 4

Thermal sensitivity of CO_2 and CH_4 emissions varies with streambed sediment properties.

This chapter aims to determine the effect of multiple controlling factors on potential rates of microbial metabolism, and CO_2 and CH_4 production, from streambed sediments. The effect of temperature was investigated, as well as how the temperature effect is influenced by sediment type, OM content and geology. Microbial metabolism and carbon emissions were determined through laboratory incubations of different sediment types of varying OM contents, at increasing temperatures. This work was collaborative with all experimental work and analysis performed by the candidate with Paul Romeijn and the statistical inference performed by Dr. Ben Marchant. This chapter is published in Nature Communications (https://doi.org/10.1038/s41467-018-04756-x).

Chapter 5

Sediment type and season as factors controlling nutrient cycling in agricultural streams: Part I. Carbon

This chapter aims to investigate streambed carbon cycling in an agriculturally-impacted catchment, focusing on concentrations of CO_2 and CH_4 within the streambed. Whether CO_2 is produced within the streambed will also be considered. Sediment type and season were investigated as drivers of streambed carbon cycling through porewater sampling in an agricultural stream. Porewater samples were analysed for DOC, CO_2 and CH_4 concentrations, and $\delta^{13}C_{CO2}$ ratios. Analysis of carbon dioxide isotopes was performed by staff at the Life Sciences Mass Spectrometry Facility at the Centre for Ecology and Hydrology.

Chapter 6

Sediment type and season as factors controlling nutrient cycling in agricultural streams: Part II. Nitrogen

This chapter aims to examine nitrogen cycling within the sediment of an agricultural stream, focusing on rates of denitrification and microbial activity. Their influence on nutrient and N_2O concentrations will then be investigated. Sediment type and season were considered as

drivers of nutrient cycling, denitrification and streambed N_2O concentrations. Laboratory enzyme activity assays were performed by co-authors to determine rates of microbial activity and nutrient uptake in different sediment types. Potential rates of denitrification in the sediment types were also considered under varying nutrient conditions. *In-situ* nutrient cycling and associated N_2O concentrations were then investigated through porewater sampling in an agricultural stream. Porewater samples were analysed for NH_4^+, NO_3^-, NO_2^- and N_2O concentrations, and $\delta^{15}N_{NO3^-+NO2^-}$ and $\delta^{18}O_{NO3^-+NO2^-}$ ratios. This work was collaborative with the candidate performing the *in-situ* sampling and subsequent laboratory analysis, all data and statistical analysis, and manuscript preparation. The laboratory enzyme activity assays were performed by co-authors and the analysis of nitrate isotopes was performed by staff at the analytical facilities at the University of East Anglia.

1.4 References

1. Battin, T. J. *et al.* The boundless carbon cycle. *Nat. Geosci.* **2,** 598–600 (2009).
2. Cole, J. J. *et al.* Plumbing the Global Carbon Cycle: Integrating Inland Waters into the Terrestrial Carbon Budget. *Ecosystems* **10,** 172–185 (2007).
3. Raymond, P. a *et al.* Global carbon dioxide emissions from inland waters. *Nature* **503,** 355–359 (2013).
4. Trimmer, M. *et al.* River bed carbon and nitrogen cycling: state of play and some new directions. *Sci. Total Environ.* **434,** 143–58 (2012).
5. Tranvik, L. J. *et al.* Lakes and reservoirs as regulators of carbon cycling and climate. *Limnol. Oceanogr.* **54,** 2298–2314 (2009).
6. Striegl, R. G., Dornblaser, M. M., McDonald, C. P., Rover, J. R. & Stets, E. G. Carbon dioxide and methane emissions from the Yukon River system. *Global Biogeochem. Cycles* **26,** (2012).
7. Duff, J. H., Tesoriero, A. J., Richardson, W. B., Strauss, E. A. & Munn, M. D. Whole-Stream Response to Nitrate Loading in Three Streams Draining Agricultural Landscapes. *J. Environ. Qual.* **37,** 1133 (2008).
8. Groffman, P. M., Gold, A. J. & Addy, K. Nitrous oxide production in riparian zones and its importance to national emission inventories. *Chemosph. - Glob. Chang. Sci.* **2,** 291–299 (2000).
9. Lansdown, K. *et al.* The interplay between transport and reaction rates as controls on nitrate attenuation in permeable, streambed sediments. *J. Geophys. Res. G Biogeosciences* **120,** 1093–1109 (2015).
10. Stelzer, R. S., Bartsch, L. A., Richardson, W. B. & Strauss, E. A. The dark side of the hyporheic zone: Depth profiles of nitrogen and its processing in stream sediments. *Freshw. Biol.* **56,** 2021–2033 (2011).

11. Baker, M. A., Dahm, C. N. & Valett, H. M. in *Streams and Ground Waters* (eds. Jones, J. B. & Mulholland, P. J.) 259–283 (Elsevier, 2000). doi:10.1016/B978-0-12-389845-6.50012-0

12. Kendall, C. in *Isotope Tracers in Catchment Hydrology* (eds. C. Kendall and J.J. McDonnell) 519–576 (Elsevier, 1998)

13. McMahon, P. B. & Dennehy, K. F. N2O emissions from a nitrogen-enriched river. *Environ. Sci. Technol.* **33,** 21–25 (1999).

14. Mosier, A., Kroeze, C., Nevison, C., Oenema, O. & Seitzinger, S. Closing the global N 2 O budget : nitrous oxide emissions through the agricultural nitrogen cycle inventory methodology. *Nutr. Cycl. Agroecosystems* **52,** 225–248 (1998).

15. Maurice, L., Rawlins, B. G., Farr, G., Bell, R. & Gooddy, D. C. The influence of flow and bed slope on gas transfer in steep streams and their implications for evasion of CO_2. *J. Geophys. Res. Biogeosciences* (2017). doi:10.1002/2017JG004045

16. Crawford, J. T. & Stanley, E. H. Controls on methane concentrations and fluxes in streams draining human-dominated landscapes. *Ecol. Appl.* 15–1330.1 (2015). doi:10.1890/15-1330.1

17. Sanders, I. a. *et al.* Emission of methane from chalk streams has potential implications for agricultural practices. *Freshw. Biol.* **52,** 1176–1186 (2007).

18. Richey, J. E., Melack, J. M., Aufdenkampe, A. K., Ballester, V. M. & Hess, L. L. Outgassing from Amazonian rivers and wetlands as a large tropical source of atmospheric CO2. *Nature* **416,** 617–620 (2002).

19. Stanley, E. H. *et al.* The ecology of methane in streams and rivers: Patterns, controls, and global significance. *Ecol. Monogr.* **86,** 146–171 (2016).

20. Anderson, B. *et al. Methane and Nitrous Oxide Emissions from Natural Sources*. (Office of Atmospheric Programs, US EPA, EPA 430-R-10-001, 2010).

21. Beaulieu, J. J. *et al.* Nitrous oxide emission from denitrification in stream and river networks. *Proc. Natl. Acad. Sci.* **108,** 214–219 (2011).

22. Bastviken, D. *et al.* Freshwater methane emissions offset the continental carbon sink. *Science (80-.).* **331,** 50 (2011).

23. Panneer Selvam, B., Natchimuthu, S., Arunachalam, L. & Bastviken, D. Methane and carbon dioxide emissions from inland waters in India - implications for large scale greenhouse gas balances. *Glob. Chang. Biol.* **20,** 3397–3407 (2014).

24. Crawford, J. T. *et al.* CO2 and CH4 emissions from streams in a lake-rich landscape: Patterns, controls, and regional significance. *Glob. Chang. Biol.* **20,** 3408–22 (2014).

25. Krause, S., Louise Heathwaite, a., Binley, A. & Keenan, P. Nitrate concentration changes at the groundwater-surface water interface of a small Cumbrian river. *Hydrol. Process.* **23,** 2195–2211 (2009).

26. Brunke, M. & Gonser, T. The ecological significance of exchange processes between rivers and groundwater. *Freshw. Biol.* **37,** 1–33 (1997).

27. McMahon, P. B. & Böhlke, J. K. Denitrification and mixing in a stream-aquifer system: Effects on nitrate loading to surface water. *J. Hydrol.* **186,** 105–128 (1996).

28. Sophocleous, M. Interactions between groundwater and surface water: The state of the science. *Hydrogeol. J.* **10,** 52–67 (2002).

29. Jones, J. B. & Mulholland, P. J. Influence of drainage basin topography and elevation on carbon dioxide and methane supersaturation of stream water. *Biogeochemistry* **40,** 57–72 (1998).

30. Baulch, H. M., Dillon, P. J., Maranger, R. & Schiff, S. L. Diffusive and ebullitive transport of methane and nitrous oxide from streams: Are bubble-mediated fluxes important? *J. Geophys. Res.* **116,** G04028 (2011).

31. Shelley, F., Abdullahi, F., Grey, J. & Trimmer, M. Microbial methane cycling in the

bed of a chalk river: oxidation has the potential to match methanogenesis enhanced by warming. *Freshw. Biol.* **60,** 150–160 (2015).

32. Trimmer, M., Maanoja, S., Hildrew, A. G., Pretty, J. L. & Grey, J. Potential carbon fixation via methane oxidation in well-oxygenated riverbed gravels. **55,** 560–568 (2010).

33. Battin, T. J., Kaplan, L. A., Newbold, J. D. & Hansen, C. M. E. Contributions of microbial biofilms to ecosystem processes in stream mesocosms. *Nature* **426,** 439–442 (2003).

34. Knapp, J. L. A. *et al.* Tracer-based characterization of hyporheic exchange and benthic biolayers in streams. *Water Resour. Res.* **53,** 1575–1594 (2017).

35. O'Connor, B. L. & Harvey, J. W. Scaling hyporheic exchange and its influence on biogeochemical reactions in aquatic ecosystems. *Water Resour. Res.* **44,** 1–17 (2008).

36. Krause, S., Tecklenburg, C., Munz, M. & Naden, E. Streambed nitrogen cycling beyond the hyporheic zone: Flow controls on horizontal patterns and depth distribution of nitrate and dissolved oxygen in the upwelling groundwater of a lowland river. *J. Geophys. Res. Biogeosciences* **118,** 54–67 (2013).

37. Lautz, L. K. & Fanelli, R. M. Seasonal biogeochemical hotspots in the streambed around restoration structures. *Biogeochemistry* **91,** 85–104 (2008).

38. McClain, M. E. *et al.* Biogeochemical Hot Spots and Hot Moments at the Interface of Terrestrial and Aquatic Ecosystems. *Ecosystems* **6,** 301–312 (2003).

39. Boulton, A. J., Findlay, S., Marmonier, P., Stanley, E. H. & Valett, H. M. The Functional Significance of the Hyporheic Zone in Streams and Rivers. *Annu. Rev. Ecol. Syst.* **29,** 59–81 (1998).

40. Grimm, N. B. & Fisher, S. G. Exchange between interstitial and surface water: Implications for stream metabolism and nutrient cycling. *Hydrobiologia* **111,** 219–228

(1984).

41. Pinay, G., O'Keefe, T. ., Edwards, R. . & Naiman, R. . Nitrate removal in the hyporheic zone of a salmon river in Alaska. *River Res. Appl.* **25,** 367–375 (2009).

42. Zarnetske, J. P., Haggerty, R., Wondzell, S. M. & Baker, M. a. Dynamics of nitrate production and removal as a function of residence time in the hyporheic zone. *J. Geophys. Res.* **116,** G01025 (2011).

43. Mulholland, P. J. *et al.* Nitrogen Cycling in a Forest Stream Determined by a 15N Tracer Addition. *Ecol. Monogr.* **70,** 471–493 (2000).

44. Jones, J. B. & Holmes, R. M. Surface-subsurface interactions in stream ecosystems. *Trends Ecol. Evol.* **11,** 239–242 (1996).

45. Krause, S. *et al.* Inter-disciplinary perspectives on processes in the hyporheic zone. **499,** 481–499 (2011).

46. Fischer, H., Kloep, F., Wilzcek, S. & Pusch, M. T. A river's liver - Microbial processes within the hyporheic zone of a large lowland river. *Biogeochemistry* **76,** 349–371 (2005).

47. Battin, T. J., Kaplan, L. a, Newbold, J. D. & Hendricks, S. P. A mixing model analysis of stream solute dynamicsand the contribution of a hyporheic zone to ecosystemfunction. *Freshw. Biol.* **48,** 995–1014 (2003).

48. Quick, A. M. *et al.* Controls on nitrous oxide emissions from the hyporheic zones of streams. *Environ. Sci. Technol.* (2016). doi:10.1021/acs.est.6b02680

49. Duff, J. H. & Triska, F. J. in *Streams and Ground Waters* (eds. Jones, J. & Mulholland, P. J.) 197–220 (Elsevier Inc., 2000). doi:10.1016/B978-0-12-389845-6.50009-0

50. Rivett, M. O., Buss, S. R., Morgan, P., Smith, J. W. N. & Bemment, C. D. Nitrate attenuation in groundwater: A review of biogeochemical controlling processes. *Water*

Res. **42,** 4215–4232 (2008).

51. Wang, L. *et al.* Prediction of the arrival of peak nitrate concentrations at the water table at the regional scale in Great Britain. *Hydrol. Process.* **26,** 226–239 (2012).
52. Hlaváčová, E., Rulík, M. & Čáp, L. Anaerobic microbial metabolism in hyporheic sediment of a gravel bar in a small lowland stream. *River Res. Appl.* **21,** 1003–1011 (2005).
53. Mulholland, P. J. *et al.* Stream denitrification across biomes and its response to anthropogenic nitrate loading. *Nature* **452,** 202–205 (2008).
54. Boano, F. *et al.* Hyporheic flow and transport processes: Mechanisms, models, and bioghemical implications. *Rev. Geophys.* 1–77 (2014). doi:10.1002/2012RG000417.Received
55. Hannah, D. M., Sadler, J. P. & Wood, P. J. Hydroecology and ecohydrology: a potential route forward? *Hydrol. Process.* **21,** 3385–3390 (2007).
56. Krause, S., Hannah, D. M. & Fleckenstein, J. H. Hyporheic hydrology: interactions at the groundwater-surface water interface. *Hydrol. Process.* **23,** 2103–2107 (2009).
57. Abbott, B. W. *et al.* Using multi-tracer inference to move beyond single-catchment ecohydrology. *Earth-Science Rev.* **160,** 19–42 (2016).
58. Lewandowski, J. & Nützmann, G. Nutrient retention and release in a floodplain's aquifer and in the hyporheic zone of a lowland river. *Ecol. Eng.* **36,** 1156–1166 (2010).
59. Welti, N. *et al.* Large-scale controls on potential respiration and denitrification in riverine floodplains. *Ecol. Eng.* **42,** 73–84 (2012).
60. Ullah, S. *et al.* In situ measurement of redox sensitive solutes at high spatial resolution in a riverbed using Diffusive Equilibrium in Thin Films (DET). *Ecol. Eng.* **49,** 18–26 (2012).
61. Mendoza-Lera, C. & Datry, T. Relating hydraulic conductivity and hyporheic zone

biogeochemical processing to conserve and restore river ecosystem services. *Sci. Total Environ.* **579,** 1815–1821 (2016).

Chapter 2: Opening opportunities for high-resolution isotope analysis - quantification of $\delta^{15}N_{NO3^-}$ and $\delta^{18}O_{NO3^-}$ in Diffusive Equilibrium in Thin–film passive samplers

Sophie A. Comer-Warner[1], Stefan Krause[1], Daren C. Gooddy[2], Sarah A. Bennett[2,3], Sarah K. Wexler[4], and Jan Kaiser[4]

1. School of Geography, Earth and Environmental Sciences, University of Birmingham, Edgbaston, Birmingham B15 2TT, UK

2. British Geological Survey (BGS), Maclean Building, Wallingford, Oxfordshire OX10 8BB, UK

3. NIGL, BGS, Keyworth, Nottingham NG12 5GG, UK

4. Centre for Ocean and Atmospheric Sciences, School of Environmental Sciences, University of East Anglia, Norwich Research Park, Norwich NR4 7TJ, UK

This chapter is published in Analytical Chemistry.

2.1 Abstract

The fate of nitrate transported across groundwater-surface water interfaces has been intensively studied in recent decades. The interfaces between aquifers and rivers or lakes have been identified as biogeochemical hotspots with steep redox gradients. However, a detailed understanding of the spatial heterogeneity and potential temporal variability of these hotspots, and the consequences for nitrogen processing, is still hindered by a paucity of adequate measurement techniques. A novel methodology is presented here, using DET gels as high-spatial-resolution passive-samplers of $\delta^{15}N_{NO3^-}$ and $\delta^{18}O_{NO3^-}$ to investigate nitrogen cycling. Fractionation of $\delta^{15}N_{NO3^-}$ and $\delta^{18}O_{NO3^-}$ during diffusion of nitrate through the DET gel was determined using varying equilibrium times and nitrate concentrations. This demonstrated that nitrate isotopes of $\delta^{15}N_{NO3^-}$ and $\delta^{18}O_{NO3^-}$ do not fractionate when sampled

with a DET gel. $\delta^{15}N_{NO3^-}$ values from the DET gels ranged between 2.3±0.2 and 2.7±0.3‰ for a NO_3^- stock solution value of 2.7±0.4‰, and $\delta^{18}O_{NO3^-}$ values ranged between 18.3±1.0 and 21.5±0.8‰ for a NO_3^- stock solution of 19.7±0.9‰. Nitrate recovery and isotope values were independent of equilibrium time and nitrate concentration. Additionally, an *in-situ* study showed that nitrate concentration and isotopes, provide unique, high-resolution data that enable improved understanding of nitrogen cycling in freshwater sediments.

The transport and transformation of nitrate across groundwater-surface water interfaces has been intensively studied over the past few decades, resulting in the identification of hotspots of increased biogeochemical turnover in these areas[1–4]. However, our understanding of the spatial patterns and temporal dynamics of nitrogen processing at the sediment interfaces between aquifers and rivers or lakes is still hampered by a critical lack of adequate monitoring methodologies[5–9]. In particular, there is a vital need for *in-situ* data providing a more detailed insight into gradients of nutrient cycling at small spatial scales[5]. Isotopic data is particularly crucial as it is able to provide additional source and process information that concentration data alone cannot[10,11]. Such information is crucial for improving mechanistic process understanding of ecosystem functioning across spatial and temporal scales, and to support integrated river and groundwater management and restoration so that freshwater systems are managed effectively[12–15].

A promising technological advancement has been the emergence of DET gel samplers, to passively collect chemical constituents in water, soil and sediment (Figure 2.1). Besides a wide range of contaminants, DET gels have been applied to analyse vertical profiles of nitrate concentrations at high spatial resolutions of 1 cm, providing significant advantages over traditional sampling methods, such as multi-level piezometers[14,16–19]. Recently, this spatial resolution has been further improved to millimetre scale using colorimetry and hyperspectral imagery to obtain simultaneous nitrate/nitrite profiles[20]. The application of DET gels at

groundwater-surface water interfaces supports the identification of discrete zones of concentrations of nitrate, nitrite and ammonium, including the characterisation of differing redox zones and hotspots of biogeochemical reactivity[14]. DET gels have been used recently to investigate coupled nitrification-denitrification and dissimilatory nitrate reduction to ammonium, however, no evidence was provided demonstrating there was no fractionation on diffusion of nitrate through the DET gel, and only $\delta^{15}N_{NO3^-}$ was considered[21,22].

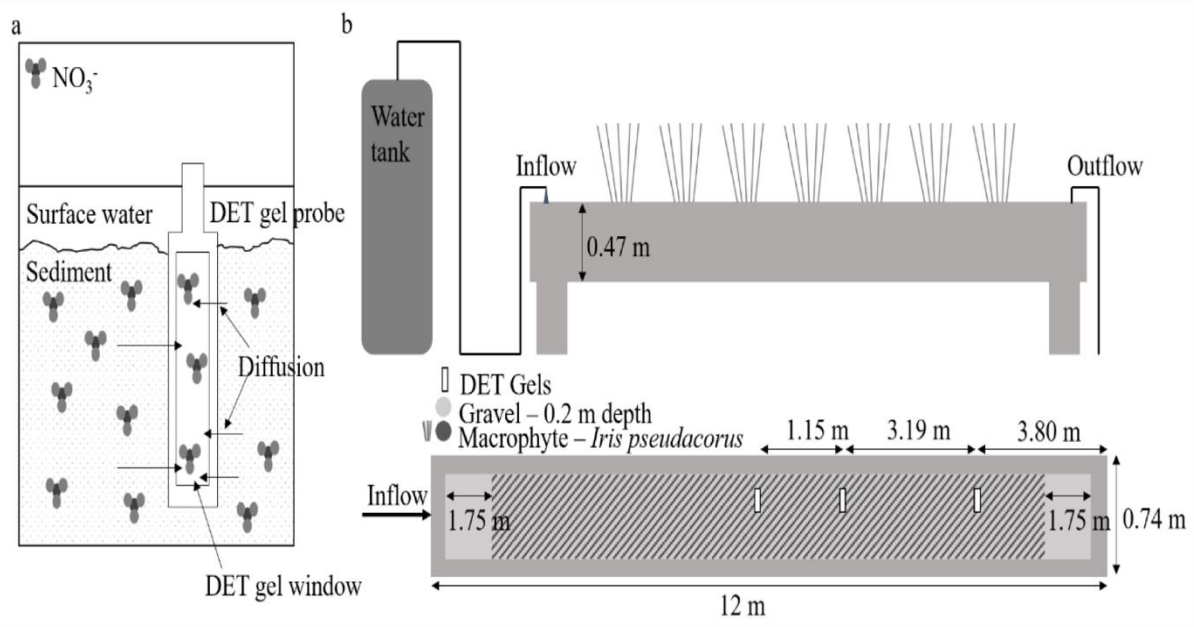

Figure 2.1a. A depiction of the DET gel deployment, showing its position in the sediment and diffusion of nitrate molecules from the higher concentration sediment environment into the lower concentration DET gel. b. A schematic of the mesocosms at the URL, Montornès del Vallès Wastewater Treatment Plant, Montornès del Vallès, Spain used for the in-situ proof of concept. Shown are the positions of the DET gels within the vegetation of the flume.

Here we present a new method, which combines the advantages of high-resolution sampling by DET technology with the analysis of nitrate isotope ratios to quantify nitrogen cycling at groundwater-surface water interfaces. Recognising the limitations of inferring biogeochemical cycling and nutrient dynamics from concentration data alone, we propose the use of DET gels as a high resolution, *in-situ* sampler, of nitrate isotopes in addition to

concentration data. The measurement of $\delta^{15}N_{NO3}^-$ and $\delta^{18}O_{NO3}^-$ provides useful information on the processes controlling nitrate concentrations in hotspots of biogeochemical turnover in areas such as aquifer-lake or aquifer-river interfaces[10]. Additionally, the sources of nitrate measured may be identified, as nitrate from differing sources often has distinct isotopic values of $\delta^{15}N_{NO3}^-$ and $\delta^{18}O_{NO3}^-$, enabling identification of nitrate sources affecting freshwater systems[10]. This combination of high-resolution sampling and process inference from tracer analysis provides significant potential for increasing our understanding of hotspots of biogeochemical turnover and differing redox zones in the HZ, therefore, allowing more effective management of freshwater systems.

2.2 Experimental

Laboratory experiments were performed to determine the potential for fractionation of $\delta^{15}N_{NO3}^-$ and $\delta^{18}O_{NO3}^-$ during the diffusion of nitrate through DET gels. Thereby, during laboratory experiments, the influences of two key controls were investigated for their impacts on fractionation; (1) the concentration of nitrate in the initial solution, and (2) the time allowed for diffusive equilibrium of the nitrate from the initial solution into the DET gel. An initial proof of concept study was conducted using an isotope technique requiring 1 mg NO_3^--N resulting in the requirement of high nitrate concentrations (up to 7.0 g NO_3^- l^{-1}). Subsequently, a more environmentally relevant experiment was performed to verify the results, using an isotope technique requiring 0.7 mg NO_3^--N, and therefore, much lower nitrate concentrations between 20.1 and 100.5 mg NO_3^- l^{-1} could be used. A field trial was then conducted to demonstrate the additional insight gained through high spatial resolution $\delta^{15}N_{NO3}^-$ and $\delta^{18}O_{NO3}^-$ data, in addition to nitrate concentration data, this was also conducted using the isotope technique requiring 0.7 mg NO_3^--N.

2.2.1 Laboratory experiments

2.2.1.1 Proof of Concept study

2.2.1.1.1 Equilibration of DET gels in nitrate solutions:

A 3x4x0.2 cm polyacrylamide DET gel (Diffusive Gradient in Thin-film (DGT) Research Ltd), was immersed in an unagitated 100 ml solution of known NO_3^- concentration, in an acid-washed (10% HCl) beaker. Solutions of 3.3±0.0, 4.8±0.0 and 7.0±0.1 g $NO_3^- l^{-1}$ were used, with each concentration being equilibrated for three different time periods: 24, 48 and 168 hours. A river sample spiked with nitrate (7.0±0.0 g $NO_3^- l^{-1}$) was also used to test for matrix effects; the river sample was collected from the River Tern, UK and filtered (0.2 µm). All experiments were performed in triplicate, and the concentration of the stock solution was compared to that of the solution in the beaker after the gel was removed. A concentration 97.7% that of the stock solution was expected due to the gel volume being 2.3% of the solution volume. The solution concentrations were found to be 95.0±3.0% that of the stock (n=12).

2.2.1.1.2 Back-equilibration from DET gels:

At the end of the equilibration period DET gels were removed from solution and weighed in a pre-weighed centrifuge tube to determine the weight of each gel. The solution volume of each gel was calculated from the weight multiplied by the assumed water content of the saturated gel (95%). 25 ml of ultrapure water was added to each gel and the gels were shaken on a reciprocating shaker for 24 hours, after which the gels were removed, and the back-equilibrated samples frozen for chemical analysis. Nitrate concentrations were determined using ion chromatography (Dionex ICS1100), standards were used as quality controls and gave an accuracy of 0.4 mg l^{-1}, precision of ±0.4 mg l^{-1}, and a limit of detection (LOD) of 0.5 mg l^{-1}.

2.2.1.2 Laboratory experiment at environmentally relevant concentrations.

The proof of concept experiment outlined above was repeated to investigate isotope fractionation at environmentally relevant nitrate concentrations, using an equilibration time of 24 hours. Solutions of 20.1±0.0, 50.8±0.2 and 100.5±0.3 mg $NO_3^- l^{-1}$ were used, as well as a filtered (0.2 µm) river sample (Wood Brook, Mill Haft, UK) with a concentration of 23.1±0.0 mg $NO_3^- l^{-1}$. During back-equilibration 20 ml of ultrapure water was added to each gel, and nitrate concentrations were determined on a Continuous Flow Analyser (Skalar Sans++). Standards were used as quality controls and gave an accuracy of 0.4 mg $NO_3^- l^{-1}$, precision of ±0.1 $NO_3^- l^{-1}$, and an LOD of 0.9 mg $NO_3^- l^{-1}$. The concentration of the stock solution was compared to that of the solution in the beaker after the gel was removed. A concentration 97.7% that of the stock solution was expected due to the gel volume being 2.3% of the solution volume, and solution concentrations were found to be 96.8±1.1% that of the stock (n=4).

2.2.2 In-situ field trial

2.2.2.1 Field Trial Study site:

For a field trial, proving the concept of DET isotope analysis in sediments, gel probes were deployed at the URL located at the Montornès del Vallès Wastewater Treatment Plant, Montornès del Vallès, Spain. The mesocosm flumes are 12 m long, 0.74 m wide, and 0.47 m deep (Figure 2.1), with waste water treatment effluent flowing into the channel. The flumes are filled to 20 cm depth with gravel and planted with *Iris pseudacorus*. Flow conditions were sub-surface during installation of the DET gels, after 49 hours a flood event was simulated, creating 8 cm surface flow, which lasted for the remaining 16 hours of the gel deployment.

2.2.2.2 DET probe deployment in sediments:

Three 0.16 x 15 x 1 cm DET gels (DGT Research) were deployed for 65 hours in the vegetated zone of the flume (Figure 2.1). The deployment period exceeded estimated

exposure times required to ensure concentration equilibrium by diffusion in order to account for resettling of any potential sediment disturbances during the probe deployment. Gel 1 was deployed closest to the inflow: 3.86 m from the beginning of the flume. Gel 2 was deployed 1.15 m downstream of gel 1, and gel 3 was deployed 3.19 m downstream of gel 2, and 3.80 m from the end of the flume (Figure 2.1).

All gels were extracted from the sediment within 10 minutes, and immediately sliced at 2.5 cm intervals within 40 minutes. The DET gels were sliced (ultrapure water-rinsed blade), on an acid-washed (10% HCl) chopping board. Once sliced, the gels were placed into 50 ml centrifuge tubes and stored at 4°C.

2.2.2.3 DET gel probe processing:

The DET gels were back-equilibrated, on ice, with 6 ml ultrapure water on a reciprocating shaker for 24 hours. Once equilibrated the gels were removed and weighed, the resulting solution was then filtered (0.2 μm) and frozen for later analysis. Samples were analysed for nitrate concentration on a continuous flow analyser (Skalar San++), standards were used as quality controls and gave an accuracy of 0.1 mg NO_3^- l^{-1}, precision of ±0.1 NO_3^- l^{-1}, and an LOD of 0.9 mg NO_3^- l^{-1}.

2.2.3 Isotope Analysis

For the laboratory proof of concept experiments the nitrate was extracted from the samples using anion and cation exchange columns, and converted to silver nitrate using the method in Chang[23] and Heaton[24] or a modified version of this as subsequently described. For river samples with the presence of interfering anions, the method by Chang[23] and Heaton[24] was used; for the pure NO_3^- solutions, the samples were not passed through anion and cation exchange columns. Instead the nitrate was converted to silver nitrate and the above method used from the point of adding the first batch of Ag_2O. The silver nitrate was analysed by mass spectrometry as in Heaton[24]. The international isotope reference materials used for $\delta^{15}N$

were International Atomic Energy Agency (IAEA)-N-1 and IAEA-N-2, with $\delta^{15}N$ values vs air of +0.4 and +20.4‰, respectively, with a measurement precision of ±0.3 and ±0.5‰, respectively. The international isotope reference materials used for $\delta^{18}O$ were IAEA-NO_3^-, United States Geological Survey (USGS)-34 and USGS-35, with $\delta^{18}O$ vs standard mean ocean water of +26.0, -28.0 and +56.4‰, respectively, with a measurement precision of ±1.2, ±1.7 and ±1.9‰, respectively. Analysis was performed at the NIGL, BGS.

For the laboratory experiment at environmentally relevant concentrations and the field study data, the denitrifier method was used as this requires a lower mass of nitrate for analysis (0.7 μg NO_3^--N)[25,26]. This method utilises denitrifying bacteria to convert sample nitrate to N_2O, with a long-term measurement precision of ±0.3 and ±0.4‰ and an accuracy of 0.0 and 0.0‰ for $\delta^{15}N_{NO3^-}$ and $\delta^{18}O_{NO3^-}$, respectively, and a measurement limit of 2 μM NO_3^-. The international isotope reference materials used were IAEA-NO_3^-, USGS-34 and USGS-35, with $\delta^{15}N$ of +4.7, -1.4 and +3.4‰, respectively, with a measurement precision of ±0.3, ±0.6 and ±0.5‰, respectively, and $\delta^{18}O$ of +25.7, -28.0 and +57.4‰, respectively, with a measurement precision of ±0.7, ±0.6 and ±0.6‰, respectively. Analysis was performed by the Analytical Facilities, University of East Anglia.

2.3 Results and Discussion

2.3.1 Laboratory experiments

2.3.1.1 Nitrate concentrations from DET gels:

Nitrate concentrations were recovered from the DET gels with ranges between 3.6±0.1 and 3.7±0.1 for a 3.3±0.0 g $NO_3^- l^{-1}$ stock solution, between 5.2±0.3 and 5.3±0.1 for a 4.8±0.0 g $NO_3^- l^{-1}$ stock solution, between 6.7±0.1 and 6.9±0.0 for a 7.0±0.1 g $NO_3^- l^{-1}$ stock solution, and 6.3±0.0 and 6.8±0.1 for a 7.0±0.0 g $NO_3^- l^{-1}$ spiked river sample (Table 2.S-1). The nitrate concentration data showed that all of the experiments reached equilibrium with a nitrate recovery between 90.4±0.3 and 112.1±4.0%, which was independent of equilibrium

time with a fitted linear model having an adjusted R^2 value of -0.01, and p-value of 0.96 (Figure 2.S-1). The concentration appears to have affected the recovery of nitrate with a fitted linear model having an adjusted R^2 value of 0.80, and p-value of 0.00 (Figure 2.S-1). However, despite the large adjusted R^2 value, solution concentrations of 3.3±0.0 and 4.8±0.0 g $NO_3^- l^{-1}$ showed similar recoveries, even though one solution is only 70% of the concentration of the other, which is unexpected if there is a strong dependence of nitrate recovery on concentration. The observed recoveries were all between 90.4 and 112.1% and we believe the differences to come from varying dilution factors between the lowest and highest concentrations used, as solutions of 7.0 g $NO_3^- l^{-1}$ were diluted by the same factor, which was twice that of the solutions of concentration 3.3 and 4. 8 g $NO_3^- l^{-1}$, which were also diluted by the same factor, to allow for machine analysis. The nitrate recoveries observed were, therefore, independent of initial solution concentration. This was supported by the independence of recovery and initial solution concentration when performing the environmentally relevant concentration experiments (Table 2.S-1). These yielded nitrate recoveries between 99.4 and 105.2%, showing that equilibrium was reached in each case. A fitted linear model gave an adjusted R^2 value of -0.3, and a p-value of 0.64, showing that the nitrate recovery was independent of initial solution concentration.

The independence from equilibration time evidenced that as long as equilibrium is reached, the time the gel is left in solution should not affect nitrate recovery, and that the DET gels were expected to equilibrate by 24 hours. When utilising the DET gels *in-situ* the deployment time should be longer than the equilibrium time required for the gel thickness used. This is because the natural conditions of the system need to be re-established after gel deployment. Field deployment times for DET gels of 72 hours have been recommended previously[14].

The high nitrate concentrations used in these experiments (up to 7.0 g $NO_3^- l^{-1}$), resulted from practical limitations of the isotope analysis method used in the proof of concept study, which

required a minimum of 1 mg NO_3^--N. As evidenced by our results, these high concentrations did not prevent the reaching of equilibrium by diffusion into the gel. This proves that DET gels can also be applied in high nitrate conditions (e.g. artificial wetlands, wastewater treatment plant outputs), as the recovery of nitrate was not dependent on the solution concentration. It is acknowledged that the large nitrate concentrations used here, due to method limitations, are much higher than those found in most natural environments, therefore, the experiment was repeated with environmentally relevant concentrations as discussed above.

2.3.1.2 Nitrate isotope ratios in DET gels

2.3.1.2.1 $\delta^{15}N_{NO3^-}$

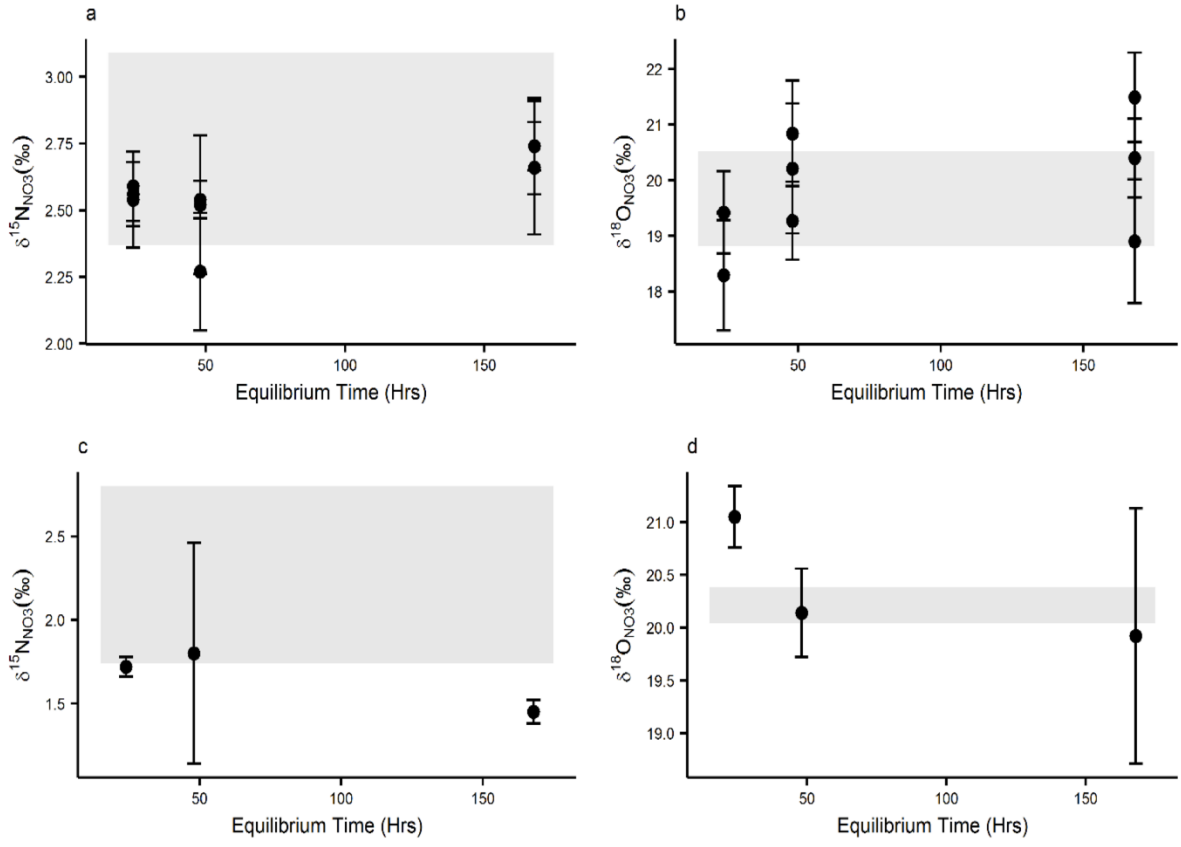

Figure 2.2a. $\delta^{15}N_{NO3^-}$ plotted against equilibrium time for DET gel solutions equilibrated in KNO_3 solutions, b. $\delta^{18}O_{NO3^-}$ plotted against equilibrium time for DET gel solutions equilibrated in KNO_3 solutions, c. $\delta^{15}N_{NO3^-}$ plotted against equilibrium time for DET gel

solutions equilibrated in nitrate-spiked river solutions, d. $\delta^{18}O_{NO3^-}$ plotted against equilibrium time for DET gel solutions equilibrated in nitrate-spiked river solutions. The grey shaded areas represent the measurement error of the stock solutions used for equilibration (σ=1).

The $\delta^{15}N_{NO3^-}$ for the nitrate solutions were the same as that of the stock solution, within error, with a range between 2.3±0.2‰ and 2.7±0.1‰, compared with 2.7±0.4‰ of the stock (Figure 2.2). The nitrate-spiked river water had a different $\delta^{15}N_{NO3^-}$ value, 2.3±0.5‰, than that of the nitrate solutions; this was expected as distinct sources of nitrate have different $\delta^{15}N_{NO3^-}$ and $\delta^{18}O_{NO3^-}$ values. The $\delta^{15}N_{NO3^-}$ for the river solutions equilibrated for 24 and 48 hours were found to be the same as the stock, within error, with $\delta^{15}N_{NO3^-}$ of 1.8±0.7‰ and 1.7±0.1‰, respectively. $\delta^{15}N_{NO3^-}$ for 168-hour equilibrium time was lower than the stock with a value of 1.5±0.1‰, however, this was not a statistically significant difference (paired t-test, p-value = 0.16).

2.3.1.2.2 $\delta^{18}O_{NO3^-}$

The $\delta^{18}O_{NO3^-}$ of the nitrate solutions were predominantly found to be the same as that of the stock solution, within error, with a range between 18.3±1.0‰ and 20.8±1.0‰, compared with 19.7±0.9‰ of the stock (Figure 2.2). The measured $\delta^{18}O_{NO3^-}$ value for the 168-hour equilibrium time with a stock solution of 4.8 g $NO_3^- l^{-1}$ was higher than the stock at $\delta^{18}O_{NO3^-}$ 21.5±0.8‰, however, this was not a statistically significant difference (paired t-test, p-value = 0.095). The $\delta^{18}O_{NO3^-}$ for the river solutions equilibrated for 48 and 168 hours were found to be the same as the stock, within error, with $\delta^{18}O_{NO3^-}$ of 19.9±1.2‰ and 20.1±0.4‰, respectively, compared with 20.2±0.2‰ of the stock. $\delta^{18}O_{NO3^-}$ for 24-hour equilibrium time was higher than the stock at 21.1±0.3‰, and this was found to be statistically significant (paired t-test, p-value=0.01).

This is believed to be due to the unusually small measurement error in the stock solution (0.2‰), as the lowest value the 24-hour sample could be is 20.8‰ and the highest value the stock could be is 20.4‰, which are similar values and would not otherwise be interpreted as having fractionated. This is evidenced by the uncertainty found in the International Energy Agency-NO_3^- standard of 0.85 and 1.46‰ (from multiple analyses), showing that two results within this range cannot be distinguished using this technique.

2.3.1.3 Determination of fractionation

The analysis of $\delta^{15}N_{NO3^-}$ and $\delta^{18}O_{NO3^-}$ revealed no significant difference between the values of the stock solution and those of the gel solutions. We, therefore, found no evidence of fractionation during the process of nitrate diffusion into and out of the gel during equilibrium and back-equilibrium. This also demonstrates that solution concentration and equilibrium time did not affect $\delta^{15}N_{NO3^-}$ and $\delta^{18}O_{NO3^-}$ (Figure 2.2). There was also no relationship between the $\delta^{15}N_{NO3^-}$ and $\delta^{18}O_{NO3^-}$ of the gel solution and nitrate recovery, with fitted linear models for the KNO_3 for $\delta^{15}N_{NO3^-}$ and $\delta^{18}O_{NO3^-}$ with adjusted R^2 values of -0.050 and 0.058, and p-values of 0.46 and 0.26, respectively, and fitted linear models for the river samples with adjusted R^2 values of -0.80 and -0.051, and p-values of 0.79 and 0.52, respectively. This again indicated that equilibrium was reached, and no fractionation was caused by diffusion (Figure 2.S-2).

This was also shown in most cases for additional environmentally relevant concentration experiments (outlined previously). Gel solutions of NO_3^- had $\delta^{15}N_{NO3^-}$ values between 0.1±0.3 and 0.5±0.3‰ for a stock value of 0.1±0.3‰, and a $\delta^{18}O_{NO3^-}$ value for a 100.5 mg NO_3^- l^{-1} solution of 22.3±0.4‰ for a stock value of 22.0±0.4‰. The $\delta^{18}O_{NO3^-}$ values for 20.1 and 50.8 mg NO_3^- l^{-1} solutions were outside of the stock's error, both having values of 23.0±0.4‰. These were found to be significantly different to the stock (paired t-test, p-value = 0.022 and 0.000, respectively, for 20.1 and 50.8 mg NO_3^- l^{-1}), however, this is believed to

be due to the small standard deviation of sample replicates (n=3), of 0.2, 0.0 and 0.0‰, respectively, for 20.1 and 50.8 mg NO_3^- l^{-1}, and the stock. Given that the difference between the highest value the stock ratio could be and the lowest value the solution ratio could be is only 0.2 for both solutions, this would not usually be considered fractionated. This is evidenced by the long-term reproducibility of the isotope technique, which is ±0.4‰, showing that two results within this range cannot be distinguished using this technique. The river sample had a $\delta^{15}N_{NO3^-}$ value of 10.3±0.3‰ for a stock of 10.2±0.3‰ and a $\delta^{18}O_{NO3^-}$ value of 4.7±0.4‰ for a stock of 4.2±0.4‰.

The nitrate-spiked river samples were used to test for any matrix effects, which may affect $\delta^{15}N_{NO3^-}$ and $\delta^{18}O_{NO3^-}$ values when this method is utilised *in-situ.* There was no fractionation of $\delta^{15}N_{NO3^-}$ and $\delta^{18}O_{NO3^-}$ in the river water samples, confirming the applicability of this method in environments where interfering ions are present.

2.3.2 Concentration and Isotope analysis from in-situ DET application

Three example profiles of *in-situ* DET sampling are discussed as proof of concept for the proposed combined DET-isotope methodology. The DET gels captured a large range of nitrate concentrations and $\delta^{15}N_{NO3^-}$ and $\delta^{18}O_{NO3^-}$ values in a 15 cm profile (Table 2.S-2, Figure 2.3), with all nitrate concentrations from the DET gels (18.6±0.1 to 82.5±0.9 mg NO_3^- l^{-1}) greater than that of the average inflow concentration of nitrate (13.4±0.7 mg NO_3^- l^{-1}). The largest concentration range was observed in gel 2, with a minimum of 20.0±0.1 mg NO_3^- l^{-1} at 11 cm depth, to a maximum of 82.5±0.9 mg NO_3^- l^{-1} at 1.25 cm depth. The largest range of $\delta^{15}N_{NO3^-}$ and $\delta^{18}O_{NO3^-}$, was shown in gels 1 and 2, respectively. $\delta^{15}N_{NO3^-}$ values in gel 1 ranged from 0.2±0.3‰ at 11 cm depth to 17.9±0.3‰ at 3.75 cm depth, and $\delta^{18}O_{NO3^-}$ values in gel 2 ranged from -9.9±0.4‰ at 1.25 depth to 9.3±0.4‰ at 6.25 cm depth. These results highlight the ability of DET gel-based passive sampling to capture hotspots of biogeochemical activity and spatially small redox zones, which would be missed with more

traditional methods i.e. multi-level piezometers, as was found previously with nitrate concentrations[14]. This is particularly shown in profile 1, where there appears to be an area of denitrification at 3.75 cm, indicated by low nitrate concentration combined with high $\delta^{15}N_{NO3^-}$ and $\delta^{18}O_{NO3^-}$ values. Concentrations at all depths in gel 1 vary over a small range between 37.3±0.4 and 47.4±0.4 mg $NO_3^- l^{-1}$, except for at a depth of 3.75 cm, where the concentration has decreased to 18.6±0.1 mg $NO_3^- l^{-1}$.

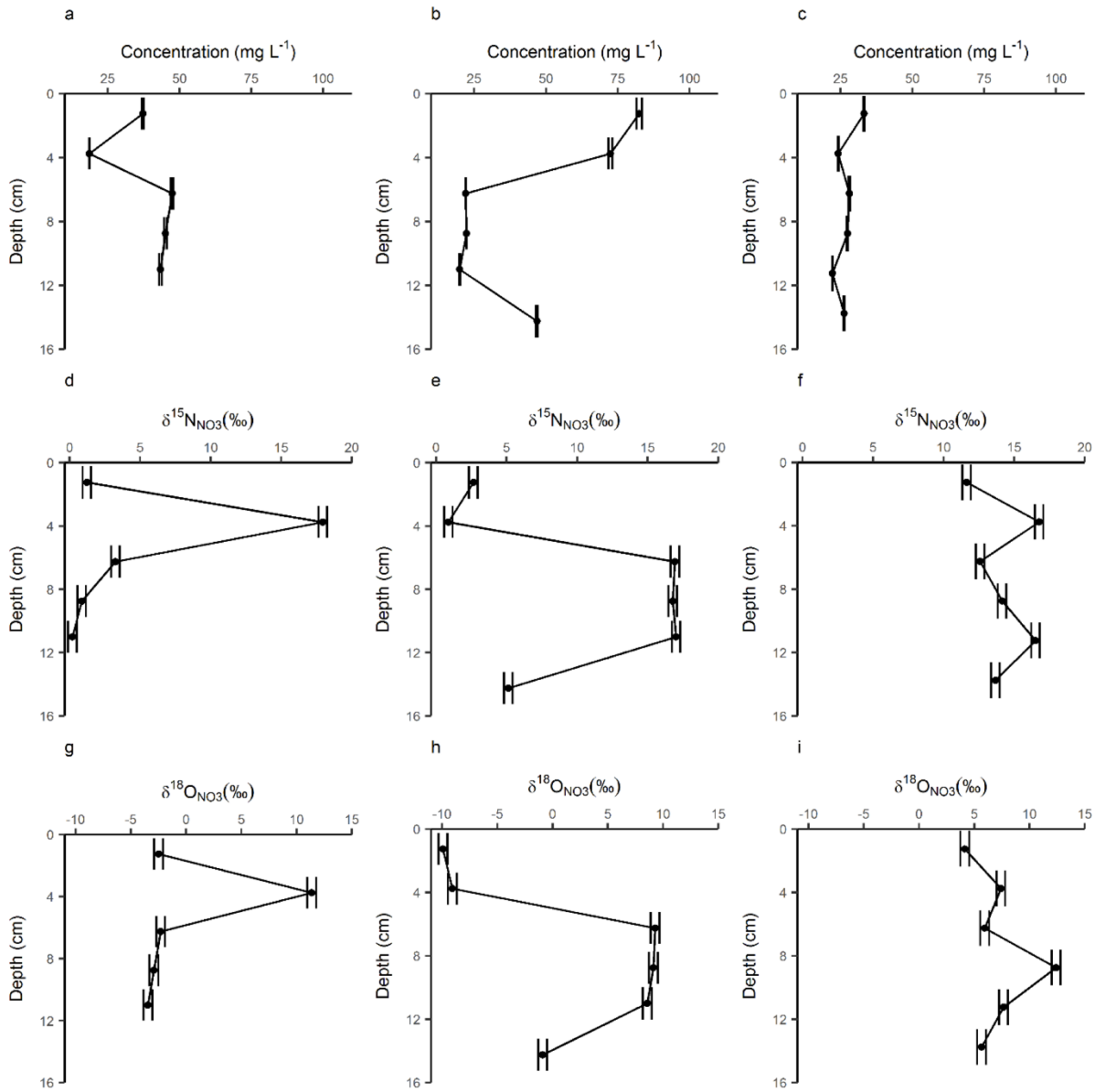

Figure 2.3. DET gel profiles from an in-situ deployment in gravel-filled mesocosms at the URL, Montornès del Vallès Wastewater Treatment Plant, Montornès del Vallès, Spain. a-c.

Concentration of nitrate plotted against depth for gels 1-3, d-f. $\delta^{15}N_{NO3^-}$ ratios plotted against depth for gels 1-3, g-i. $\delta^{18}O_{NO3^-}$ ratios plotted against depth for gels 1-3.

This is also reflected in the isotopic data where $\delta^{15}N_{NO3^-}$ varies over a small range between 0.2±0.3‰ and 3.3±0.3‰, except at 3.75 cm, where the $\delta^{15}N_{NO3^-}$ value has increased to 17.9±0.3‰, and $\delta^{18}O_{NO3^-}$ varies over a small range between -2.3±0.4‰ and -3.5±0.4‰, except at 3.75 cm where the $\delta^{18}O_{NO3^-}$ value has increased to 11.4±0.4‰.

The analysis of vertical profiles of nitrate isotope ratios and concentrations indicate differences in concentration patterns at the three locations (Figure 2.3). Gel 1 shows slightly higher concentrations at greatest depths (43.4±0.5 to 47.4±0.4 mg $NO_3^- l^{-1}$) compared to the shallowest depth (37.3±0.4 mg $NO_3^- l^{-1}$), with a local minimum of 18.6±0.1 mg $NO_3^- l^{-1}$ at 3.75 cm. This could be due to zones of nitrification associated with the mineralisation of nitrogen from the macrophytes[14,27–29]. The $\delta^{15}N_{NO3^-}$ and $\delta^{18}O_{NO3^-}$ profiles show little variation with depth, only varying between 0.2±0.3‰ and 3.3±0.3‰, and -2.3±0.4‰ and -3.5±0.4‰, respectively, except at 3.75 cm where there is a large increase in $\delta^{15}N_{NO3^-}$ to 17.9±0.3‰ and $\delta^{18}O_{NO3^-}$ to 11.4±0.4‰. Although similar, $\delta^{15}N_{NO3^-}$ values between 6.25 and 11 cm depth do decrease with depth, perhaps pointing to the onset of denitrification at 6.25 cm depth. The combination of low nitrate concentration, with high $\delta^{15}N_{NO3^-}$ and $\delta^{18}O_{NO3^-}$ values is indicative of denitrification, therefore, there appears to be a localised zone of denitrification at 3.75 cm[30].

In gel 2 an overall decrease in nitrate was observed at greater depths than in gel 1, although there was a concentration of 46.9±0.3 mg $NO_3^- l^{-1}$ at 14.25 cm, which was intermediate of the concentrations found at 1.25 and 3.75 cm (82.5±0.9 and 72.4±0.7 mg $NO_3^- l^{-1}$, respectively) and 6.25 to 11 cm (20.0±0.1 to 22.4±0.2 mg $NO_3^- l^{-1}$). The $\delta^{15}N_{NO3^-}$ values showed little variation between the shallowest and the largest depth; $\delta^{15}N_{NO3^-}$ was slightly higher at the greatest depth than at the shallowest depth, with values of 5.1±0.3‰ and 2.7±0.3‰,

respectively, and the lowest $\delta^{15}N_{NO3^-}$ value of 0.9±0.3‰ was found at 3.75 cm depth. The shallowest depth $\delta^{18}O_{NO3^-}$ values were also lower than at the greatest depth, however, the difference from -9.9±0.4‰ to -0.9±0.4‰, was greater than seen for $\delta^{15}N_{NO3^-}$. A substantial increase in $\delta^{15}N_{NO3^-}$ values was observed between 6.25 and 11 cm depth, with values between 16.8±0.3 and 16.9±0.3‰. This large increase was also present in the $\delta^{18}O_{NO3^-}$ profile, where peak concentrations range between 8.6±0.4‰ and 9.3±0.4‰, between 6.25 and 11 cm. In combination with $\delta^{15}N_{NO3^-}$ and $\delta^{18}O_{NO3^-}$ values, the concentrations observed at these depths indicate denitrification.

Vertical variation of nitrate concentrations in gel 3 seems to be minimal, with a narrow concentration range of 22.2±0.2 to 33.1±0.2 mg $NO_3^- l^{-1}$ for the whole 15 cm gel. It is worth noting that the maximum concentration found in gel 3 is at 1.25 cm, which is the same as is found in gel 2. The $\delta^{15}N_{NO3^-}$ and $\delta^{18}O_{NO3^-}$ values in gel 3 did not cover as wide a range as in gels 1 and 2; the range in $\delta^{15}N_{NO3^-}$ and $\delta^{18}O_{NO3^-}$ here was just 11.6±0.3 to 16.8±0.3‰, and 4.1±0.4 to 12.4±0.4‰, respectively. $\delta^{15}N_{NO3^-}$ values showed little variation ranging from 11.6±0.3 to 14.2±0.3‰, at all depths except 3.75 and 11.25 cm, where two areas of higher $\delta^{15}N_{NO3^-}$ values were found, with values of 16.8±0.3 and 16.5±0.3‰, respectively. These high $\delta^{15}N_{NO3^-}$ values at 3.75 and 11.25 cm, were not reflected in the $\delta^{18}O_{NO3^-}$ data, which showed a higher $\delta^{18}O_{NO3^-}$ value of 12.4±0.4‰ at 8.75 cm depth, with all other depths having similar $\delta^{18}O_{NO3^-}$ values between 4.1±0.4 and 7.7±0.4‰. The profile shows low nitrate concentrations with high $\delta^{15}N_{NO3^-}$ and $\delta^{18}O_{NO3^-}$ values for all depths, indicating denitrification throughout the profile. Considering $\delta^{15}N_{NO3^-}$:$\delta^{18}O_{NO3^-}$ is also useful in identifying areas of denitrification, with a ratio between approximately 2.1-2.5 considered indicative of denitrification[10]. In gel 3 this ratio is found at depths of 3.75, 6.25, 11.25 and 13.75 cm, where the $\delta^{15}N_{NO3^-}$:$\delta^{18}O_{NO3^-}$ is 2.3, 2.1, 2.2 and 2.4, respectively, providing further evidence

of denitrification. This denitrification throughout the profile is likely related to an overall increase in denitrification towards the downstream end of the flume as the residence time of the porewater and nitrate increased, and due to the cumulative effect of vegetation described previously.

Generally, enhanced denitrification appears to be correlated with the occurrence of vegetation in the flume, which has been previously observed to particularly affect depths between 5-12 cm[27,28]. Possible mechanisms by which vegetation enhances sediment denitrification can be of biotic or abiotic nature, generally leading to high biogeochemical reactivity[31]. These include, uptake by macrophytes, increased surface water downwelling, and enhanced residence times of water in the sediment that are facilitated by vegetation, and may, therefore, have led to the increased denitrification seen here[3,28]. Similar zones of vegetation-associated denitrification were found in the River Leith, UK[28]. Nitrate concentrations ranging from 0.05 to 7.31 mg NO_3^--N l^{-1} were found in vegetated areas, compared to 0.41 to 9.83 mg NO_3^--N l^{-1} in non-vegetated areas, indicating denitrification associated with the vegetation.

Horizontal patterns along the flume indicate a general trend of denitrification with an increased observation of low nitrate concentration samples from gel 1 through to gel 3, combined with an increased frequency of high $\delta^{15}N_{NO3^-}$ and $\delta^{18}O_{NO3^-}$ values. This longitudinal profile is overlain by local effects, where hotspots of biogeochemical reactivity can be seen, thought to be influenced by the vegetation effect described previously.

Comparing the gel data to the nitrate concentration of the inflow shows an increase in nitrate from the inflow to the sub-surface water of the flume, indicating net nitrification within the flume itself. This is the opposite of the denitrification trend shown by the gel profiles, and seems to show high nitrification within the flume, even upstream of the first gel, which increased nitrate concentrations before these decreased again through denitrification.

The *in-situ* results of the DET gel and isotope method presented here, have allowed the investigation of detailed processes at a spatial scale, which exceeds that of previous studies. Particularly, hotspots of denitrification were easily identified using both concentration and isotope data. The isotopic data were invaluable in showing that the gel profiles indicated generally high nitrate concentrations, with zones of denitrification leading to low nitrate concentrations. This is in contrast to the concentration data alone, which along with the inflow concentration, indicates varying degrees of nitrification in the gel profiles. This is increasingly important in the study of nutrient fate at aquifer and river or lake interfaces; research areas that are often limited by a lack of sufficient monitoring methods. Thus, this field trial has successfully demonstrated the value of this new approach for *in-situ* applications.

To assess natural waters in which this DET-isotope technique could be applied, the concentration of nitrate in porewaters needed to provide a solution of 50 nmol NO_3^- required to perform the isotope analysis was calculated. Using a 1.56 mm thick DET gel and slicing at 1 cm would require a porewater nitrate concentration of 10.5 mg l^{-1} and slicing at 2.5 cm would reduce this to 4.2 mg NO_3^- l^{-1}. The nitrate concentrations required limit this technique to sediments in non-pristine environments[3,32].

2.4 Conclusions

The laboratory proof of concept demonstrates that $\delta^{15}N_{NO3}^-$ and $\delta^{18}O_{NO3}^-$ do not fractionate when sampled with a DET gel. Nitrate recovery and $\delta^{15}N_{NO3}^-$ and $\delta^{18}O_{NO3}^-$ values were independent of both equilibrium time and nitrate concentration, suggesting the applicability of DET technology for sampling isotope ratios from sediment porewater at high spatial resolution.

Additionally, the *in-situ* application of DET gel probes in a field trial provide evidence of the potential of this methodology to sample nitrate concentration and isotopic data with DET technology in the field at higher resolution than previously possible.

Based on the promising results of the presented lab and field trials we recommend the application of this combined methodology at aquifer-river and aquifer-lake interfaces in order to enhance mechanistic process understanding of hotspots in nitrogen cycling. Future research may elaborate to what degree the application of the proposed methodologies can be extended also to brackish and marine systems.

2.5 Acknowledgements

The authors would like to thank Dr. Tim Heaton at the NIGL for his help in sample analysis and data interpretation, Dr. Eugènia Martí at the Centre D'Estudis Avancats de Blanes and the URL for allowing us to use their facilities and data, and Dr. Hao Zhang of DGT Research and Lancaster Environment Centre, University of Lancaster, for providing the DET gels and advice on the gel's capabilities. We would also like to thank the Natural Environment Research Council (NERC) and the Central England NERC Training Alliance for their funding of this project, as well as the NIGL for providing an in-kind grant for isotopic analysis.

Supporting Information (SI) Available: A 4-page listing of data Tables 2.S-1 and 2.S-2, and figures showing nitrate recovery against equilibrium time and nitrate concentration (Figure 2.S-1) and nitrate recovery against nitrate isotope values (Figure 2.S-2) is available as SI.

2.6 References

1. McClain, M. E. *et al.* Biogeochemical Hot Spots and Hot Moments at the Interface of Terrestrial and Aquatic Ecosystems. *Ecosystems* **6,** 301–312 (2003).

2. Lautz, L. K. & Fanelli, R. M. Seasonal biogeochemical hotspots in the streambed around restoration structures. *Biogeochemistry* **91,** 85–104 (2008).

3. Krause, S., Tecklenburg, C., Munz, M. & Naden, E. Streambed nitrogen cycling beyond the hyporheic zone: Flow controls on horizontal patterns and depth distribution of nitrate and dissolved oxygen in the upwelling groundwater of a lowland river. *J. Geophys. Res. Biogeosciences* **118,** 54–67 (2013).

4. Krause, S., Boano, F., Cuthbert, M. O., Fleckenstein, J. H. & Lewandowski, J. Understanding process dynamics at aquifer-surface water interfaces: An introduction to the special section on new modeling approaches and novel experimental technologies. *Water Resour. Res.* **50,** 1847–1855 (2014).

5. Krause, S. *et al.* Inter-disciplinary perspectives on processes in the hyporheic zone. **499,** 481–499 (2011).

6. Boano, F. *et al.* Hyporheic flow and transport processes: Mechanisms, models, and biochemical implications. *Rev. Geophys.* 1–77 (2014). doi:10.1002/2012RG000417.Received

7. Hannah, D. M., Sadler, J. P. & Wood, P. J. Hydroecology and ecohydrology: a potential route forward? *Hydrol. Process.* **21,** 3385–3390 (2007).

8. Krause, S., Louise Heathwaite, a., Binley, A. & Keenan, P. Nitrate concentration changes at the groundwater-surface water interface of a small Cumbrian river. *Hydrol. Process.* **23,** 2195–2211 (2009).

9. Krause, S., Hannah, D. M. & Fleckenstein, J. H. Hyporheic hydrology: interactions at the groundwater-surface water interface. *Hydrol. Process.* **23,** 2103–2107 (2009).

10. Kendall, C. in *Isotope Tracers in Catchment Hydrology* (eds. C. Kendall and J.J. McDonnell) 519–576 (Elsevier, 1998)

11. Abbott, B. W. *et al.* Using multi-tracer inference to move beyond single-catchment ecohydrology. *Earth-Science Rev.* **160,** 19–42 (2016).

12. Lewandowski, J. & Nützmann, G. Nutrient retention and release in a floodplain's aquifer and in the hyporheic zone of a lowland river. *Ecol. Eng.* **36,** 1156–1166 (2010).

13. Welti, N. *et al.* Large-scale controls on potential respiration and denitrification in riverine floodplains. *Ecol. Eng.* **42,** 73–84 (2012).

14. Ullah, S. *et al.* In situ measurement of redox sensitive solutes at high spatial resolution in a riverbed using Diffusive Equilibrium in Thin Films (DET). *Ecol. Eng.* **49,** 18–26 (2012).

15. Mendoza-Lera, C. & Datry, T. Relating hydraulic conductivity and hyporheic zone biogeochemical processing to conserve and restore river ecosystem services. *Sci. Total Environ.* **579,** 1815–1821 (2016).

16. Krom, M. ., Davison, P., Zhang, H. & Davison, W. High-resolution pore-water sampling with a gel sampler. (1994).

17. Mortimer, R. J. ., Krom, M. ., Hall, P. O. ., Hulth, S. & Ståhl, H. Use of gel probes for the determination of high-resolution solute distributions in marine and estuarine pore waters. *Mar. Chem.* **63,** 119–129 (1998).

18. Docekalova, H., Clarisse, O., Salomon, S. & Wartel, M. Use of constrained DET probe for a high-resolution determination of metals and anions distribution in the sediment pore water. **57,** 145–155 (2002).

19. Palmer-Felgate, E. J., Mortimer, R. J. G., Krom, M. D. & Jarvie, H. P. Impact of point-source pollution on phosphorus and nitrogen cycling in stream-bed sediments. *Environ. Sci. Technol.* **44,** 908–914 (2010).

20. Metzger, E. *et al.* Simultaneous Nitrite/Nitrate Imagery at Millimeter Scale through the Water–Sediment Interface. *Environ. Sci. Technol.* acs.est.6b00187 (2016). doi:10.1021/acs.est.6b00187

21. Kessler, A. J., Glud, R. N., Cardenas, M. B. & Cook, P. L. M. Transport Zonation Limits Coupled Nitrification-Denitrification in Permeable Sediments. (2013).

22. Roberts, K. L., Kessler, A. J., Grace, M. R. & Cook, P. L. M. Increased rates of dissimilatory nitrate reduction to ammonium (DNRA) under oxic conditions in a periodically hypoxic estuary. *Geochim. Cosmochim. Acta* **133,** 313–324 (2014).

23. Chang, C. C. . *et al.* A method for nitrate collection for δ15N and δ18O analysis from waters with low nitrate concentrations. *Can. J. Fish. Aquat. Sci.* **56,** 1856–1864 (1999).

24. Heaton, T. H. E., Wynn, P. & Tye, A. M. Low 15N/14N ratios for nitrate in snow in the High Arctic (79°N). *Atmos. Environ.* **38,** 5611–5621 (2004).

25. Casciotti, K. L., Sigman, D. M., Hastings, M. G., Bohlke, J. K. & Hilkert, A. Measurement of the oxygen isotopic composition of nitrate in seawater and freshwater using the denitrifier method. *Anal. Chem.* **74,** 4905–4912. (2002).

26. Sigman, D., Karsh, K. & Casciotti, K. Ocean Process Tracers: Nitrogen Isotopes in the Ocean. *Encycl. Ocean Sci.* 4138–4153 (2009). doi:10.1006/rwos.2001.0172

27. Byrne, P. *et al.* Diffusive equilibrium in thin films provides evidence of suppression of hyporheic exchange and large-scale nitrate transformation in a groundwater-fed river. *Hydrol. Process.* n/a-n/a (2014). doi:10.1002/hyp.10269

28. Ullah, S. *et al.* Influence of emergent vegetation on nitrate cycling in sediments of a groundwater-fed river. *Biogeochemistry* **118,** 121–134 (2014).

29. Mortimer, R. J. G. *et al.* Evidence for suboxic nitrification in recent marine sediments. *Mar. Ecol. Prog. Ser.* **236,** 31–35 (2002).

30. Amberger, A. & Schmidt, H.-L. Naturliche Isotopengehalte von Nitrat als Indikatoren fur dessen Herkunft. *Geochim. Cosmochim. Acta* **51,** 2699–2705 (1987).

31. Forshay, K. J. & Dodson, S. I. Macrophyte presence is an indicator of enhanced denitrification and nitrification in sediments of a temperate restored agricultural stream. *Hydrobiologia* **668,** 21–34 (2011).

32. Lefebvre, S., Marmonier, P. & Pinay, G. Stream regulation and nitrogen dynamics in sediment interstices: comparison of natural and straightened sectors of a third-order stream. *River Res. Appl.* **20,** 499–512 (2004).

2.7 SI

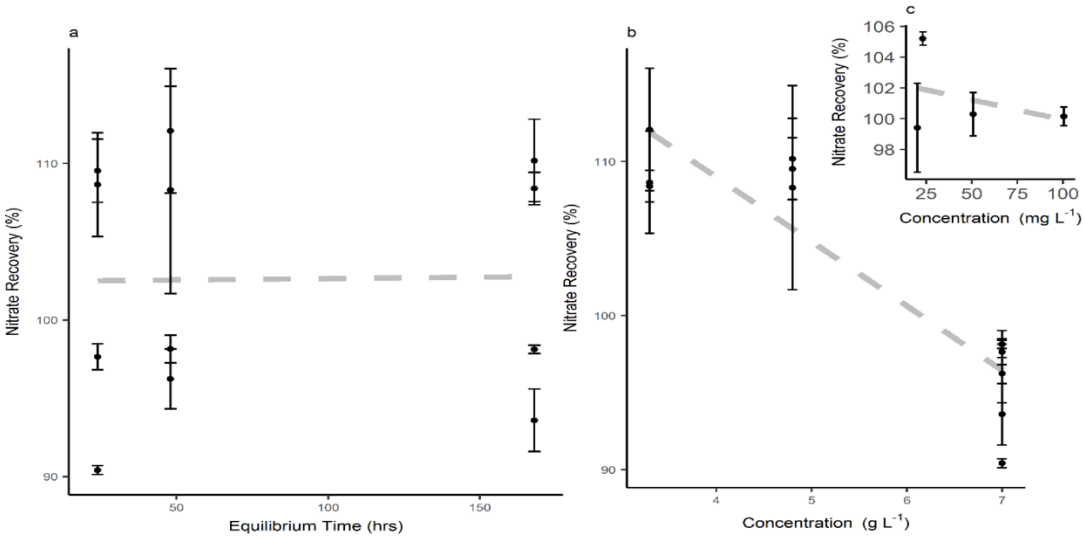

Figure 2.S-1a. The nitrate recovery (%) obtained from the laboratory DET gel experiments plotted against equilibrium time (hrs), the fitted linear model has an adjusted R^2 of -0.01, and p-value of 0.96, b. The nitrate recovery (%) obtained from the laboratory DET gel experiments plotted against concentration (g l^{-1}), the fitted linear model has an adjusted R^2 of 0.80, and p-value of 0.00, and c. The nitrate recovery (%) obtained from lower concentration DET gel experiments plotted against concentration (mg l^{-1}), the fitted linear model has an adjusted R^2 of -0.3, and p-value of 0.64.

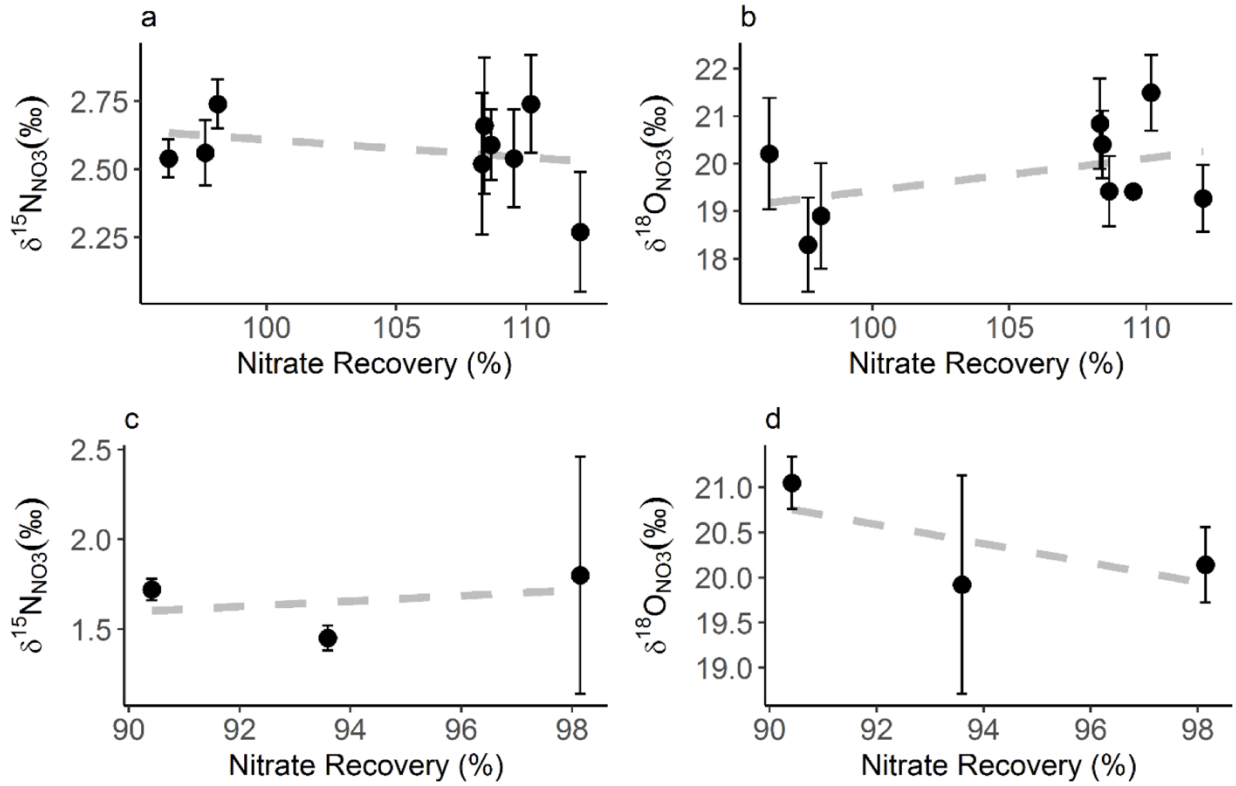

Figure 2.S-2a. Nitrate recovery plotted against $\delta^{15}N_{NO3^-}$ for DET gel solutions equilibrated in KNO_3 solutions, the fitted linear model has an adjusted R^2 of -0.050 and a p-value of 0.46, b. Nitrate recovery plotted against $\delta^{18}O_{NO3^-}$ for DET gel solutions equilibrated in KNO_3 solutions, the fitted linear model has an adjusted R^2 of 0.058 and a p-value of 0.26, c. Nitrate recovery plotted against $\delta^{15}N_{NO3^-}$ for DET gel solutions equilibrated in nitrate-spiked river solutions, the fitted linear model has an adjusted R^2 of -0.8 and a p-value of 0.79, d. Nitrate recovery plotted against $\delta^{15}N_{NO3^-}$ for DET gel solutions equilibrated in nitrate-spiked river solutions, the fitted linear model has an adjusted R^2 of -0.051 and a p-value of 0.52

Table 2.S-1. Nitrate concentration, nitrate recovery and nitrate isotopes from laboratory DET gel experiments, the top table shows the results from the primary experiments at high concentration, the bottom table shows the data from the lower concentration experiments. Values associated with river solutions are shown in grey.

Equilibrium Time	Gel nitrate Concentration (g L^{-1})	Nitrate Recovery (%)	$\delta^{15}N_{NO3}$(‰)	$\delta^{18}O_{NO3}$(‰)
168	3.6±0.0	108.4±1.0	2.7±0.3	20.4±0.7
48	3.7±0.1	112.1±4.0	2.3±0.2	19.3±0.7
24	3.6±0.1	108.6±3.3	2.6±0.1	19.4±0.7
168	5.3±0.1	110.2±2.6	2.7±0.2	21.5±0.8
48	5.2±0.3	108.3±6.6	2.5±0.3	20.8±1.0
24	5.2±0.1	109.5±2.0	2.5±0.2	19.4±0.0
168	6.9±0.0	98.1±0.3	2.7±0.1	18.9±1.1
48	6.7±0.1	96.2±1.9	2.5±0.1	20.2±1.2
24	6.8±0.1	97.6±0.8	2.6±0.1	18.3±1.0
168	6.5±0.1	93.6±2.0	1.5±0.1	19.9±1.2
48	6.8±0.1	98.1±0.9	1.8±0.7	20.1±0.4
24	6.3±0.0	90.4±0.3	1.7±0.1	21.1±0.3
Stock NO_3	-	-	2.7±0.4	19.7±0.9
Stock River	-	-	2.3±0.5	20.2±0.2

Equilibrium Time	Gel nitrate Concentration (mg L^{-1})	Nitrate Recovery (%)	$\delta^{15}N_{NO3}$(‰)	$\delta^{18}O_{NO3}$(‰)
24	20.0±0.6	99.4±2.9	0.5±0.3	23.0±0.4
24	50.9±0.7	100.3±1.4	0.4±0.3	23.0±0.4
24	100.6±0.6	100.2±0.6	0.1±0.3	22.3±0.4
24	24.3±0.1	105.2±0.4	10.3±0.3	4.7±0.4
Stock NO_3	-	-	0.1±0.3	22.0±0.4
Stock River	-	-	10.2±0.3	4.2±0.4

Table 2.S-2. Nitrate concentration and nitrate isotopes for three DET gels deployed into the gravel sediment of a vegetated mesocosm at the URL, Montornès del Vallès Wastewater Treatment Plant, Montornès del Vallès, Spain.

Gel profile	Depth (cm)	Nitrate Concentration (mg L^{-1})	$\delta^{15}N_{NO3}$(‰)	$\delta^{18}O_{NO3}$(‰)
1	1.25	37.3±0.4	1.2±0.3	-2.5±0.4
1	3.75	18.6±0.1	17.9±0.3	11.4±0.4
1	6.25	47.4±0.4	3.3±0.3	-2.3±0.4
1	8.75	45.1±0.5	0.9±0.3	-2.9±0.4
1	11	43.4±0.5	0.2±0.3	-3.5±0.4
2	1.25	82.5±0.9	2.7±0.3	-9.9±0.4
2	3.75	72.4±0.7	0.9±0.3	-9.1±0.4
2	6.25	22.1±0.1	16.9±0.3	9.3±0.4
2	8.75	22.4±0.2	16.8±0.3	9.1±0.4
2	11	20.0±0.1	17.0±0.3	8.6±0.4
2	14.25	46.9±0.3	5.1±0.3	-0.9±0.4
3	1.25	33.1±0.2	11.6±0.3	4.1±0.4
3	3.75	24.2±0.2	16.8±0.3	7.4±0.4
3	6.25	28.0±0.2	12.6±0.3	6.0±0.4
3	8.75	27.4±0.2	14.2±0.3	12.4±0.4
3	11.25	22.2±0.2	16.5±0.3	7.7±0.4
3	13.75	26.3±0.2	13.7±0.3	5.7±0.4

Chapter 3: A comparison of available field methodologies for nutrient sampling in streambed porewaters

Sophie Comer-Warner[1], Julia L.A. Knapp[2], Jay P. Zarnetske[3], Phillip J. Blaen[1,4], Megan J. Klaar[5], Felicity Shelley[6], Sami Ullah[1], Daren C. Gooddy[7], Nick Kettridge[1] and Stefan Krause[1]

1. School of Geography, Earth and Environmental Sciences, University of Birmingham, Edgbaston, Birmingham B15 2TT, UK

2. University of Tübingen, Institut for Geoscience, Hölderlinstr. 12, Germany

3. Department of Earth and Environmental Sciences, 220 Trowbridge Rd, East Lansing, MI 48824, USA

4. Birmingham Institute of Forest Research, University of Birmingham, Edgbaston, Birmingham B15 2TT, UK

5. Garstang School of Geography, University of Leeds, Leeds, LS2 9JT, UK

6. School of Biological and Chemical Sciences, Queen Mary University of London, Mile End Road, London E1 4NS, UK

7. British Geological Survey (BGS), Maclean Building, Wallingford, Oxfordshire OX10 8BB, UK

3.1 Abstract

The HZ is the transition region within the streambed, where groundwater and surface water mix, creating unique environmental characteristics, which result in the HZ being a 'hotspot' of biogeochemical activity. Despite this, streambed biogeochemical processes remain poorly understood, in part due to difficulties associated with sampling porewater from the streambed. This paper provides a critical assessment of the key techniques available for streambed porewater sampling to investigate biogeochemical cycling. Nitrate and ammonium

concentration profiles from three sampling techniques (multilevel mini-piezometers, DET gels and USGS Minipoint samplers) were compared to identify key differences in profiles obtained through the use of these different techniques. We found that nitrate concentrations did not differ significantly between methods, however, ammonium concentrations did, and tended to be greatest using multilevel mini-piezometers and smallest using USGS Minipoint samplers. Subsequently, we present a review of the available techniques for streambed biogeochemical sampling, including the achievable spatial and temporal resolution, and advantages and limitations, of each technique. This review aims to provide guidance of the most appropriate sampling method to answer specific research questions, and address gaps within our understanding and knowledge of streambed biogeochemistry. This has wide implications for interdisciplinary HZ research, which has typically suffered from a lack of systematic sampling protocols.

3.2 Introduction

Ecohydrological and biogeochemical process dynamics in streambed environments have recently received increasing attention by the research community, regulators, policy makers and restoration organisations[1–4]. This increasing interest is due to the observation of 'hotspots' and 'hot moments' of biogeochemical reactivity in the HZ, where surface water and groundwater mix[3,5,6]. This mixing produces unique physical characteristics of, for example, pH, temperature and flow, which enable the HZ to support a large proportion of the microbial stream community[2]. Streambed environments, therefore, are characterised by high rates of microbial activity, enhanced nutrient cycling and steep redox gradients, leading to its description as the "river's liver" [2,7–10].

The investigation of streambed biogeochemical processes, in particular, requires the sampling (extraction) and analysis of interstitial porewaters, at multiple spatial and temporal scales. However, despite the growing volume of interdisciplinary research in the HZ, there remains

controversy and a lack of systematic protocols for sampling methodologies to facilitate transferability between studies[3]. Sampling, as well as data interpretation, therefore, can be challenging[11,12]. Current standard techniques have had varying success with adequately capturing nutrient conditions across the respectively relevant spatial and temporal scales, and selecting the most appropriate methodology for a specific research question remains a challenge.

Standard porewater sampling methodologies have typically been developed to address subject-specific research questions and the challenges of working with sediments, which are consolidated to different degrees. Thus, we are confronted with a range of different porewater sampling methods and variations of how these methods are applied in practice. Depending on the application, the chosen methods may be based on permanent (e.g. piezometers) or temporary (e.g. USGS Minipoint samplers (Minipoints from here onwards)[13,14]) installations (Figure 3.1). While the extraction of porewater samples warrants the capturing of a snap shot in time only, the spatial and temporal resolutions vary significantly between Minipoints with discrete, high-resolution depth sampling and often permanently installed, single well piezometers with large (up to several 10s of cm) screened sections (Figure 3.1). Hence, extracted sample volumes vary from a few millilitres to several litres[11–13,15–19], as well as, maximum sampling depths (mm's to 200 cm) and sampling intervals (mm's to >10 cm) (Figure 3.1)[3,12,13,15,17,19–22].

Sampling techniques developed for extracting porewater samples for biogeochemical analysis predominantly focus on the upper metre of the streambed, often targeting the top 20 cm at a higher spatial resolution[12,13,20,22]. Sampling techniques may be active (through the application of negative pressure) or passive (based on diffusion), with a wide range of different sample volumes extracted. The vertical scale achievable depends heavily on the technique used, e.g. screened piezometer vs multilevel mini-piezometer, and the volume of porewater extracted.

There are many porewater sampling methods available for biogeochemical investigation, which include multilevel mini-piezometers, Minipoints and DET gels (Figure 3.1).

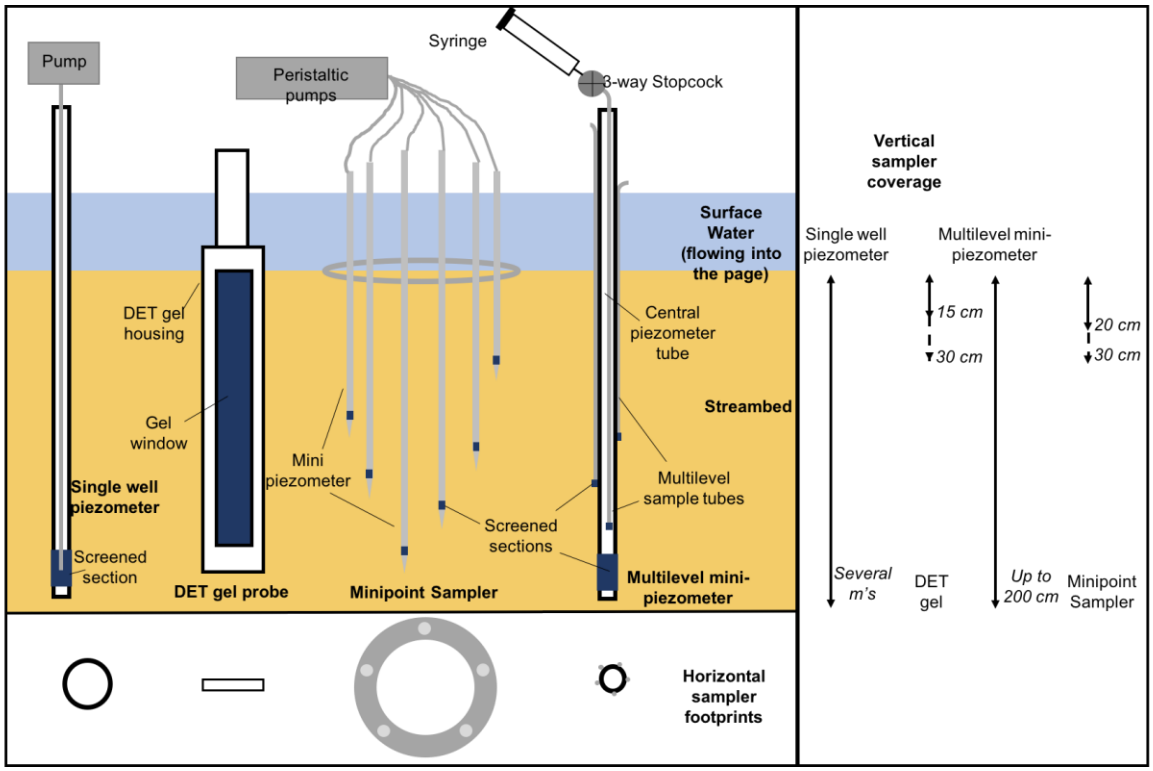

Figure 3.1. A conceptual diagram showing the practical setup of the main biogeochemical streambed sampling techniques of single well piezometers, DET gels, USGS Minipoint samplers, and multilevel mini-piezometers. Also shown are the vertical coverage and horizontal footprint of the samplers.

This paper aims to compare the information achieved with the most frequently used of the aforementioned methods, in particular with regards to their ability to capture nutrient patterns in streambed porewaters across a stream reach at varying spatial resolution. We, therefore, analyse the depth-related variability in streambed nitrogen concentrations captured by three different sampling methods. We present data from a comparative field study comprising multilevel mini-piezometers, Minipoints and DET gel probes applied to sample streambed porewater for analysis of different nitrogen fractions. These field experiments are complemented by a laboratory control experiment comparing NH_4^+ concentrations gained

from multilevel piezometers and DET gels, to elaborate on observed differences in field applications. Based on these observations, a comparison of the different available sampling techniques is presented, discussing their specific advantages and limitations for different applications.

3.3 Comparison of sampling techniques

This study focusses on streambed sampling methodologies developed to sample vertical biogeochemical profiles of nutrients, which enable ecohydrological questions across varying interfaces to be investigated. As such, only techniques which allow chemical sampling at multiple depths are summarised here, and the advantages and limitations of each method are outlined with respect to this application.

3.3.1 Active Samplers

3.3.1.1 Single well piezometers

Single well piezometers are typically constructed from a steel or polyvinyl chloride (PVC) pipe, which is screened at one end over the desired vertical range; the end of the pipe closest to the screen is then blocked (Figure 3.1)[30–32]. These piezometers are usually used at a single depth up to several metres, but can be used in a nested design to allow sampling at multiple depths, which are typically sampled consecutively[33,34]. A screened section varying between 10 and 100s of mm's is utilised depending on whether depth specific or depth-integrated sampling is required[31,35]. The footprint of a single piezometer is typically 1-4 cm in diameter[16,34,36], which can result in a relatively large footprint when a nested design is utilised. Piezometers are deployed into the streambed over temporal scales of several weeks to years[31], and the extracted porewater sample represents a snapshot of the conditions at the time of sampling. Prior to sampling the piezometer is purged of water by pumping until dry or until 3 times the water volume has been removed, if complete purging is not feasible[34,37,38]. The water is sampled from the piezometer once it has refilled, hence, the porewater is not

extracted through suction from the sediment, but through flow into the piezometer[31]. This allows large volumes of water to be sampled, with extraction achieved either with a pump or a syringe.

3.3.1.1.1 Advantages:

Vertical hydraulic gradients can be measured in the piezometer at the depth of sampling, allowing hydrological and chemical information to be gained at the same location. Piezometer installation is straightforward in sandy and silt sediments.

3.3.1.1.2 Disadvantages:

Single well piezometers must be installed with sufficient time prior to sampling for the natural conditions of the streambed to re-establish, this time can be long (hours to days), especially when installing into clay, silt or shale sediment[39]. Piezometer installation in gravel and clay sediments can be difficult, and requires substantial hammering or pre-drilling of the sediment[30]. Additionally, the footprint of the piezometer is relatively large, and the achievable vertical resolution is low compared to other techniques.

3.3.1.2 Multilevel mini-piezometers

Multilevel mini-piezometers consist of a number of small Tygon© or Polytetrafluoroethylene tubes of varying length (as sampling points), which are fitted around a larger central PVC or High-density polyethylene tube (acting as a more traditional piezometer) (Figure 3.1)[12,18,24,32]. The design allows the extraction of porewater at a number of discrete sampling depths and sampling intervals, which are defined by the user and determined by the length of the small tubes and their spacing. Sampling depths are typically between 10 and 200 cm[18,24,40–43], with a sampling interval of 10 cm[24,43], although a spatial resolution up to 5 cm is achievable with a low extraction rate[12]. The footprint of the multilevel mini-piezometer setup is small, usually ~ 3 cm in diameter, allowing samples to be taken at multiple depths over a discrete area[12,18,24]. Multilevel mini-piezometers are deployed into the streambed over temporal scales of several

weeks to years, and the extracted pore-water sample represents a snapshot of the conditions at the time of sampling. Sample volumes are typically small and collected slowly with a syringe or with a peristaltic pump at a low flow rate, which prevents the natural hyporheic flow from being disturbed, as well as allowing a higher vertical resolution to be achieved[18]. The multiple depths of the multilevel mini-piezometers may be sampled simultaneously or consecutively from shallowest to deepest depths or vice versa. A sampler combining attributes of the single well piezometer and the multilevel minipiezometers has recently been developed, using a relatively large central piezometer (32 mm outer diameter) up to 4 m depth[44]. Sampling ports are connected to the central tube so that the sampling resolution varies from 0.05 to 0.5 m, depending on which zone is being sampled at that depth. Although this affords high-resolution sampling at critical zones with a large depth profile, this sampling methodology retains the issues associated with a large sampler footprint as it is not a minipiezometer.

3.3.1.2.1 Advantages:

Multilevel mini-piezometers allow porewater samples to be extracted from discrete depths, enabling vertical solute profiles to be captured. Their design, which is both compact and user-defined, leads to easy installation in soft sediment[31], and a small sampling diameter, as well as a flexible vertical depth and resolution to address desired research questions. The central piezometer tube is flexible and so bends with surface water flow, which results in a more storm-resilient piezometer than more traditional, rigid single-well piezometers[12]. Furthermore, the depth extension of sampling available when using multilevel mini-piezometers allows deeper streambed biogeochemistry to be investigated.

3.3.1.2.2 Disadvantages:

The hydrological information gained via hydraulic gradients is difficult to determine in the discrete depths of the multilevel mini-piezometers, due to the small diameter of the multilevel

sampling tubes. Only the central piezometer tube, therefore, can be dip-metered to provide information on vertical hydraulic gradient. It is, therefore, not possible to ascertain this information for each sampling depth and only information at the deepest location of the piezometer is available. Additionally, the central tube is too small to allow continuous monitoring of hydraulic heads using a pressure transducer. It is possible to disrupt the vertical solute profile during sampling, as drawing samples at too high flow rate or at too great a negative pressure may cause overlap in the sample area between depths or alter preferential flow (artificially increasing horizontal or vertical flow) in the streambed[18]. The sampling interval achievable using multilevel mini-piezometers is relatively coarse compared to other discrete depth-sampling techniques. The piezometers must be installed in advance of sampling to allow the sediment to re-collapse around the piezometer and for the natural conditions to re-establish. In gravel or clay sediments, installation can be more difficult and may require pre-drilling of a hole or substantial hammering to install the piezometer into the streambed. Additionally, although currently a suggestion, the evidence presented in this study appears to suggest that multilevel mini-piezometers may underestimate ammonium concentrations.

3.3.1.3 Mini Drivepoint Samplers

Arrays of mini-piezometers, such as the USGS Minipoint sampler, have been utilised to sample streambed chemistry[13,14,22]. The Minipoint sampler consists of six ~0.3 cm-diameter, stainless steel piezometers with drivepoints, which are arranged around a ring (Figure 3.1)[13], and an alternative design of nine 0.8 cm diameter mini-piezometers has also been developed[22]. The piezometers are fixed at discrete, user-defined depths to enable the upper 20-30 cm of the streambed to be sampled at high vertical resolution, up to 1 cm[10]. The footprint of the Minipoint sampler is relatively large, ~10 cm[13], resulting in porewater samples collected from different depths over a wider area than those from a multilevel piezometer. The Minipoint sampler is usually installed shortly before sampling, enabling it to

be used as a roaming sampler, and extracted samples represent a snapshot of the conditions at the time of sampling. Samples collected using Minipoint samplers tend to be of small volume and are extracted slowly using a syringe or a peristaltic pump with very low flow rates. This prevents the natural hyporheic flow from being disturbed, as well as maintaining a high vertical resolution[14]. The discrete sampling depths may be sampled simultaneously or consecutively.

3.3.1.3.1 Advantages:

The Minipoint sampler design, with short and thin (typically up to 20 cm in length and 0.3 cm diameter) piezometers[13], enables easy and rapid installation with minimal disturbance to the streambed. This allows the Minipoints to be sampled shortly after deployment and they can, therefore, be used effectively as roaming samplers where probes are installed, sampled and then removed, before installation at a new location. The tip of the Minipoint piezometers may be filled with glass wool, enabling pre-filtration of samples prior to porewater collection[22], or filtered in-line during pumping[10]. The Minipoint sampler allows high-resolution porewater extraction, which is difficult to achieve with other piezometer methods[14].

3.3.1.3.2 Disadvantages:

Minipoint sampler installation success is heavily dependent on sediment type, with deployment in gravel sediments sometimes impractical or if deployment is achievable, preventing accurate spacing of the Minipoint piezometers. The relatively large sampler footprint[13], resulting in samples from different depths not being vertically aligned, may result in inaccurate vertical profiles where small-scale heterogeneity in sediment properties occur. Porewater samples must be extracted from Minipoint samplers at a low rate to prevent porewater being drawn from outside of the intended sampling depth, and to prevent changes in preferential flow, in order to preserve the high spatial resolution. It is not possible to dip-meter Minipoint samplers and so

no information on vertical hydraulic gradients can be yielded from them. Additionally, although requiring further investigation, the evidence presented in this study suggests that Minipoints may underestimate NH_4^+ concentrations.

3.3.2 Passive Equilibration Samplers

3.3.2.1 DET gel probes

DET gel probes[45,46] are passive samplers consisting of a polyacrylamide hydrogel[47], which is ~95% water, between ~0.4 to 1.8 mm thick and housed in a plastic probe[28,45]. DET gels are typically supplied in a $NaNO_3$ buffer, therefore, if to be utilised for NO_3^- sampling, it is necessary to request a buffer of NaCl. Porewater is not extracted to obtain a sample, instead solutes diffuse across the DET gel membrane, into and out of the gel, until equilibrium with the porewater is reached. The gel is then removed from the sediment, sliced at the required vertical resolution, and placed into a vial. The gel is processed in the laboratory by weighing the gel (to determine the volume of water in the gel) and back-equilibrating with a known volume of ultrapure water[20,48]. The concentration in the resulting solution is determined and this, along with the volume of water in the gel slice and added during back-equilibration, is used to determine the concentration of solute in the DET gel slice and hence, the porewater. Commercially available DET gels are typically 15 cm in length and so this vertical range is usually sampled, however, they have also been modified and used up to 30 cm (Figure 3.1)[28]. The vertical resolution attained by the DET gel is determined by the interval at which the gel is immediately sliced at upon removal from the sediment. DET gels are able to obtain a high vertical resolution of 1 cm, although 1 mm is also theoretically possible if slicing occurs after removal prior to vertical diffusion within the gel or if the DET gel is constrained at the desired resolution[20,28,49]. Recently, DET gels have been combined with colorimetry and hyperspectral imagery, which enables two-dimensional nitrite and nitrate distributions to be simultaneously measured at millimetre scale[21]. The footprint of the DET gel is small, ~0.5 cm

x 4 cm, preventing the gel samples from integrating biogeochemical patterns from a large area within the streambed. The DET gel probe is deployed into the sediment for at least 72 hours prior to sampling to allow natural conditions to re-establish and equilibrium with the porewater to be reached[28]. Due to the DET gel being an equilibration technique the samples collected represent a snapshot of conditions during equilibrium, and therefore, represent an average of the biogeochemical conditions over the past 1-2 hours depending on equilibrium times within the sediment. The nature of this technique means that all depths are sampled simultaneously.

3.3.2.1.1 Advantages:

The DET gel is a passive sampler, relying on equilibrium of solutes rather than physical extraction of porewater, which prevents alteration of preferential flow or crossover between depths from occurring during sampling. This vertical resolution is then maintained as long as the gel is sliced immediately after removal from the sediment. The DET gel sampler has a very high spatial resolution, up to 0.1-1 mm, although 1 cm is more common for streambed nutrient applications. The design of the gel results in any biogeochemical features lesser or equal to the slicing resolution being lost[46], and so the high spatial resolution is crucial to capturing detailed vertical solute profiles. Additionally, although requiring further investigation, the evidence presented in this study appears to suggest that DET gels capture weakly-bound NH_4^+, which piezometer-based methods may not.

3.3.2.1.2 Disadvantages:

Although the DET gel probes are easy to install in soft sediments, difficulty can arise in deployment in gravel sediments, although Ullah et al. (2012)[28] developed a stainless-steel installation device and successfully deployed the DET gel probes in an armoured gravel bed. As the DET gel probe is not a piezometer, no information on vertical hydraulic gradient or hyporheic flow can be ascertained from the device, and so information is limited to

biogeochemistry alone. The DET gel should be left for at least 72 hours[28] after installation before it is removed from the sediment, which requires some planning prior to sampling. This 72 hours is suggested to allow the natural conditions to re-establish around the gel, and for the gel to then equilibrate with the surrounding porewater, before removal. Furthermore, as the DET gel is not partitioned, vertical diffusion within the gel is possible, especially once removed from the porewater environment. It is crucial, therefore, to slice or fix the DET gel immediately after removal. If this is not achieved before equilibrium within the DET gel itself, then the vertical profile may be smoothed across slicing intervals[20,46]. The speed with which this is required depends on the slicing resolution, and it is possible to use a constrained DET gel with separate compartments at the desired resolution to avoid this issue.

3.4 Materials and Methods

3.4.1 In-situ field applications

3.4.1.1. Study site

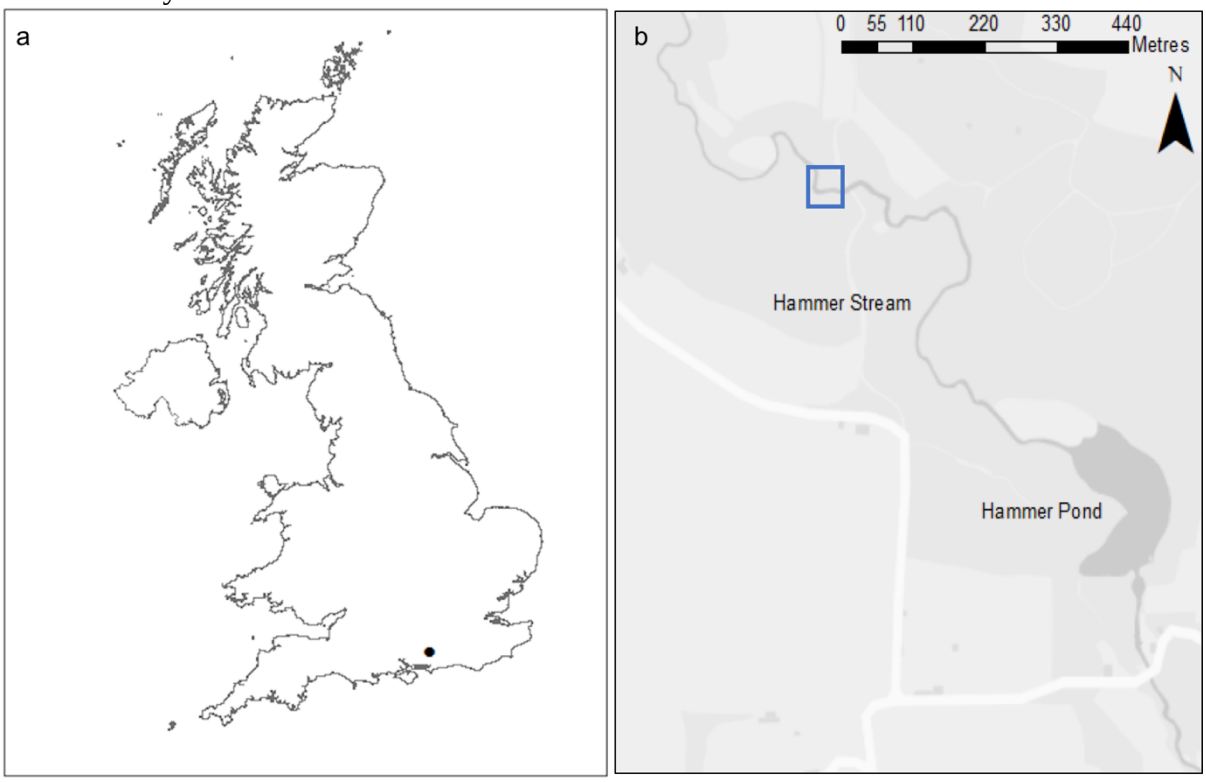

Figure 3.2. The location of a. the Hammer stream within the UK, and b. the study reach

(indicated by the blue rectangle) within the wider Hammer stream (contains Ordnance Survey data).

The field comparison of the different experimental methods in this study focussed on the Hammer Stream in West Sussex, UK, (Figure 3.2) which drains a 24.6 km^2 sandstone and mudstone catchment (BGS 2016). Land-use within the catchment is predominantly agricultural, with smaller patches of deciduous broad-leafed woodland present (BGS 2016). The application of the different field sampling methods focussed on an approximately 40 m meandering reach of the stream, where the streambed was dominated by spatially-homogeneous, sandy sediment[24].

3.4.1.2 Field methods

Porewater samples for the field analysis were collected between 16th June and 9th July 2015 from 40 multilevel piezometers, 32 Minipoints and 21 DET gels. Multi-level piezometers were installed more than 1 year in advance, Minipoints were installed on the day of sampling and DET gels were deployed at least 6 days prior to removal. Porewater samples of 50 ml were manually collected from the multilevel piezometers at depths of 10, 20, 30, 50 and 100 cm using syringes, and by slow pumping rates with a multi-channel peristaltic pump from the Minipoints (20 ml) at depths of 0, 2.5, 5, 7.5, 10, 12.5 and 15 cm (Figure 3.1). All samples were subsequently filtered on site (0.45 μm Whatman) into acid-washed (10% HCl) vials. The DET gels were removed one at a time over a 90-minute duration, and sliced at 5 cm intervals (ultrapure water-rinsed blade on an acid-washed (10% HCl) chopping board) within 5 minutes of removal. The DET gel slices were stored in acid-washed (10% HCl) centrifuge tubes at 4°C, and the porewater samples were frozen, until laboratory analysis.

3.4.1.3 Laboratory processing

3.4.1.3.1 DET gels

The gels were weighed and 5 ml of ultrapure (18.2 MΩ) water added to each tube. The gels were then shaken, on ice, for 20 hours, after which, the gels were removed and the resulting solution frozen for storage until analysis.

All porewater samples were analysed for nitrate and ammonium concentration using a continuous flow analyser (Skalar San++), with an LOD of 0.02 mg N l^{-1} for ammonium and nitrate. The accuracy and precision was 0.1 and ±0.02 mg NH_4^+-N l^{-1} and 0.14 and ±0.01 mg NO_3^--N l^{-1}, respectively.

3.4.2 Laboratory Experiment

Fine, sand-dominated sediment was collected from the Mill Brook at the Birmingham Institute of Forest Research (BIFoR) facility in May 2016. The sediment was sieved (16 mm), homogenised and placed into three separate buckets. Solutions of varying concentrations (0.0, 4.9 and 10.0 mg NH_4^+ l^{-1}) were made from a stock of NH_4Cl and added to the buckets, and DET gels and multilevel mini-piezometers, with sampling depths of 2.5, 7.5 and 12.5 cm, were installed into the sediment. After 3 days, the DET gels were removed and sliced at 5 cm intervals, and the mini-piezometers were sampled. Porewater samples were stored frozen until analysis. The DET gels were processed as detailed previously.

3.5 Results and discussion

3.5.1 Field Study

3.5.1.1 Nitrate

The nitrate depth profiles observed from the three techniques varied greatly (Figure 3.3); the nitrate concentrations in the piezometers were predominantly low (<3 mg l^{-1}), and the DET gels showed the largest variation in concentration, with the largest nitrate concentrations found with this technique (25.5 and 34.2 mg l^{-1}). The Minipoints, however, showed the largest consistent variation in nitrate concentration, with little bias towards low

concentrations, which was seen in the piezometers, and the DET gels to a lesser extent.

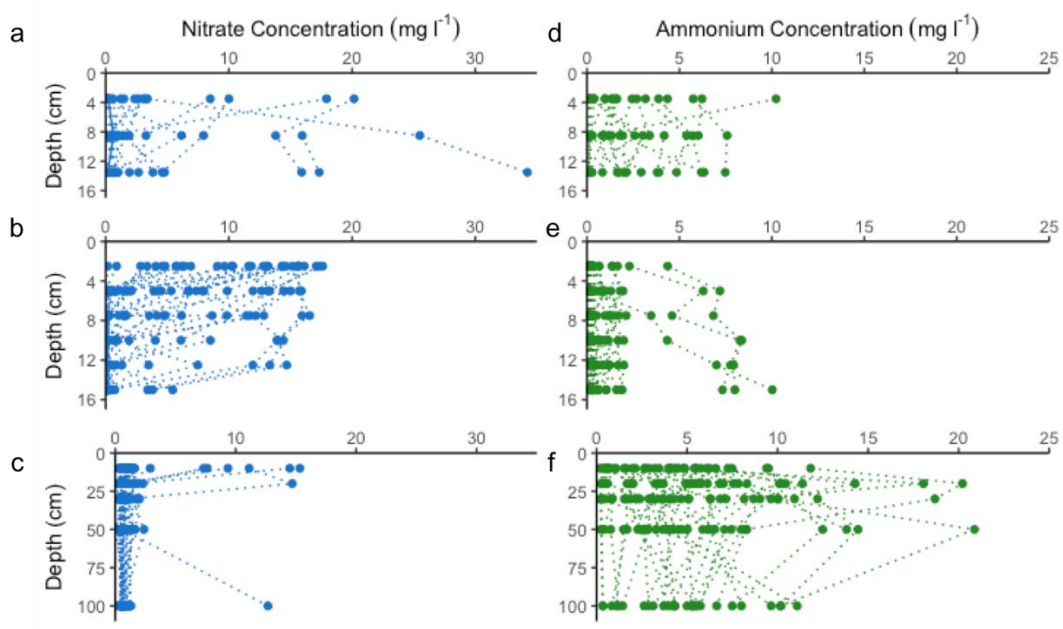

Figure 3.3. Vertical profiles of nitrate concentration (mg l^{-1}) in the streambed of the Hammer Stream, Sussex, UK in a. DET gels, b. Minipoint samplers and c. multilevel mini-piezometers and vertical profiles of ammonium concentration (mg l^{-1}) in the streambed of the Hammer Stream, Sussex, UK in d. DET gels, e. Minipoint samplers and f. multilevel mini-piezometers.

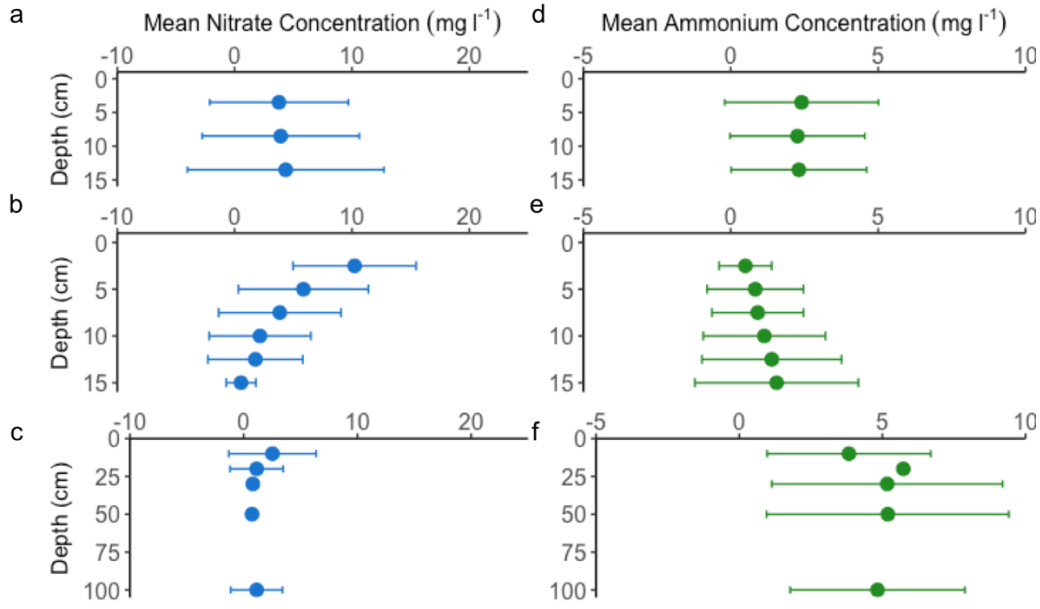

Figure 3.4. Mean nitrate concentrations (mg l^{-1}) ±1 standard deviation found at each sampled depth in the streambed of the Hammer Stream, Sussex, UK in a. DET gels, b.

Minipoint samplers and c. multilevel mini-piezometers and mean ammonium concentrations (mg l^{-1}) ±1 standard deviation found at each sampled depth in the streambed of the Hammer Stream, Sussex, UK in d. DET gels, e. Minipoint samplers and f. multilevel mini-piezometers.

Observed average nitrate concentrations per depth were between 3.78 and 4.34, 0.54 and 10.2, and 0.73 and 2.53 mg l^{-1}, for the DET gels, Minipoints and piezometers, respectively (Figure 3.4). Lower average concentrations were observed in the Minipoints and piezometers than in the DET gels. The Minipoints, therefore, captured the greatest range of average concentrations, over 9.67 mg l^{-1}, compared to only 0.56 and 1.79 mg l^{-1} in the DET gels and piezometers, respectively. There was, however, no statistically significant difference in nitrate concentrations between the methods used (Table 3.S-1), although care should be taken when comparing results obtained from different sampling methods, as these can be heavily dependent on how samples were collected. Passive and active sampling techniques, for example, may lead to differences in the porewater collected.

For a more direct comparison of the methods only data from the top 15 cm was considered. The highest average nitrate concentration (4.08 mg NO_3^- l^{-1}) was observed in the Minipoints, which was slightly higher than that of the DET gels (4.02 mg NO_3^- l^{-1}). The lowest average nitrate concentration (2.53 mg NO_3^- l^{-1}) was observed in the piezometers. This was perhaps due to nitrate generally decreasing with depth in the upper 15 cm (Figure 3.3), and the piezometer setup used was unable to sample at the shallowest depths. The DET gels captured the largest array of nitrate concentrations with a standard deviation, variance and range of 6.97, 48.6 and 34.2 mg NO_3^- l^{-1}, respectively (Table 3.S-2). The piezometers captured the lowest variation of nitrate concentrations, which was probably due to their restriction to one depth (10 cm) in the upper 15 cm of sediment, with a standard deviation, variance and range of 3.84, 14.8 and 15.0 mg NO_3^- l^{-1}, respectively. The standard deviation and variance of the Minipoint data was slightly lower than that of the DET gels (5.51 and 30.4 mg NO_3^- l^{-1},

respectively), while the range was closer to that of the piezometer data (17.6 mg NO_3^- l^{-1}). There was, however, no statistically significant difference in nitrate concentrations in the upper 15 cm between the methods used (Table 3.S-1).

The clearest trend in average nitrate concentration with depth was observed in the Minipoint data, where nitrate decreased non-linearly with depth, from 10.2 to 0.54 mg l^{-1} over a depth interval of 2.5 to 15 cm. The small concentration ranges captured by the DET gels and piezometers resulted in no real trend with depth in the DET gels (3.78 to 4.34 mg l^{-1} from 3.5 to 13.5 cm depth) and only a weak trend with depth in the piezometers (2.53 to 1.13 mg l^{-1} from 10 to 100 cm depth), although this pattern was similar to that observed in the Minipoints. In sandy or fine grained sediments, characteristic of the study site, the variability in concentration is usually greatest in the first few centimetres of the streambed[25–27]. The design of the multi-level piezometers used here, therefore, may have limited the ability of this method to fully capture the profiles seen in the Minipoints, where sampling was focussed in the first 15 cm. It is important to note that multilevel piezometers may be designed to sample at a finer resolution in the top 20 cm of the streambed, with an achievable sampling resolution of 5 cm. Here we used the more common setup of multilevel minipiezometers, with a coarser resolution and a greater depth range, to compare techniques as they are more generally used. The difference in profiles between the DET gels and the Minipoints was unexpected, given that both techniques sample the top 15 cm of the streambed at high resolution. It is possible that the difference in sampling resolution (2.5 cm in the Minipoints and 5 cm in the DET gels), caused some smoothing effect of the profiles, however, there should still have been a trend in the profile of the DET gels, which was not observed.

3.5.1.2 Ammonium

The ammonium depth profiles observed varied greatly between the three techniques (Figure 3.3); the ammonium concentrations in the Minipoints were predominantly low (<2.5 mg l^{-1}),

and the piezometers showed the largest variation in concentration (between 0.18 and 20.9 mg l^{-1}). The average ammonium concentrations observed per depth were between 2.26 and 2.40, 0.50 and 1.56, and 3.83 and 5.73 mg l^{-1}, for the DET gels, Minipoints and piezometers, respectively. The average concentrations in the Minipoints were lower than in the DET gels and piezometers, with the highest average concentrations observed in the piezometers (Figure 3.4). The piezometers and Minipoints captured relatively large ranges of average concentrations, 1.90 and 1.06 mg l^{-1}, respectively, compared to only 0.14 mg l^{-1} for the DET gels. The DET gels consistently measured larger concentrations than the Minipoints, at comparable depths, which may be due to the difference in sampling principles between these methods, as Minipoints are active samplers and DET gels are passive samplers (see laboratory experiment discussion below). The differences in ammonium concentrations between the three methods were statistically significant, and were significantly different in all three methods (Table 3.S-1).

For a more direct comparison of the three methods only data from the top 15 cm was considered. The highest average ammonium concentration (3.83 mg NH_4^+ l^{-1}) was observed in the piezometers, with the DET gels capturing the second highest average ammonium concentration (2.32 mg NH_4^+ l^{-1}). The lowest average ammonium concentration (1.05 mg NH_4^+ l^{-1}) was, therefore, observed in the Minipoints. This may be because ammonium increased with depth in the upper 15 cm in the Minipoints (Figure 3.3), and the piezometer setup used was only able to sample at 10 cm, which may result in the piezometers capturing the greater concentrations found at depth. The piezometer and DET gel data had similar, relatively large standard deviation and variance of 2.86 and 8.17, and 2.36 and 5.57 mg NH_4^+ l^{-1}, for the piezometers and DET gels, respectively (Table 3.S-2). The Minipoints captured the lowest standard deviation and variance of 1.98 and 3.90 mg NH_4^+ l^{-1}, respectively. The greatest range of ammonium concentration was found in the piezometers (11.6 mg NH_4^+ l^{-1}),

although the Minipoint and DET gel data were also similar (10.0 and 10.2 mg NH_4^+ l^{-1}, respectively). The DET gels captured larger average concentrations than the Minipoints, which sampled similar depths. This has been observed previously with co-located piezometers and DET gels, where ammonium concentrations were also greatest in the DET gels[28]. This was investigated further in the laboratory experiment discussed below. The differences in ammonium concentrations, in the upper 15 cm, between the three methods were statistically significant, and were significantly different in all three methods (Table 3.S-1). Although significant differences between the methodologies were observed, as mentioned above, care should be taken when comparing the results gained from differing sampling techniques.

The clearest trend in average ammonium concentration with depth was observed in the Minipoint data, where concentrations increased linearly with depth from 0.50 to 1.56 mg l^{-1} over a depth of 2.5 to 15 cm. The small concentration range captured by the DET gels resulted in no real trend with depth in the DET gels (2.40 to 2.31 mg l^{-1} from 3.5 to 13.5 cm depth). Although there was no concentration trend with depth in the piezometers (3.83 to 4.83 mg l^{-1} from 10 to 100 cm depth), there was a general increase in ammonium concentration up to 50 cm (to 5.19 mg l^{-1}), followed by a decrease from 50 to 100 cm depth. The lack of trend in both ammonium and nitrate concentrations with depth observed in the DET gels was unexpected, especially given that DET gels have previously been used to capture biogeochemically active zones within sediment[28,29]. Furthermore, the upper 15 cm of the streambed sampled by the DET gels typically has the greatest biogeochemical variation and the Minipoints captured clear vertical trends over the same depth. The piezometers captured the greatest range of ammonium concentration, which was unexpected given that they predominantly sampled at depths greater than 20 cm.

3.5.2 Laboratory Experiment

The ammonium concentrations observed in the DET gels were predominantly greater than those observed in the multilevel mini-piezometers (Figure 3.5), which has been observed previously[28]. Two samples at 2.5 cm depth in the high concentration solution, however, had ammonium concentrations which were slightly greater in the piezometer than in the DET gel (2.13 and 1.55, and 1.99 and 1.47 mg l^{-1}, in the piezometers and the DET gels, respectively). A comparison of the mean ammonium concentration at each depth from the DET gels and the multilevel mini-piezometers showed that the concentration in the DET gels was statistically significantly greater than in the multilevel mini-piezometers at all depths (Table 3.S-3, p-values between 0.00 and 0.02, Figure 3.6). To confirm this difference was not a result of ammonium contained within the DET gels themselves, we allowed new DET gels to equilibrate in ultrapure (18.2 MΩ) water. This gave ammonium concentrations below detection and confirmed that the DET gels were not a source of ammonium. We believe that the discrepancy between techniques, between 31 and 56% over the different depths in this experiment, is due to the differing nature of these methods and not an experimental artefact. The DET gel is a passive, diffusive equilibrium sampler, which is in contact with the sediment, whereas, the piezometers are active samplers relying on a negative pressure or pumping action to sample the porewater. We suggest, therefore, that the DET gels (and other passive techniques) are able to capture highly sorptive ammonium from sediment surfaces, whereas the piezometers (or any active technique relying on the extraction of porewater via pumping or a syringe) only sample the 'free' porewater, potentially not capturing the residual water (and any solutes therein) that is bound to sediment surfaces.

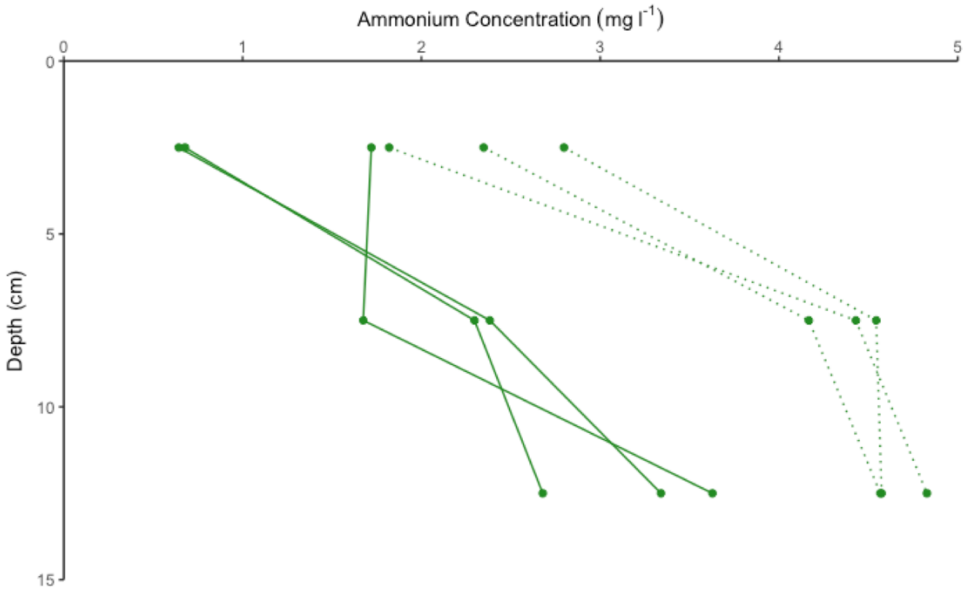

Figure 3.5. Vertical profiles of ammonium concentration (mg l^{-1}) for all data from the laboratory experiments, with the piezometer data plotted with a solid line and the DET gel data plotted with a dotted line.

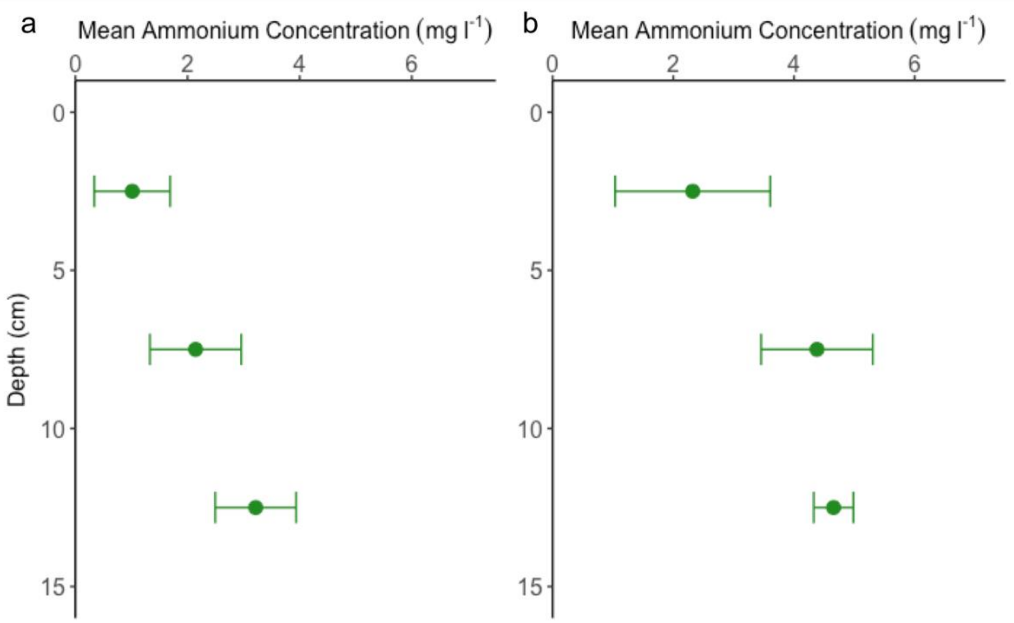

Figure 3.6. Mean ammonium concentrations (mg l^{-1}) ±1 standard deviation found at each sampled depth in the laboratory experiments in a. multilevel mini-piezometers and b. DET gels

3.6 Conclusions

As interest in streambed biogeochemistry continues to increase, along with the volume of interdisciplinary research conducted in the HZ, the development of standard sampling protocols and further sampling methods is required. Although samplers such as Minipoints and DET gels provide high-resolution nutrient profiles in the upper few centimetres of the streambed, where the majority of the biogeochemistry occurs, multilevel and single well piezometers remain a valuable tool for the investigation of deeper influences of groundwater and larger scale processes. Furthermore, the sampling method used may significantly affect the resulting ammonium concentrations, and may produce differences in vertical trends in both nitrate and ammonium. The research question, and desired spatial and temporal resolution will, therefore, determine which sampling technique is most appropriate to use, with each one characterised by specific advantages and limitations.

3.7 Acknowledgements

This research was funded by The Leverhulme Trust project “Where rivers, groundwater and disciplines meet: A hyporheic research network”, and from the authors’ institutions. The authors would like to thank the Leverhulme project team for their help, guidance and insight.

3.8 References

1. Boano, F. *et al.* Hyporheic flow and transport processes: Mechanisms, models, and bioghemical implications. *Rev. Geophys.* 1–77 (2014). doi:10.1002/2012RG000417.Received
2. Harvey, J. W. & Gooseff, M. River corridor science: Hydrologic exchange and ecological consequences from bedforms to basins. *Water Resour. Res.* **51,** 6893–6922 (2015).
3. Krause, S. *et al.* Inter-disciplinary perspectives on processes in the hyporheic zone. **499,** 481–499 (2011).
4. Krause, S., Boano, F., Cuthbert, M. O., Fleckenstein, J. H. & Lewandowski, J. Understanding process dynamics at aquifer-surface water interfaces: An introduction to the special section on new modeling approaches and novel experimental technologies. *Water Resour. Res.* **50,** 1847–1855 (2014).
5. Lautz, L. K. & Fanelli, R. M. Seasonal biogeochemical hotspots in the streambed around restoration structures. *Biogeochemistry* **91,** 85–104 (2008).
6. McClain, M. E. *et al.* Biogeochemical Hot Spots and Hot Moments at the Interface of Terrestrial and Aquatic Ecosystems. *Ecosystems* **6,** 301–312 (2003).
7. Fischer, H., Kloep, F., Wilzcek, S. & Pusch, M. T. A river's liver - Microbial processes within the hyporheic zone of a large lowland river. *Biogeochemistry* **76,** 349–371 (2005).
8. Brunke, M. & Gonser, T. The ecological significance of exchange processes between rivers and groundwater. *Freshw. Biol.* **37,** 1–33 (1997).
9. Boulton, A. J., Findlay, S., Marmonier, P., Stanley, E. H. & Valett, H. M. The Functional Significance of the Hyporheic Zone in Streams and Rivers. *Annu. Rev. Ecol. Syst.* **29,** 59–81 (1998).

10. Harvey, J. W., Böhlke, J. K., Voytek, M. a., Scott, D. & Tobias, C. R. Hyporheic zone denitrification: Controls on effective reaction depth and contribution to whole-stream mass balance. *Water Resour. Res.* **49,** 6298–6316 (2013).

11. Kalbus, E., Reinstorf, F. & Schirmer, M. Measuring methods for groundwater – surface water interactions: a review. *Hydrol. Earth Syst. Sci* **10,** 873–887 (2006).

12. Rivett, M. *et al.* Cost-effective mini drive-point piezometers and multilevel samplers for monitoring the hyporheic zone. *Q.J.Eng.Geol.Hydrogeol.* **41,** 49–60 (2008).

13. Duff, J. H. *et al.* A mini drivepoint sampler for measuring pore water solute concentrations in the hyporheic zone of sand-bottom streams. *Limnol. Ocean.* **43,** 1378–1383 (1998).

14. Harvey, J. W. & Fuller, C. C. Effect of enhanced manganese oxidation in the hyporheic zone on basin-scale geochemical mass balance. *Water Resour. Res.* **34,** 623 (1998).

15. Bou, C. & Rouch, R. Un nouveau champ de recherches sur la faune aquatique souterraine. *Cr Acad Sci* **265,** 369–370 (1967).

16. Conant, B., Cherry, J. A. & Gillham, R. W. A PCE groundwater plume discharging to a river: Influence of the streambed and near-river zone on contaminant distributions. *J. Contam. Hydrol.* **73,** 249–279 (2004).

17. Hunt, G. W. & Stanley, E. H. An evaluation of alternative procedures using the Bou-Rouch method for sampling hyporheic invertebrates. *Can. J. Fish. Aquat. Sci.* **57,** 1545–1550 (2000).

18. Krause, S., Tecklenburg, C., Munz, M. & Naden, E. Streambed nitrogen cycling beyond the hyporheic zone: Flow controls on horizontal patterns and depth distribution of nitrate and dissolved oxygen in the upwelling groundwater of a lowland river. *J. Geophys. Res. Biogeosciences* **118,** 54–67 (2013).

19. Palmer, M. A., Strayer, D. L. & Rundle, S. D. Meiofauna. 415–433 (2006). doi:10.1016/B978-0-12-332908-0.50027-9

20. Krom, M. ., Davison, P., Zhang, H. & Davison, W. High-resolution pore-water sampling with a gel sampler. (1994).

21. Metzger, E. *et al.* Simultaneous Nitrite/Nitrate Imagery at Millimeter Scale through the Water–Sediment Interface. *Environ. Sci. Technol.* acs.est.6b00187 (2016). doi:10.1021/acs.est.6b00187

22. Sanders, I. A. & Trimmer, M. In situ application of the $15NO_3^-$- isotope pairing technique to measure denitrification in sediments at the surface water-groundwater interface. *Limnol. Oceanogr. Methods* **4,** 142–152 (2006).

23. Survey, B. G. British Geological Survey. (2016) BGS 1:50,000 [Shapefile geospatial data], Scale 1:50,000,. Retrieved from http://edina.ac.uk/digimap.

24. Shelley, F., Klaar, M., Krause, S. & Trimmer, M. Enhanced hyporheic exchange flow around woody debris does not increase nitrate reduction in a sandy streambed. *Biogeochemistry* **136,** 1–20 (2017).

25. Knapp, J. L. A. *et al.* Tracer-based characterization of hyporheic exchange and benthic biolayers in streams. *Water Resour. Res.* **53,** 1575–1594 (2017).

26. Battin, T. J., Kaplan, L. A., Newbold, J. D. & Hansen, C. M. E. Contributions of microbial biofilms to ecosystem processes in stream mesocosms. *Nature* **426,** 439–442 (2003).

27. O'Connor, B. L. & Harvey, J. W. Scaling hyporheic exchange and its influence on biogeochemical reactions in aquatic ecosystems. *Water Resour. Res.* **44,** 1–17 (2008).

28. Ullah, S. *et al.* In situ measurement of redox sensitive solutes at high spatial resolution in a riverbed using Diffusive Equilibrium in Thin Films (DET). *Ecol. Eng.* **49,** 18–26 (2012).

29. Comer-Warner, S. A. *et al.* Opening Opportunities for High-Resolution Isotope Analysis - Quantification of $\delta^{15}N_{NO3^-}$ and $\delta^{18}O_{NO3^-}$ in Diffusive Equilibrium in Thin–Film Passive Samplers. *Anal. Chem.* **89,** 4139–4146 (2017).

30. Grimm, N. B., Baxter, C. V. & Crenshaw, C. L. in *Methods in Stream Ecology* (eds. Hauer, F. R. & Lamberti, G. A.) 761–782 (Elsevier Inc., 2007). doi:10.1016/B978-012332908-0.50046-2

31. Dahm, C. N., Maurice Valett, H., Baxter, C. V. & Woessner, W. W. in *Methods in Stream Ecology* (eds. Hauer, F. R. & Lamberti, G. A.) 119–142 (Elsevier Inc., 2007). doi:10.1016/B978-012332908-0.50008-5

32. Lewandowski, J., Meinikmann, K., Nützmann, G. & Rosenberry, D. O. Groundwater - the disregarded component in lake water and nutrient budgets. Part 2: Effects of groundwater on nutrients. *Hydrol. Process.* **29,** 2922–2955 (2015).

33. Käser, D. H., Binley, A., Heathwaite, A. L. & Krause, S. Spatio-temporal variations of hyporheic flow in a riffle-step-pool sequence. *Hyrological Process.* **23,** 2138–2149 (2009).

34. Krause, S., Louise Heathwaite, a., Binley, A. & Keenan, P. Nitrate concentration changes at the groundwater-surface water interface of a small Cumbrian river. *Hydrol. Process.* **23,** 2195–2211 (2009).

35. Winter, T. C., Harvey, J. W., Franke, O. L. & Alley, W. M. in *Ground Water and Surface Water: A Single Resource* (eds. Winter, T. C., Harvey, J. W., Franke, O. L. & Alley, W. M.) 3–32 (U.S. Government Printing Office, 1998).

36. Blume, T., Krause, S., Meinikmann, K. & Lewandowski, J. Upscaling lacustrine groundwater discharge rates by fiber-optic distributed temperature sensing. *Water Resour. Res.* **49,** 7929–7944 (2013).

37. Johnson, A. *et al.* The role of microbial community composition and groundwater

chemistry in determining isoproturon degradation potential in UK aquifers. **49,** 71–82 (2004).

38. Lapworth, D. J., Gooddy, D. C., Allen, D. & Old, G. H. Understanding groundwater, surface water, and hyporheic zone biogeochemical processes in a Chalk catchment using fluorescence properties of dissolved and colloidal organic matter. *J. Geophys. Res.* **114,** G00F02 (2009).

39. *Technical Guidance Manual for Ground Water Investigations: Ground Water Sampling*. (n.d.). Retrieved from http://www.epa.ohio.gov/Portals/28/documents/TGM-10_final0512W.pdf.

40. Gooddy, D. C., Macdonald, D. M. J., Lapworth, D. J., Bennett, S. A. & Griffiths, K. J. Nitrogen sources, transport and processing in peri-urban floodplains. *Sci. Total Environ.* **494–495,** 28–38 (2014).

41. Heppell, C. *et al.* Interpreting spatial patterns in redox and coupled water–nitrogen fluxes in the streambed of a gaining river reach. *Biogeochemistry* **117,** 491–509 (2013).

42. Krause, S., Hannah, D. . & Blume, T. Interstitial pore-water temperature dynamics across a pool-riffle-pool sequence. *Ecohydrology* **4,** 549–563 (2011).

43. Lansdown, K. *et al.* The interplay between transport and reaction rates as controls on nitrate attenuation in permeable, streambed sediments. *J. Geophys. Res. G Biogeosciences* **120,** 1093–1109 (2015).

44. Gassen, N., Griebler, C., Werban, U., Trauth, N. & Stumpp, C. High Resolution Monitoring above and below the Groundwater Table Uncovers Small-Scale Hydrochemical Gradients. *Environ. Sci. Technol.* **51,** 13806–13815 (2017).

45. Davison, W., Grime, G. W., Morgan, J. A. W. & Clarke, K. Distribution of dissolved iron in sediment pore waters at submillimetre resolution. *Nature* **352,** 323–325 (1991).

46. Harper, M. P., Davison, W. & Tych, W. Temporal, Spatial, and Resolution Constraints for in situ Sampling Devices Using Diffusional Equilibration : Dialysis and DET. *Environ. Sci. Technol.* **31,** 3110–3119 (1997).

47. Davison, W. & Zhang, H. In-situ speciation measurements of trace components in natural waters using thin-film gels. *Nature* **237,** 546–548 (1994).

48. Mortimer, R. J. ., Krom, M. ., Hall, P. O. ., Hulth, S. & Ståhl, H. Use of gel probes for the determination of high resolution solute distributions in marine and estuarine pore waters. *Mar. Chem.* **63,** 119–129 (1998).

49. Docekalova, H., Clarisse, O., Salomon, S. & Wartel, M. Use of constrained DET probe for a high-resolution determination of metals and anions distribution in the sediment pore water. **57,** 145–155 (2002).

3.9 SI

Table 3.S-1. Statistical test results from all data from the Hammer stream, UK, where the Kruskal-Wallis rank sum test indicated a significant difference between the methods, a Dunn test was used to determine which groups were significantly different.

Groups	p-value	d.f.	Test
Nitrate	0.54	2	Kruskal-Wallis rank sum
Ammonium	**$2.2x10^{-16}$**	2	Kruskal-Wallis rank sum
DET-Minipoint	**$1.21x10^{-5}$**	-	Dunn Test
DET-Piezometer	**$1.84x10^{-6}$**	-	Dunn Test
Minipoint-Piezometer	**$2x10^{-38}$**	-	Dunn Test
Nitrate (15 cm)	0.27	2	Kruskal-Wallis rank sum
Ammonium (15 cm)	**$2.08x10^{-14}$**	2	Kruskal-Wallis rank sum
DET-Minipoint (15 cm)	**1.4x10-6**	-	Dunn Test
DET-Piezometer (15 cm)	**$9.36x10^{-3}$**	-	Dunn Test
Minipoint-Piezometer (15 cm)	**$3.65x10^{-12}$**	-	Dunn Test

Table 3.S-2 – Descriptive statistics for all data from the DET gels, Minipoints and multilevel mini-piezometers sampled in the Hammer Stream, Sussex, UK

	Nitrate (mg l^{-1})				Ammonium (mg l^{-1})			
Method	**Mean**	**Standard Deviation**	**Variance**	**Range**	**Mean**	**Standard Deviation**	**Variance**	**Range**
Multilevel mini-piezometer	2.53	3.84	14.75	15.00	3.83	2.86	8.17	11.64
Minipoint	4.08	5.51	30.35	17.62	1.05	1.98	3.90	10.02
DET gel	4.02	6.97	48.58	34.23	2.32	2.36	5.57	10.18

Table 3.S-3 – Statistical test results from all data from the laboratory experiments, p-values <0.05 show a significant difference between the DET gel and piezometer data at that depth.

Groups	p-value	d.f.	Test
DET gel v piezometer 2.5 cm	**0.02**	-	Wilcoxon signed rank
DET gel v piezometer 7.5 cm	**0.02**	-	Wilcoxon signed rank
DET gel v piezometer 12.5 cm	**$2.39x10^{-4}$**	8	Paired t-test

Chapter 4: Thermal sensitivity of CO_2 and CH_4 emissions varies with streambed sediment properties

Sophie A. Comer-Warner[1], Paul Romeijn[1†], Daren C. Gooddy[2], Sami Ullah[1], Nick Kettridge[1], Benjamin Marchant[2], David M. Hannah[1] and Stefan Krause[1]

1. School of Geography, Earth and Environmental Sciences, University of Birmingham, Edgbaston, Birmingham, B15 2TT, UK

2. BGS, Maclean Building, Wallingford, Oxfordshire, OX10 8BB, UK.

†Joint first authorship

This chapter is published in Nature Communications (https://doi.org/10.1038/s41467-018-04756-x).

4.1 Abstract

Globally, rivers and streams are important sources of carbon dioxide and methane, with small rivers contributing disproportionately relative to their size. Previous research on GHG emissions from surface water lacks mechanistic understanding of contributions from streambed sediments. We hypothesise that streambeds, as known biogeochemical hotspots, significantly contribute to the production of GHGs. With global climate change, there is a pressing need to understand how increasing streambed temperatures will affect current and future GHG production. Current global estimates assume exponential and linear relationships between temperature and GHG emissions from surface water. Here we show non-linearity and threshold responses of streambed GHG production to warming. We reveal that temperature sensitivity varies with substrate (of variable grain size), OM content and geological origin. Our results confirm that streambeds, with their non-linear response to projected warming, are integral to estimating freshwater ecosystem contributions to current and future global GHG emissions.

Carbon fluxes from freshwaters, particularly rivers and streams, have been largely overlooked, as these were conceptualised as unreactive 'pipelines' transporting water from terrestrial to marine environments[1–4]. However, up to 50% of carbon is lost annually from inland waters through gas exchange as CO_2[5–7], returning 0.8 Pg of carbon directly to the atmosphere[1]. Previous research has mainly quantified surface water contributions[8–11] estimating global fluxes from streams and rivers to be 1.8 Pg CO_2-C yr^{-1} [8], and 26.8 Tg CH_4-C yr^{-1} [12]. Small streams appear to be particularly important, contributing ~15% of the CO_2 flux[8]. Although the CH_4 flux is dwarfed by that for CO_2, CH_4 fluxes may be regionally significant, and are seen to offset over 25% of the terrestrial C sink when considered as C equivalents[13–15]. Streambeds have been identified as 'hotspots' of carbon turnover[5,16–18], characterised by enhanced metabolic activity and nutrient spiralling[19–23]. GHG concentrations in streambeds are elevated with respect to surface waters, and concentrations between 71 nmol CH_4 l^{-1} [24] and 134 μmol CH_4 l^{-1} [25], and 130 μmol CO_2 l^{-1} [26] to 5 mmol CO_2 l^{-1} [27] have been observed in sediment porewaters. Despite recent advances in analysing freshwater carbon cycling, the spatially and temporally variable drivers of enhanced GHG production in streambed sediments, CH_4:CO_2 ratios and the relative importance of sediment GHG to overall C emissions[2,5,7,28,29] remain insufficiently understood[1,5,7].

Temperature is the prime control of biogeochemical processing rates and exponential and linear correlations between water temperature and GHG production have been observed previously over a large temperature range[28,30]. Additionally, long-term warming has been shown to increase CH_4 emissions, and decrease CO_2 absorption and carbon sequestration in small ponds[31]. The impact of temperature on sediment C cycling and GHG production is likely to vary for streambed sediments of different geological origin, substrate, OM and nutrient content. Initial research suggests the potential of substantial GHG production from fine and organic carbon-rich sediments[28,32,33], but didn't allow for any systematic analysis of

sediment controls on GHG production. It is expected that temperature increases will be particularly important in agricultural lowland rivers and streams representing large areas of Europe, North America and Asia[34], which are characterised by excess nutrient loadings and OM-rich, fine sediments[12].

Herein, we investigate the temperature impacts on streambed sediment aerobic microbial metabolic activity (MMA) and GHG production, along a gradient of OM content in streambed sediments of different geological origin. Geological origin was investigated as different geologies have varying biogeochemical properties and, therefore, are expected to have different GHG production rates. We incubated three substrates of differing grain size: Fine (silt-dominated underneath vegetation), medium (sand-dominated from unvegetated zones) and coarse (gravel-dominated from unvegetated zones) from the River Tern and River Lambourn - two agricultural, lowland, UK streams of contrasting geology (Sandstone and Chalk, respectively, Figure 4.1).

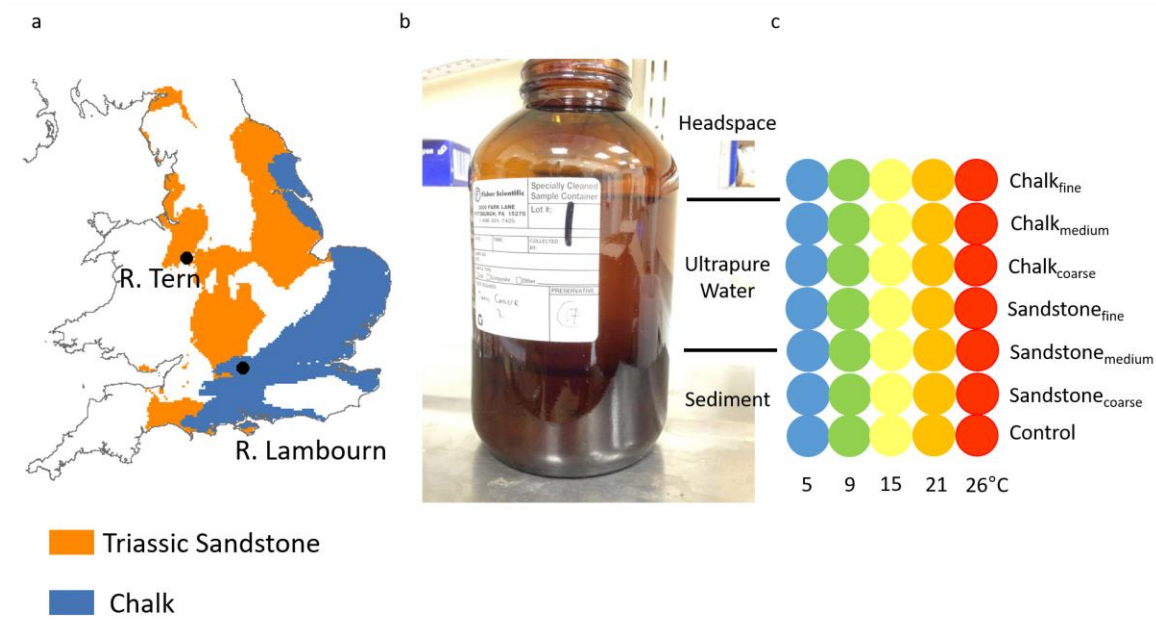

Figure 4.1a. Map of England and Wales, UK, showing the spatial distribution of Triassic Sandstone and Chalk aquifers, and the two study streams (River Tern and River Lambourn) [Contains BGS materials Copyright NERC [2016] and gadm.org]. b. Incubation bottle used

for the experiment, including a depiction of the distribution of sediment, water and headspace. C. Experimental setup with each dot representing a triplicate of repeats.

Sandstone and carbonate were investigated as these are the dominant aquifer materials of the globe, therefore, allowing any conclusions to be more generally applied. Incubation experiments were performed in triplicate at 5, 9, 15, 21 and 26 °C, with the potential GHG production at 5 hours investigated here. The smart tracer resazurin (Raz)-Rru system was used as a proxy for aerobic MMA, so that Rru production represented MMA (see methodology for a detailed explanation)[35]. GHG samples were collected from the headspace of the incubation jars, and so fluxes measured here include both diffusive and ebullitive pathways.

4.2 Results and discussion

4.2.1 MMA

Details of the method and results of the statistical analysis are found in section 2.7 and Table 4.S-1. MMA results are presented as ng of Rru produced per μg of Raz added to the jar at time zero, all reported errors represent ± 1 standard deviation.

MMA increased significantly with temperature across all substrates (Figure 4.2, p-value = <0.01). MMA in $Chalk_{fine}$ increased by 1260% from 5 to 21°C, producing MMA rates 400% larger than the second highest production ($Chalk_{medium}$ at 21°C). The only other substantial activity was observed in $Sandstone_{fine}$ and $Chalk_{medium}$ sediments at higher temperatures, resulting in significantly greater MMA in fine sediments for both geologies (p-value = <0.01 for Chalk, and <0.01 for Sandstone). There was a significant increase in MMA with temperature in the fine sediments, compared with the control experiments. This was expected as fine sediments are predicted to have greater activities and there was a significant temperature-gradient across all sediment types. This was also the case for CO_2 and CH_4 production.

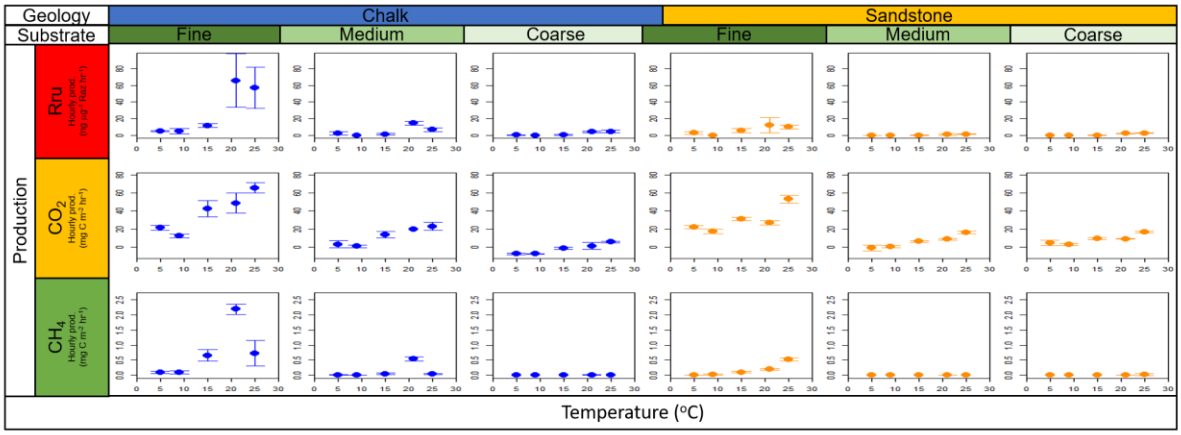

Figure 4.2. Hourly production of Rru, CO_2 and CH_4 plotted against temperature for each substrate type across the different geological origins (Triassic Sandstone, Chalk).

MMA was higher in $Chalk_{fine}$ than $Sandstone_{fine}$, despite the same OM content in both geologies (3.6%). We suggest that this is due to differences in the aromaticity of the carbon, which was 17.3% in $Chalk_{fine}$ and 20.9% in $Sandstone_{fine}$ sediments. Carbon in $Chalk_{fine}$ had a lower aromaticity, hence, the carbon was more bioavailable, producing greater MMA.

An exponential relationship between temperature and MMA, as reported previously to be consistent across ecosystems[36], was not observed in this study. Greater microbial metabolism was observed in $Chalk_{fine}$, $Chalk_{medium}$ and $Sandstone_{fine}$ sediments at 21°C than at 26°C. Anaerobic conditions may cause a reduction in MMA; but water column oxygen concentrations for $Chalk_{fine}$, $Chalk_{medium}$ and $Sandstone_{fine}$ sediments increased between 21°C and 26°C, thus oxygen concentration cannot explain the observed decrease in metabolism (SI, Figure 4.S-1).

OM content and geological origin had a substantial impact on MMA at higher temperatures (Figure 4.3). Most sediments exhibited low rates of MMA between 5 and 15°C, with only $Chalk_{fine}$ producing larger rates at 15°C (11.8±2.2 ng Rru μg^{-1} Raz hr^{-1}), indicating an onset of increased reactivity at 15°C in $Chalk_{fine}$. MMA was not significantly different between the two geologies (p-value = 0.14), however, MMA was greater in the Chalk sediments at 21 and 26°C. The difference in rates between geological origin was greater at 21 than 26°C

reflecting the higher MMA at 21°C (maximum of 65.7±32.1 ng Rru μg^{-1} Raz hr^{-1}) than 26°C (maximum of 56.8±24.7 ng Rru μg^{-1} Raz hr^{-1}) in the Chalk sediments. The metabolic rate was greatest in the fine sediments at higher temperatures, with the $Chalk_{fine}$ greater than the $Sandstone_{fine}$ at 21 and 26°C.

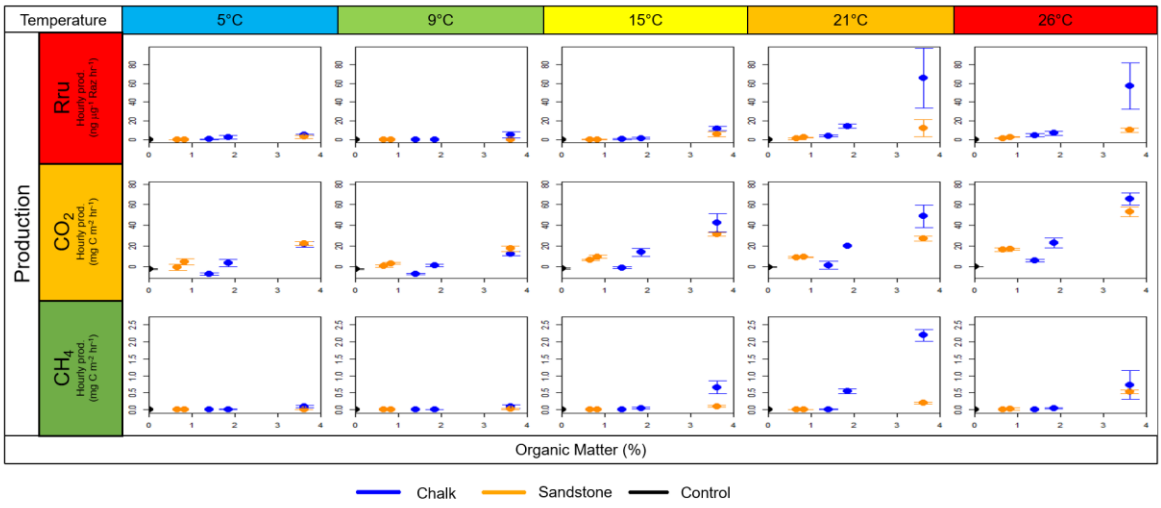

Figure 4.3. Hourly production of Rru, CO_2 and CH_4 plotted against OM content for each temperature.

Differences in small production rates produced unrealistic temperature coefficient (Q_{10}) values, therefore, only Q_{10} values where notable activity rates were observed, are discussed herein. This is also the case for the CO_2 and CH_4 discussions below.

Q_{10MMA} values generally ranged between 0.0 and 3.3 (SI, Table 4.S-4), confirming previously reported values[34,37]. High Q_{10MMA} values of 9.0 between 9 and 15°C in $Chalk_{fine}$, 22.2 between 15 and 21°C in $Chalk_{fine}$, and 1425.3 between 15 and 21°C in $Chalk_{medium}$ sediments, reflected the elevated respiration rates observed in these sediments at the given temperatures. The observed Q_{10MMA} value for $Chalk_{medium}$ between 15 and 21°C was substantially larger than previously reported values (above), which is due to insignificant rates of MMA at 15°C, followed by high rates at 21°C once the microbial community responded to the elevated temperature. These Q_{10MMA} values highlight the difference in temperature response between

geological origin, with large increases in respiration rates only observed in the Chalk sediments at higher temperatures.

4.2.2 CO_2 Production

Details of the results of the statistical analysis are found in Table 4.S-2. $Chalk_{fine}$ and $Sandstone_{fine}$ yielded the highest CO_2 production rates, with a 220 and 150% increase from 5 to 26°C, respectively, with a maximum potential CO_2 production rate of 65.6±5.9 mg C m^{-2} hr^{-1} observed in the $Chalk_{fine}$ sediment at 26°C. CO_2 production rates increased significantly with temperature across all substrates compared to the controls (Figure 4.2, p-value = <0.01). These results accord with the findings of previous research, which showed CO_2 production may increase linearly with rising temperatures, however, CO_2 production also increased exponentially with rising temperatures[28]. The relationship between temperature and potential CO_2 production observed in this study was linear and varied with substrate as previously seen[28], with significantly (p-value = <0.01 for Chalk, and <0.01 for Sandstone) greater production rates in fine sediments than in medium and coarse sediments. The CO_2 production rates did not vary greatly between $Chalk_{fine}$ and $Sandstone_{fine}$ sediments, which was expected given the similar OM content between these sediments (3.6%). However, the MMA was greater in $Chalk_{fine}$ than $Sandstone_{fine;}$ it has been noted that the CO_2 production rates did not mirror the Rru production rates observed, despite Rru production often used as a proxy for MMA. Somewhat surprisingly, in $Chalk_{coarse}$ at 5 and 9°C, negative production of CO_2 was observed under aerobic conditions, which may be due to two processes. Firstly, negative production of CO_2 may occur at a high pH due to the aqueous carbonate system acting as a CO_2 sink. This has been observed previously at pH greater than 8.5,[38] and the average pH of $Chalk_{coarse}$ at 5 and 9°C was 8.3±0.1, close to this threshold. It is possible, therefore, that the CO_2 produced here did not diffuse into the headspace, but remained in solution as carbonate. Secondly, the production rates were calculated from the difference in concentration between

0 and 5 hours. As $Chalk_{coarse}$ had such low headspace CO_2 concentrations, it is possible that CO_2 from the atmosphere dissolved into the water column at these low temperatures, reducing the CO_2 concentration in the headspace over time.

OM content and geological origin had a significant influence on potential CO_2 production rates, particularly at higher temperatures (Figure 4.3). Both streams had similar rates of CO_2 production for fine sediments, which significantly exceeded production rates in medium and coarse sediments. Slightly higher CO_2 production rates were found in the medium and coarse sediments of Sandstone than in Chalk, with an OM content below 2%. In general, CO_2 production was significantly greater in Chalk than Sandstone sediments (p-value = <0.01). At 15°C, $Chalk_{fine}$, $Chalk_{medium}$ and $Sandstone_{fine}$ responded to increased temperature with enhanced production rates compared to 9°C, indicating a threshold of 15°C was required to enhance biogeochemical processing in both geological settings. At 21°C, CO_2 production rates were similar to those at 15°C; with no substantial increase in production observed. Large increases in CO_2 production rates were observed at 26°C in the fine sediments to 65.6±5.9 mg C m^{-2} hr^{-1} for Chalk, and 53.1±4.7 mg C m^{-2} hr^{-1} for Sandstone. This is in contradiction to the observed MMA, which may indicate there is no metabolic reason for the observed decrease in MMA from 21 to 26°C. The difference between CO_2 production rates in the fine sediments decreased between 21 and 26°C.

Q_{10CO2} values generally ranged between 0.1 and 4.0 (SI, Table 4.S-4), which were similar to previously reported values in lake sediments[39]. Higher values indicated a greater temperature dependency in some cases, with Q_{10CO2} values of 8.1 for $Chalk_{fine}$ between 9 and 15°C, and 4.9 for $Sandstone_{fine}$ between 21 and 26°C. These Q_{10CO2} values highlight the difference in response of the two geological origins, with $Chalk_{fine}$ reacting to temperature increases earlier than $Sandstone_{fine}$ (15 and 26°C, respectively).

Potential CO_2 production rates ranging from approximately 70 to 156 nmol CO_2 g^{-1} hr^{-1}, from 9.73 to 25.31°C in sandy sediments, and 147 to 261 nmol CO_2 g^{-1} hr^{-1}, from 3 to 22°C in anoxic, fine sediments, have been observed previously[28,40]. These values for previous studies are greater than those observed here, where a range of 18 to 53 nmol CO_2 g^{-1} hr^{-1} in $Chalk_{fine}$, and 18 to 45 nmol CO_2 g^{-1} hr^{-1} in $Sandstone_{fine}$ from 5 to 26°C were observed. Different units are discussed above due to lack of available information to convert published values into mg m^{-2} hr^{-1}. The fine sediments were characterised by high carbon turnover rates of 82 days for Chalk and 105 days for Sandstone at 15°C (representative of the current climate). When warming was considered these rates became 71 days for Chalk and 122 days for Sandstone at 21°C, and 50 days for Chalk and 62 days for Sandstone at 26°C. Our findings, thus, indicate that the turnover time for sediment C could almost halve under future climates where streambed temperatures reach 26°C (representative of many Mediterranean streams), which bears severe consequences for biogeochemical cycling and nutrient spiralling in freshwater ecosystems.

4.2.3 CH_4 Production

Details of the results of the statistical analysis are found in Table 4.S-3. A maximum potential CH_4 production rate of 2.2±0.2 mg C m^{-2} hr^{-1} was observed in $Chalk_{fine}$ at 21°C. CH_4 production rates did not increase substantially with temperature across all substrates (Figure 4.2), which contrasts with observations of previous studies that report CH_4 fluxes to vary greatly with temperature across different ecosystems[30], although the increase was significant in all sediment types compared to the controls (p-value = <0.01). Instead, high CH_4 production was only observed in $Chalk_{fine}$, $Chalk_{medium}$ and $Sandstone_{fine}$ sediments, where production rates increased from 5°C to 26°C, this may be due to the suggestion that local factors are the dominant control on CH_4 production[12]. Ebullition may be responsible for this observation as it is related to finer sediments[41], explaining high production rates in $Chalk_{fine}$

and $Sandstone_{fine}$, and OM-rich sediments[41,42], resulting in elevated production rates in the three highest OM content sediments investigated here. The temperature sensitivity of CH_4 production rates was not consistent between the Chalk and Sandstone sediments. Rates were greater at 21 than 26°C in the $Chalk_{fine}$ and $Chalk_{medium}$ sediments, whereas rates increased with temperature in $Sandstone_{fine}$ sediments. Patterns in $Chalk_{fine}$ and $Chalk_{medium}$ CH_4 production rates were consistent with trends observed in microbial metabolism and may be explained by an increase in CH_4 oxidation with temperature, alongside anoxic conditions[28]. A further explanation for the observed geological difference is that Chalk streams are thermally buffered due to groundwater, resulting in reduced thermal extremes in the summer and winter[43]; the Chalk microbial community is, therefore, expected to be adapted to lower temperatures, and may not respond well to extreme temperatures, e.g. 26°C. Patterns in $Sandstone_{fine}$ CH_4 production rates, however, did not correspond to those of MMA, with a more obvious increase in CH_4 production than MMA with increasing temperature, which was non-linear.

Ratios of CH_4:CO_2 generally increased with temperature for fine sediments, with an increase in CH_4:CO_2 of 10% in $Chalk_{fine}$ and 2840% in $Sandstone_{fine}$ observed for a 1°C temperature increase from 5 to 26°C (SI, Figure 4.S-2). The differences in increase in ratios between geological origin show that the relative increase was substantially higher in the Sandstone sediments than the Chalk sediments, indicating a larger proportion of C being released as CH_4 than CO_2 in the Sandstone sediments. The decrease in CH_4 production from 21 to 26°C caused a decrease in CH_4:CO_2 in the $Chalk_{fine}$ sediment, resulting in an increase in ratio of 58% for a 1°C temperature increase from 5 to 21°C. An increase in CH_4:CO_2 ratio with temperature has been observed previously and is due to the high temperature dependence of CH_4 production, the variation between CH_4 and CO_2 kinetics, and the possible release of CH_4 from sediments before conversion to CO_2[28–30,44]. The ratios found herein are greater than

those previously reported in fine, anoxic Chalk sediments, which found a 1°C temperature increase produced a 4% increase in CH_4:CO_2 ratio, over a temperature range of 3 to 22°C[28]. The medium and coarse sediments showed relatively little variation in CH_4:CO_2 ratio with temperature (between 4 and 15% with 1°C increase from 5 to 26°C), except at 21°C in the $Chalk_{medium}$ sediment, which resulted in a 159% increase in CH_4:CO_2 ratio with 1°C increase in temperature from 5 to 21°C. Although most of the increases in medium and coarse CH_4:CO_2 ratios were relatively low compared to the fine sediments, they were still consistently higher (up to 4 times) than previously observed[28]. High CH_4:CO_2 ratios are frequently interpreted as indicators of significant human influence[12], which may explain the high values observed in this study for agricultural streams wherein CH_4:CO_2 ratios markedly exceeded values reported previously. The observed ratios highlight the relevance of investigating biogeochemical cycling to allow mitigation of GHG production, particularly in agricultural streams.

OM content and geological origin had a large influence on CH_4 production rates, especially at higher temperatures (Figure 4.3), resulting in significantly different production rates between geologies (p-value = <0.01). The fine sediments had similar production rates at both 9°C and 26°C. At 15 and 21°C, an increase in production rates in the $Chalk_{fine}$ sediments resulted in a clear difference between the geological origins in the fine sediments. This indicates an onset of increased production rates at 15°C in the $Chalk_{fine}$. There was a large decrease in CH_4 production rates in the $Chalk_{fine}$ sediments from 21 to 26°C, alongside an increase in CH_4 production in $Sandstone_{fine}$, resulting in similar production rates at 26°C (see above). Medium and coarse sediments had similar, low production rates across all temperatures, except at 21°C where there was an increase in CH_4 production rate in the $Chalk_{medium}$ sediment to 0.548±0.075 mg C m^{-2} hr^{-1}. This resulted in significantly greater production rates in fine

sediments than medium and coarse sediments (p-value = <0.01 for Chalk, and <0.01 for Sandstone).

48% of the Q_{10CH4} values ranged between 0.0 and 4.1 (SI, Table 4.S-4), similar to previously reported values in lake sediments[39], with large values indicating a greater temperature dependency. $Chalk_{fine}$ sediments resulted in high Q_{10CH4} values of 134.9 between 9 and 15°C, and 9.3 between 15 and 21°C. $Sandstone_{fine}$ resulted in high Q_{10CH4} values of 227.6 between 9 and 15°C, and 12.2 between 21 and 26°C. These fine sediment, Q_{10CH4} values, highlight the difference in response of the two geological origins, with both initially responding to increased temperature at 15°C, then $Chalk_{fine}$ producing high CH_4 production rates earlier than $Sandstone_{fine}$ (21 and 26°C, respectively). $Chalk_{medium}$ produced a high Q_{10CH4} value of 163.2 between 15 and 21°C, highlighting the elevated CH_4 production rate observed at 21°C. The large Q_{10CH4} values observed here were produced from initially insignificant rates of CH_4 production, followed by increased rates as the microbial community responded to increased temperatures.

CH_4 production rates have been observed to increase exponentially with increasing temperature in anoxic, fine sediments of Chalk streams, increasing from 22 nmol CH_4 g^{-1} hr^{-1} at 3°C to 80 nmol CH_4 g^{-1} hr^{-1} at 22°C[28]. These rates were far greater than those observed here, which ranged from 0.1 nmol CH_4 g^{-1} hr^{-1} at 5°C to 0.6 nmol CH_4 g^{-1} hr^{-1} at 26°C in $Chalk_{fine}$, and 0.0 nmol CH_4 g^{-1} hr^{-1} at 5°C to 0.4 nmol CH_4 g^{-1} hr^{-1} at 26°C in $Sandstone_{fine}$. The low, similar CH_4 production rates observed here in the medium and coarse substrates across all temperatures, except in $Chalk_{medium}$ at 21°C, (maximum of 0.03 nmol CH_4 g^{-1} hr^{-1}) has been observed previously, although previous experiments used seasonally collected sediments and so other environmental factors, such as substrate availability, may have also been affecting production rates. These previously observed rates were approximately 1.0 nmol CH_4 g^{-1} hr^{-1} [40], higher than those observed here in the medium and coarse sediments,

which may be due to the larger quantity of total organic carbon present in the sediments of the previous study.

Increased temperature generally led to a rise in sediment respiration and GHG production in the investigated streambed sediments. Importantly, in contrast to previous studies the non-linear relationship with temperature was not exponential for MMA and CH_4 production, and threshold responses were observed instead[28,30,36]. Although Rru production has been developed as a proxy for aerobic microbial respiration, it is possible that Rru is produced in the jar alongside methanogenesis, due to oxic and anoxic sediments existing simultaneously[45]. This explains, therefore, the observations in some sediment types of simultaneous Rru, CO_2 and CH_4 production, especially at higher temperatures. Control experiments showed negligible production of metabolic activity and GHG production (SI, Figure 4.S-3).

We found the temperature sensitivity of streambed sediment respiration and GHG production to be dependent on substrate, OM content and geological origin, with the greatest reactivity, and largest responses to increased temperature, found in the fine, high OM content sediments. This observation is likely explained by the large surface area provided by fine sediment, which leads to greater microbial populations[46]. Reactivity was generally greater in the Chalk than the Sandstone sediments; which resulted in $Chalk_{fine}$ sediments being characterised by the highest rates of MMA and GHG production. GHG production in Chalk sediments responded to increased temperatures earlier than Sandstone sediments. Increased rates of sediment respiration and GHG production associated with fine, OM-rich sediments, as well as increased temperature, are consistent with previous research[28,30,32,33,36,40,41,47–49], with CH_4 results explained by the promotion of methanogenesis in fine, OM-rich sediments[12,28].

4.3 Implications of drivers of GHG production

Our results demonstrate that biogeochemical processes in streambed sediments, such as respiration, are affected by temperature, substrate, OM content, and geological origin. The upscaling of GHG production, both temporally and spatially, should, therefore, consider the spatial variability of these confounding factors. When considering variations and trends in GHG production, increased temperature is a key driver of greater GHG production, and is expected to increase under future climates, global change and increased groundwater abstraction[12,29,50,51]. Fine, OM-rich sediments were also found to enhance GHG production, which are expected to increase due to land-use change and greater weathering rates[12]. Additionally, fine, OM-rich sediments introduce spatial variability in biogeochemical cycling, along with varying geological backgrounds. Of particular importance, therefore, are agricultural, lowland rivers, typically characterised by high nutrient loading and fine, OM-rich sediments[12,52]. The investigated sediments of agricultural rivers are representative for a wide range of ecosystems across much of Europe, North America and Asia, contributing significantly to the atmospheric burden of GHG.

Comparing the average potential CO_2 production rates from all sediments at 15°C (representing typical present-day temperatures) to previous estimates, demonstrates an increase in stream and river CO_2 emissions to the atmosphere of 269% in this study[8]. If the streambed temperature was to increase to 21 or 26°C this would result in a 329 and 552% increase in CO_2 flux, respectively, relative to current emissions estimates[8]. This rises to a 340 and 557% increase when methane is included, showing that substantial increases in C emission from streams are expected under future warming of streambed sediments up to 26°C. These fluxes were calculated per COSCAT region 402 (Coastal Segmentation and related catchments of the UK, Ireland and Iceland). Comparisons between incubation experiment results and global observations allow the quantification of the effect of streambed GHG production, in relation to increasing temperature, on GHG efflux from streams and

rivers. Incubation experiments and global observations represent different scales and natural conditions; therefore, these increases in effluxes represent an estimate of the influence of streambed GHG production at different temperatures and some caution needs to be exercised when predicting field fluxes under future climate change.

While the issues with upscaling incubation experiments to surface water emissions are appreciated, when used as an approximation (as above), the temperature-induced increase in CO_2 emissions identified in this study contradicts previous research that warming does not increase CO_2 emissions from surface waters[53]. Previous research has focused on surface water only (not accounting for streambed sediment contributions) and noted that CO_2 emissions may be affected by temperature if ecosystem respiration and gross primary production are independent[53]. Our results indicate the importance of considering streambed respiration, which has been largely unaccounted for in C efflux despite knowledge of its importance[8,54], and subsequent CO_2 production, in C fluxes from streams and rivers, as this may alter the temperature-dependence of CO_2 emissions.

4.4 Summary

Future research on the environmental factors driving high GHG production rates in streambed sediments is required to fully understand stream carbon dynamics and emissions, and their response to future climates, to enable upscaling of GHG emissions to national and global scales. Research presented herein demonstrated that upscaling estimates of stream global carbon cycling in response to temperature must account for local and regional scale complexity in streambed geology and sedimentology. Previous research has predominantly displayed exponential responses of GHG production to warming[28,30]. Our results highlight non-linearity, which is not exponential, and threshold responses of streambed GHG production in response to streambed warming, with temperature sensitivity varying greatly with substrate, OM content, and geological origin. Our results, therefore, demonstrate the

importance of considering streambed production when estimating the contribution of freshwater ecosystems to global GHG emissions; especially due to observed non-linearity in streambed GHG production with increased temperature.

4.5 Methods

4.5.1 Sediment Collection

Sediment was collected from the top 10 cm of the streambed in the River Tern and the River Lambourn, UK in September 2015. To achieve a gradient of OM contents in the samples the sediment was collected from areas with the following characteristics: silt-dominated sediment underneath vegetation (1), sand-dominated sediment from unvegetated zones (2) and gravel-dominated sediment from unvegetated zones (3). The sediment was sieved (type 1 at 0.8 cm, and types 2 and 3 at 1.6 cm), to avoid large stones dominating a large proportion of the sediment within the incubation jar, and homogenised. The sediment was then stored air tight, in the dark, at 4±1°C, for 9 weeks between collection and the beginning of the last temperature incubation. To minimise any potential effects of sediment storage the order of the temperature treatments was randomised, rather than performed in sequence e.g. from the lowest to highest temperature.

4.5.2 Incubation experiments

The incubations were performed with 300 ml sediment and 500 ml ultrapure water (18.2 MΩ) in pre-weighed 1 l amber glass jars (acid (10% HCl) and ultrapure water-rinsed) with lids with septa. Ultrapure water was used to allow sediment processes to be investigated independently of stream water solutes and microbes. Controls of 500 ml ultrapure water (18.2 MΩ) with no sediment were also prepared. The 3 substrate types from the 2 geological origins, as well as the control experiments, gave a total of 7 substrates, which were ran in triplicate resulting in 21 incubation jars per temperature treatment (Figure 4.1). Once the samples were added the jars were placed, with lids ajar, into an incubation oven at treatment

temperature for 3 days prior to the beginning of the incubation time period. The incubations were performed for 5 hours at 5, 9, 15, 21 and 26°C. Sampling occurred at 0 and 5 hours as described below.

To enable the results from these incubation experiments to reflect *in-situ* processes, real world conditions were emulated as closely as possible by manually swirling sediment slurries after the addition of the ultrapure water. This allowed for re-sorting of sediments with heavier particles at the base and finer particles settled on the top, to mimic natural sediment sorting and deposition conditions. Additionally, once incubated, the disturbance within the system was minimised to avoid any impact either on dissolution of headspace O_2 into the water and sediments, and the ebullition-based fluxes of GHG, particularly CH_4. This allowed for comparing fluxes from sediments of different texture and OM content, across the different geologies, under a constant sediment surface area. Thus, differences in sediment porosity constraints on oxygen diffusion were minimized to avoid experimental anomalies, and subsequent effects on production rates and CH_4:CO_2 ratios.

Prior to the start of the experiment a 15 ml water sample was also taken and ran as a background sample on the fluorometer, this water was then returned to the correct incubation jar. One sample each for the Lambourn and the Tern were kept for later use in fluorometer calibration.

4.5.2.1 T=0 hours

At t=0 a jar was removed from the incubation oven, opened and 5 ml of (between 14.5 and 15.4 ppb) Raz solution was added to the water column and stirred. A 15 ml water sample was taken and filtered (0.45μm ultrapure water-washed (18.2 MΩ) nylon) into the fluorometer to measure the Raz and Rru absorbance, after measurement the sample was returned to the incubation jar to maintain water volume. The fluorometer was rinsed with ultrapure water (18.2 MΩ) between samples. The oxygen concentration of the water column

was measured (FireSting Fibreoptic DO probe), and the headspace of the jar was equilibrated with the surrounding air and the jar closed. The oxygen concentration of the headspace was measured with a needle probe (FireSting Fibreoptic DO probe) through the septa of the lid, and 2x15 ml gas samples were taken in a syringe (helium-rinsed) into pre-evacuated 12 ml exetainers. The jar was then placed back into the incubation oven. This procedure was repeated for all jars.

4.5.2.2 T=5 hours

The incubation jar was removed from the incubation oven and oxygen of the headspace and gas samples taken as described above. The jar was then opened and the procedure for t=0 was followed to measure Raz, Rru, and oxygen.

4.5.3 Determination of water, sediment, OM and carbonate content

Following the incubation experiments the jars were weighed to give a wet weight, and dried in an oven at 65°C for 3 days, followed by 105°C for 1 day. The jars were then weighed again to provide a dry sediment weight and a water weight for each jar. The dry sediment of 5°C was used to determine the OM and carbonate contents of the sediment types[55]. The sediment was sieved (2 mm), homogenised and a sub-sample of each jar sediment was placed into a pre-weighed crucible. The sample was dried at 105°C overnight and weighed, resulting in subsamples of 14.8 to 24.8 g of dry sediment. The crucibles were then placed into a furnace at 550°C for 6 hours and then weighed to determine the OM content of the sediment. The crucible was replaced in the furnace at 950°C for 6 hours and then weighed to determine the carbonate content of the sediment.

4.5.4 Aerobic MMA- Raz and Rru Concentration

The Raz-Rru system has been developed as a reactive tracer due to the utilisation of Raz as an electron acceptor in aerobic respiration, resulting in the irreversible conversion of Raz to Rru[56,57]. Rru production can, therefore, be used as a proxy for aerobic MMA[56,57], Rru

production is usually normalised by the amount of Raz detected in samples, to account for any losses of the tracer from the system. As we performed experiments in closed jars, we only measured Rru in the samples. The concentration of Rru in the samples were measured on a fluorometer (GGUN FL30 (Albilia Sarl, Switzerland)) as a proxy for aerobic microbial metabolism[56], with lamps set to detect the fluorescence of Rru[58]. Two fluorometers were used to ensure reading accuracy and the fluorometers were calibrated once a week with background water, Rru (100 ppb) and a mixture (50 ppb Raz, 50 ppb Rru). Fluorometer performance data was calculated using a 93.1 ppb standard of Rru, which resulted in an accuracy and precision of 0.4 and ±0.7 ppb. The LOD for the GGUN FL30 fluorometers is 1 ppb for Rru[58]. The concentration of Rru in the measured samples ranged from 0.0 to 139.6 ppb, therefore, some samples were below the LOD of the fluorometers. The maximum hourly production rate (dependent on the amount of Raz added to the jar) yielded from a Rru concentration of 1 ppb was 1.7 ng Rru μg^{-1} Raz hr^{-1}, and any samples below the LOD are presented here as actual values, accounting for some of the low MMA rates observed.
The design of the GGUN FL30 fluorometer allows a one-point calibration of 100 ppb Rru to be sufficient for these concentrations, here a two-point calibration was performed to improve data quality.

4.5.5 Carbon Dioxide and Methane Concentration

The concentration of carbon dioxide and methane in the gas samples was determined using an Agilent 7890A Gas Chromatograph (GC) - Flame Ionisation Detector (FID). The FID measures methane and so the carbon dioxide was methanised with a catalyst before passing to the FID. The GC had a 1 ml sample loop in a splitless orientation, and an oven temperature of 60°C. The FID was set to 250°C with a hydrogen flow of 48 ml min^{-1}, air flow of 500 ml min^{-1} and a make-up nitrogen (pure) flow of 2 ml min^{-1}. The run time was 7 minutes and the gases eluted at 3.5 and 5.7 minutes for methane and carbon dioxide, respectively. Machine

performance data was calculated using an external standard with concentrations of 1051 ppm CO_2 and 9.8 ppm CH_4. This resulted in an accuracy, precision and LOD of 13.4, ±14.8 and 8.2 ppm, and 0.07, ±0.11 and 0.15 ppm, for CO_2 and CH_4, respectively.

4.5.6 Temperature coefficient values (Q_{10})

The temperature coefficient value (Q_{10}) quantifies the temperature dependence of a biological process, and is here used to investigate the biological processes of MMA, and CO_2 and CH_4 production. The Q_{10} value of a process is calculated using equation 1[59].

$$Q_{10} = \left(\frac{Process_{T_2}}{Process_{T_1}}\right)^{\left(\frac{10}{(T_2 - T_1)}\right)} \quad (1)$$

Where Process is the biological process under consideration at T_1 and T_2, and T_1 and T_2 are the respective temperatures at which Process was measured. Although Q_{10} values are typically calculated where T_1 and T_2 are 10°C apart, using the form of the Q_{10} equation given above allows T_1 and T_2 to have different temperature intervals. Q_{10} values were calculated between the different incubation temperatures, so that T_1 and T_2 were 5 and 9, 9 and 15, 15 and 21, and 21 and 26°C (see Table 4.S-4).

4.5.7 Statistical Inference

We base our inference regarding the relationships between temperature, sediment type and GHG emissions upon the linear model:

$$y(s,t) = \sum_{i=0}^{6} \{I_i(s)\alpha_i + I_i(s)\beta_i t\} + \varepsilon, \quad (2)$$

where $y(s,t)$ is the measured emission from sediment class s at temperature t, $I_i(s)$ is an indicator function that is equal to one when $i = s$ and is zero otherwise, the α_i and β_i are model coefficients for the intersect and gradient terms and each ε is independent and realized from a Gaussian distribution with zero mean and constant variance. Thus, each response curve is represented by a linear function. The seven sediment classes are: 0 – control, 1 –

chalk fine, 2 – chalk medium, 3 – chalk coarse, 4 – sandstone fine, 5 – sandstone medium and 6 – sandstone coarse.

We estimate the model coefficients $\boldsymbol{\mu} = [\alpha_0, \ldots, \alpha_6, \beta_1, \ldots, \beta_6]^{\mathrm{T}}$ for each GHG variable (where T denotes the transpose) by maximum likelihood. Where the residuals that result are inconsistent with the Gaussian assumption, a shift and a log transform are applied to the data and the model is re-estimated until approximately Gaussian residuals are achieved.

We initially apply ANOVA tests to the null hypotheses that $\alpha_0 = \alpha_1 = \cdots = \alpha_6$ and $\beta_0 = \beta_1 = \cdots = \beta_6$. If these hypotheses can be rejected at the 0.05 level we then explore the factors causing variation in the α_i and/or β_i. We control the Type-1 errors across the experiment by testing a series of planned orthogonal contrasts. For the intersect terms these contrasts are:

C1: $\alpha_0 - \frac{1}{6}\sum_{i=1}^{6} \alpha_i$, *i.e.* comparing the intersect of the control to the average of the six sediment types;

C2: $\frac{1}{3}\sum_{i=1}^{3} \alpha_i - \frac{1}{3}\sum_{i=4}^{6} \alpha_i$, *i.e.* comparing the intersects for chalk to those for sandstone;

C3: $\alpha_1 - \frac{\alpha_2+\alpha_3}{2}$, *i.e.* comparing the intersect for chalk fine to the average of that for the other chalk classes;

C4: $\alpha_4 - \frac{\alpha_5+\alpha_6}{2}$, *i.e.* comparing the intersect for sandstone fine to the average of that for the other sandstone classes;

C5: $\alpha_0 - \frac{\alpha_1+\alpha_4}{2}$, *i.e.* comparing the intersect for the control to the average of those for fine sediment classes.

If appropriate, the same comparisons were applied to the β_i gradient coefficients. The probability of achieving the estimated value of each contrast if the true value is zero, was then calculated by a Wald test following the methodology described by Lark and Cullis (2004).

If either of the initial ANOVA hypotheses cannot be rejected then the corresponding α_i or β_i in the model are replaced by a single constant coefficient and the remaining parameters are re-estimated before the above contrasts are tested.

4.6 Acknowledgments

The authors would like to thank NERC and the Central England NERC Training Alliance, as well as the European Union Marie Curie Initial Training Network 'Interfaces' for their funding of this project.

4.7 References

1. Cole, J. J. *et al.* Plumbing the Global Carbon Cycle: Integrating Inland Waters into the Terrestrial Carbon Budget. *Ecosystems* **10,** 172–185 (2007).

2. Battin, T. J. *et al.* The boundless carbon cycle. *Nat. Geosci.* **2,** 598–600 (2009).

3. Leopold, L., Wolman, M. & Miller, J. *Fluvial processes in geomorphology*. (Dover Publishers).

4. Denman, K.L., G. & Brasseur, A. Chidthaisong, P. Ciais, P.M. Cox, R.E. Dickinson, D. Hauglustaine, C. Heinze, E. Holland, D. Jacob, U. Lohmann, S Ramachandran, P.L. da Silva Dias, S. C. W. and X. Z. in *Climate Change 2007: The Physical Science Basis. Contribution of Working Group I to the Fourth Assessment Report of the Intergovernmental Panel on Climate Change* (eds. Solomon, S. et al.) **21,** 499–587 (Cambridge University Press, 2007).

5. Trimmer, M. *et al.* River bed carbon and nitrogen cycling: state of play and some new directions. *Sci. Total Environ.* **434,** 143–58 (2012).

6. Tranvik, L. J. *et al.* Lakes and reservoirs as regulators of carbon cycling and climate. *Limnol. Oceanogr.* **54,** 2298–2314 (2009).

7. Striegl, R. G., Dornblaser, M. M., McDonald, C. P., Rover, J. R. & Stets, E. G. Carbon dioxide and methane emissions from the Yukon River system. *Global Biogeochem. Cycles* **26,** (2012).

8. Raymond, P. a *et al.* Global carbon dioxide emissions from inland waters. *Nature* **503,** 355–359 (2013).

9. Hotchkiss, E. R. *et al.* Sources of and processes controlling CO2 emissions change with the size of streams and rivers. *Nat. Geosci.* **8,** 696–699 (2015).

10. Richey, J. E., Melack, J. M., Aufdenkampe, A. K., Ballester, V. M. & Hess, L. L. Outgassing from Amazonian rivers and wetlands as a large tropical source of atmospheric CO2. *Nature* **416,** 617–620 (2002).

11. De Fátima F. L. Rasera, M. *et al.* Estimating the surface area of small rivers in the southwestern amazon and their role in CO2 outgassing. *Earth Interact.* **12,** 1–16 (2008).

12. Stanley, E. H. *et al.* The ecology of methane in streams and rivers: Patterns, controls, and global significance. *Ecol. Monogr.* **86,** 146–171 (2016).

13. Panneer Selvam, B., Natchimuthu, S., Arunachalam, L. & Bastviken, D. Methane and carbon dioxide emissions from inland waters in India - implications for large scale greenhouse gas balances. *Glob. Chang. Biol.* **20,** 3397–3407 (2014).

14. Crawford, J. T. *et al.* CO2 and CH4 emissions from streams in a lake-rich landscape: Patterns, controls, and regional significance. *Glob. Chang. Biol.* **20,** 3408–22 (2014).

15. Bastviken, D. *et al.* Freshwater methane emissions offset the continental carbon sink. *Science.* **331,** 50 (2011).

16. McClain, M. E. *et al.* Biogeochemical Hot Spots and Hot Moments at the Interface of Terrestrial and Aquatic Ecosystems. *Ecosystems* **6,** 301–312 (2003).

17. Lautz, L. K. & Fanelli, R. M. Seasonal biogeochemical hotspots in the streambed around restoration structures. *Biogeochemistry* **91,** 85–104 (2008).

18. Krause, S., Tecklenburg, C., Munz, M. & Naden, E. Streambed nitrogen cycling beyond the hyporheic zone: Flow controls on horizontal patterns and depth distribution of nitrate and dissolved oxygen in the upwelling groundwater of a lowland river. *J. Geophys. Res. Biogeosciences* **118,** 54–67 (2013).

19. Jones, J. B. & Holmes, R. M. Surface-subsurface interactions in stream ecosystems.

Trends Ecol. Evol. **11,** 239–242 (1996).

20. Krause, S. *et al.* Inter-disciplinary perspectives on processes in the hyporheic zone. **499,** 481–499 (2011).

21. Seitzinger, S. *et al.* Denitrification across landscaes and waterscapes: a synthesis. *Ecol. Appl.* **16,** 2064–2090 (2006).

22. Boulton, A. J., Findlay, S., Marmonier, P., Stanley, E. H. & Valett, H. M. The Functional Significance of the Hyporheic Zone in Streams and Rivers. *Annu. Rev. Ecol. Syst.* **29,** 59–81 (1998).

23. Krause, S., Louise Heathwaite, a., Binley, A. & Keenan, P. Nitrate concentration changes at the groundwater-surface water interface of a small Cumbrian river. *Hydrol. Process.* **23,** 2195–2211 (2009).

24. Trimmer, M., Hildrew, A. G., Jackson, M. C., Pretty, J. L. & Grey, J. Evidence for the role of methane-derived carbon in a free-flowing , lowland river food web. **54,** 1541–1547 (2009).

25. Hlaváčová, E., Rulík, M. & Čáp, L. Anaerobic microbial metabolism in hyporheic sediment of a gravel bar in a small lowland stream. *River Res. Appl.* **21,** 1003–1011 (2005).

26. Schindler, J. E. & Krabbenhoft, D. P. The hyporheic zone as a source of dissolved organic carbon and carbon gases to a temperate forested stream. 157–174 (1998).

27. Trimmer, M., Sanders, I. A. & Heppell, C. M. Carbon and nitrogen cycling in a vegetated lowland chalk river impacted by sediment. **2238,** 2225–2238 (2009).

28. Shelley, F., Abdullahi, F., Grey, J. & Trimmer, M. Microbial methane cycling in the bed of a chalk river: oxidation has the potential to match methanogenesis enhanced by warming. *Freshw. Biol.* **60,** 150–160 (2015).

29. Yvon-Durocher, G., Montoya, J. M., Woodward, G., Jones, J. I. & Trimmer, M. Warming increases the proportion of primary production emitted as methane from freshwater mesocosms. *Glob. Chang. Biol.* **17,** 1225–1234 (2011).

30. Yvon-Durocher, G. *et al.* Methane fluxes show consistent temperature dependence across microbial to ecosystem scales. *Nature* **507,** 488–91 (2014).

31. Yvon-Durocher, G., Hulatt, C. J., Woodward, G. & Trimmer, M. Long-term warming amplifies shifts in the carbon cycle of experimental ponds. *Nat. Clim. Chang.* **7,** 209–214 (2017).

32. Sanders, I. a. *et al.* Emission of methane from chalk streams has potential implications for agricultural practices. *Freshw. Biol.* **52,** 1176–1186 (2007).

33. Crawford, J. T. & Stanley, E. H. Controls on methane concentrations and fluxes in streams draining human-dominated landscapes. *Ecol. Appl.* 15–1330.1 (2015). doi:10.1890/15-1330.1

34. Sand-Jensen, K., Pedersen, N. L. & Søndergaard, M. Bacterial metabolism in small temperate streams under contemporary and future climates. *Freshw. Biol.* **52,** 2340–2353 (2007).

35. Haggerty, R., Argerich, A. & Martí, E. Development of a 'smart' tracer for the assessment of microbiological activity and sediment-water interaction in natural waters: The resazurin-resorufin system. *Water Resour. Res.* **46,** 1–10 (2008).

36. Yvon-Durocher, G. *et al.* Reconciling the temperature dependence of respiration across timescales and ecosystem types. *Nature* **487,** 472–476 (2012).

37. Perkins, D. M. *et al.* Consistent temperature dependence of respiration across ecosystems contrasting in thermal history. *Glob. Chang. Biol.* **18,** 1300–1311 (2012).

38. Therrien, J., Tremblay, A. & Jacques, R. . in *Greenhouse Gas Emissions — Fluxes and*

Processes. Environmental Science. Springer, Berlin, Heidelberg (eds. Tremblay, A., Varfalvy, L., Roehm, C. & Garneau, M.) 233–250 (Springer, 2005).

39. Liikanen, A., Murtoniemi, T., Tanskanen, H., Väisänen, T. & Martikainen, P. J. Effects of temperature and oxygen availability on greenhouse gas and nutrient dynamics in sediment of a eutrophic mid-boreal lake. *Biogeochemistry* **59,** 269–286 (2002).

40. Tortosa, G. *et al.* Effects of nitrate contamination and seasonal variation on the denitrification and greenhouse gas production in La Rocina Stream (Donana National Park, SW Spain). *Ecol. Eng.* **37,** 539–548 (2011).

41. Baulch, H. M., Dillon, P. J., Maranger, R. & Schiff, S. L. Diffusive and ebullitive transport of methane and nitrous oxide from streams: Are bubble-mediated fluxes important? *J. Geophys. Res.* **116,** G04028 (2011).

42. Crawford, J. T. *et al.* Ebullitive methane emissions from oxygenated wetland streams. *Glob. Chang. Biol.* **20,** 3408–22 (2014).

43. Garner, G., Hannah, D. M., Sadler, J. P. & Orr, H. G. River temperature regimes of England and Wales: Spatial patterns, inter-annual variability and climatic sensitivity. *Hydrol. Process.* **28,** 5583–5598 (2014).

44. Marotta, H., Pinho, L. & Gudasz, C. Greenhouse gas production in low-latitude lake sediments responds strongly to warming. *Nat. Clim. Chang.* **4,** 11–14 (2014).

45. Parkin, T. B. Soil Microsites as a Source of Denitrification Variability1. *Soil Sci. Soc. Am. J.* **51,** 1194 (1987).

46. Coyne, M. S., Howell, J. M. & Cornelius, P. L. Particle Size and Temperature Affect Fecal Bacteria Survival in Sediment. *Agron. Notes* **30,** Paper 140 (1997).

47. Hedin, L. O. Factors Controlling Sediment Community Respiration in Woodland

Stream Ecosystems. *Oikos* **57,** 94–105 (1990).

48. Hargrave, B. T. Aerobic Decomposition of Sediment and Detritus As a Function of Particle Area and Organic Content. *Limnol. Oceanogr.* **17,** 583–596 (1972).

49. Baker, J. H. Relationship Between Microbial Activity of Stream Sediments, Determined by Three Different Methods, and Abiotic Variables. *Microb. Ecol.* **12,** 193–203 (1986).

50. Orr, H. G. *et al.* Detecting changing river temperatures in England and Wales. *Hydrol. Process.* **29,** 752–766 (2015).

51. Kaushal, S. S. *et al.* Rising stream and river temperatures in the United States. *Front. Ecol. Environ.* **8,** 461–466 (2010).

52. Graeber, D., Gelbrecht, J., Pusch, M. T., Anlanger, C. & von Schiller, D. Agriculture has changed the amount and composition of dissolved organic matter in Central European headwater streams. *Sci. Total Environ.* **438,** 435–446 (2012).

53. Demars, B. O. L. *et al.* Impact of warming on CO2 emissions from streams countered by aquatic photosynthesis. *Nat. Geosci.* **1,** (2016).

54. Ciais, P. *et al.* in *Climate Change 2013: The Physical Basis. Contribution of Working Group I to the Fifth Assessment Report of the Intergovernmental Panel on Climate Change* (eds. Stocker, T. . et al.) 465–570 (Cambridge University Press, 2013). doi:10.1017/CBO9781107415324.015

55. Hoogsteen, M. J. J., Lantinga, E. A., Bakker, E. J., Groot, J. C. J. & Tittonell, P. A. Estimating soil organic carbon through loss on ignition: Effects of ignition conditions and structural water loss. *Eur. J. Soil Sci.* **66,** 320–328 (2015).

56. Haggerty, R., Martí, E., Argerich, A., Von Schiller, D. & Grimm, N. B. Resazurin as a 'smart' tracer for quantifying metabolically active transient storage in stream

ecosystems. *J. Geophys. Res. Biogeosciences* **114,** 1–14 (2009).

57. Karakashev, D., Galabova, D. & Simeonov, I. A simple and rapid test for differentiation of aerobic from anaerobic bacteria. *World J. Microbiol. Biotechnol.* **19,** 233–238 (2003).

58. Lemke, D., Schnegg, P. A., Schwientek, M., Osenbrück, K. & Cirpka, O. A. On-line fluorometry of multiple reactive and conservative tracers in streams. *Environ. Earth Sci.* **69,** 349–358 (2013).

59. Davidson, E. A., Janssens, I. A. & Lou, Y. On the variability of respiration in terrestrial ecosystems: Moving beyond Q10. *Glob. Chang. Biol.* **12,** 154–164 (2006).

4.8 SI

4.8.1 Statistical Analysis

Table 4.S-1. Estimated value of each intersect and gradient contrast and the probability of these estimates being achieved under the null model Ci=0 for $log(Rru + 0.1)$*. Significant p-values are in bold.*

Contrast	Intersect: α_i		Gradient: β_i	
	Estimated value	p	Estimated value	p
ANOVA		**<0.01**		**<0.01**
C1	-0.13	0.82	-0.16	**<0.01**
C2	1.16	0.14	0.01	0.64
C3	3.28	**<0.01**	-0.04	0.35
C4	2.11	**<0.01**	0	0.95
C5	-1.57	0.11	-0.29	**<0.01**

Table 4.S-2. Estimated value of each intersect and gradient contrast and the probability of these estimates being achieved under the null model Ci=0 for $log(CO_2 + 0.1)$*. Significant p-values are in bold.*

Contrast	Intersect: α_i		Gradient: β_i	
	Estimated value	p	Estimated value	p
ANOVA		**<0.01**		**<0.01**
C1	-1.82	**<0.01**	-1.01	**<0.01**
C2	-6.01	**<0.01**	0.46	**<0.01**
C3	10.59	**<0.01**	1.47	**<0.01**
C4	12.93	**<0.01**	0.65	**<0.01**
C5	-15.79	**<0.01**	-3.57	**<0.01**

Table 4.S-3. Estimated value of each intersect and gradient contrast and probability of these estimate being achieved under the null model Ci=0 for $log(CH_4 + 0.01)$*. Significant p-values are in bold.*

Contrast	Intersect: α_i		Gradient: β_i	
	Estimated value	p	Estimated value	p
ANOVA		0.17		**<0.01**
C1	NA	NA	-0.08	**<0.01**
C2	NA	NA	0.06	**<0.01**
C3	NA	NA	0.16	**<0.01**
C4	NA	NA	0.14	**<0.01**
C5	NA	NA	-0.36	**<0.01**

4.8.2 Oxygen results

In general, the oxygen concentration of the water column decreased with increasing temperature, resulting in a large difference between the lower and higher temperatures. For example, $Chalk_{fine}$ had an oxygen concentration of 7.22±0.41 mg l^{-1} at 5°C and 2.23±0.37 mg l^{-1} oxygen at 26°C. The oxygen concentration of the water column showed a similar trend for both the Chalk and the Sandstone sediments, and was similar from 5 to 15°C, between 5.45±0.88 and 9.38±0.47 mg l^{-1}, before decreasing to a similar concentration for 21 and 26°C between 0.53±0.12 and 6.28±0.47 mg l^{-1}, resulting in anaerobic conditions in some sediments. However, the oxygen content was lower in Chalk fine than Sandstone fine, with 2.23±0.37 mg O_2 l^{-1} in the Chalk and 3.70±0.25 mg O_2 l^{-1} in the Sandstone at 26°C.

The controls showed a decrease in oxygen concentration with increasing temperature, as expected due to the physical controls over oxygen solubility, with oxygen being more soluble in colder water. This decrease is not as pronounced in the control as in the sediment treatments, decreasing by 37% from 5 to 26°C, whereas the Chalk fine oxygen concentration decreased by 69% over the same temperature range.

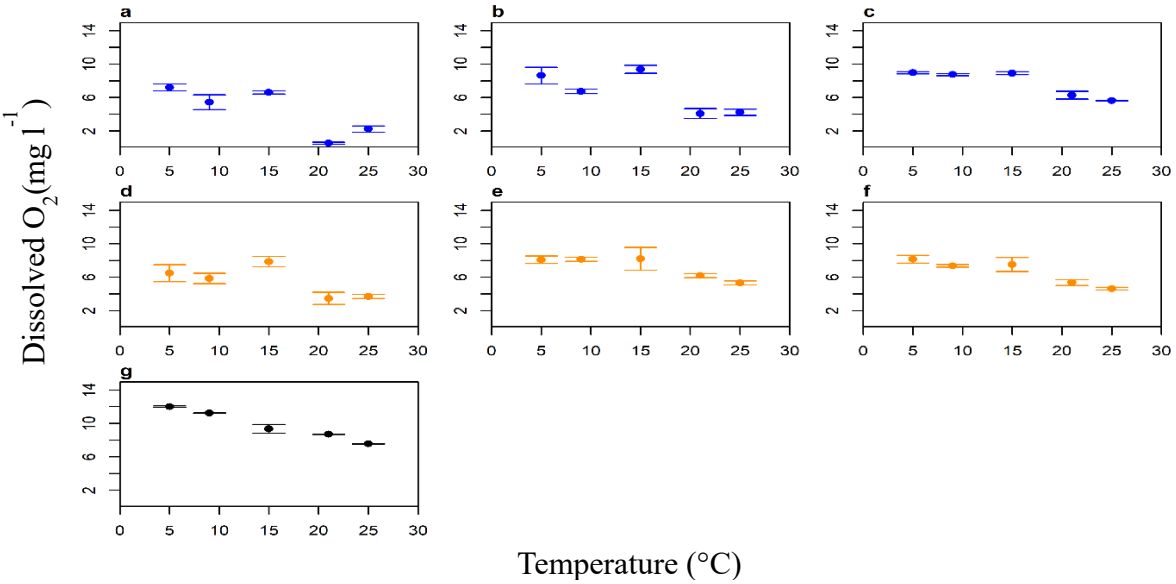

Figure 4.S-1. DO concentration plotted against temperature for a. Chalk$_{fine}$, b. Chalk$_{medium}$, c. Chalk$_{coarse}$, d. Sandstone$_{fine}$, e. Sandstone$_{medium}$, f. Sandstone$_{coarse}$ and g. Control. Also shown are the slope and adjusted r^2 of the linear models.

Table 4.S-4 Temperature coefficient (Q_{10}) values of CO_2, CH_4 and MMA with temperature increase. In some cases where production was negative or zero, no Q_{10} values could be calculated.

Temperature (°C)	Substrate	Q_{10MMA}	Q_{10CO2}	Q_{10CH4}
5 and 9	$Chalk_{fine}$	2.1	0.3	2.6
5 and 9	$Chalk_{medium}$	0.0	0.1	0.6
5 and 9	$Chalk_{coarse}$	0.0	1.1	0.0
5 and 9	$Sandstone_{fine}$	0.0	0.6	421.1
5 and 9	$Sandstone_{medium}$	0.0	0.5	-
5 and 9	$Sandstone_{coarse}$	-	3.5	-
5 and 9	Control	-	1.0	-
9 and 15	$Chalk_{fine}$	9.0	8.1	134.9
9 and 15	$Chalk_{medium}$	-	80.6	115.6
9 and 15	$Chalk_{coarse}$	-	0.1	9.5
9 and 15	$Sandstone_{fine}$	-	2.7	227.6
9 and 15	$Sandstone_{medium}$	-	4.0	7.2
9 and 15	$Sandstone_{coarse}$	-	9.1	0.9
9 and 15	Control	-	0.7	1.0
15 and 21	$Chalk_{fine}$	22.2	1.4	9.3
15 and 21	$Chalk_{medium}$	1425.3	2.3	163.2
15 and 21	$Chalk_{coarse}$	13.0	3505.2	78.8
15 and 21	$Sandstone_{fine}$	3.3	0.8	4.1
15 and 21	$Sandstone_{medium}$	52.6	1.8	4.1
15 and 21	$Sandstone_{coarse}$	65.9	1.0	10.1
15 and 21	Control	-	0.2	-
21 and 26	$Chalk_{fine}$	0.9	2.3	0.1
21 and 26	$Chalk_{medium}$	0.2	1.5	0.0
21 and 26	$Chalk_{coarse}$	2.0	100.3	0.0
21 and 26	$Sandstone_{fine}$	2.0	4.9	12.2
21 and 26	$Sandstone_{medium}$	2.3	4.6	0.1
21 and 26	$Sandstone_{coarse}$	2.3	4.0	10.1
21 and 26	Control	-	0.6	-

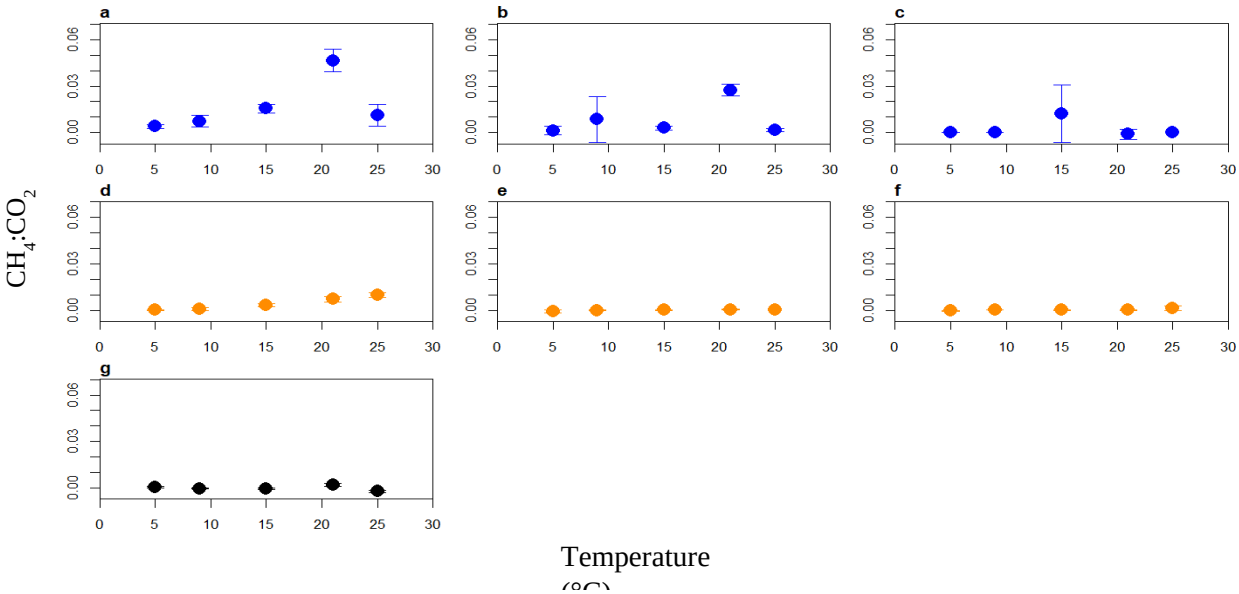

Figure 4.S-2. CH_4:CO_2 ratios plotted against temperature for a. $Chalk_{fine}$, b. $Chalk_{medium}$, c. $Chalk_{coarse}$, d. $Sandstone_{fine}$, e. $Sandstone_{medium}$, f. $Sandstone_{coarse}$ and g. Control.

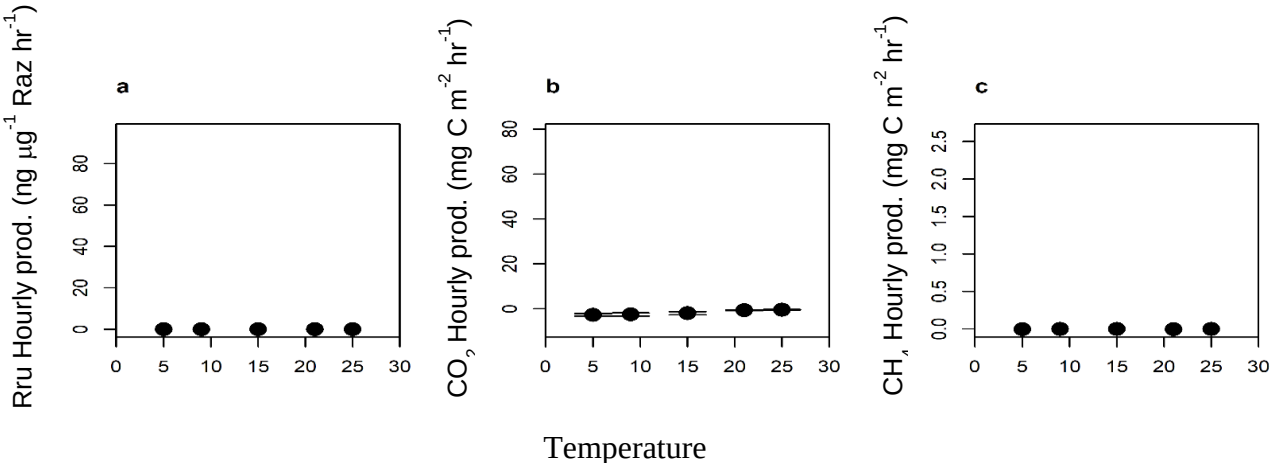

Figure 4.S-3. Hourly production plotted against temperature for control experiments, also shown are the slope and adjusted r^2 of the linear models. A. Rru production, b. CO_2 production and c. CH_4 production.

Chapter 5: Sediment type and season as factors controlling nutrient cycling in agricultural streams: Part I Carbon

Sophie A. Comer-Warner[1], Daren C. Gooddy[2], Nick Kettridge[1], Sami Ullah[1] and Stefan Krause[1]

1. School of Geography, Earth and Environmental Sciences, University of Birmingham, Edgbaston, Birmingham B15 2TT, UK

2. British Geological Survey (BGS), Maclean Building, Wallingford, Oxfordshire OX10 8BB, UK

5.1 Introduction

Since streams and rivers have been recognised as 'active pipelines', where biogeochemical processes alter solutes transported in their water, there has been an increase in interest in their role in the carbon cycle[1–4]. Carbon turnover in inland waters is substantial, with 0.8 Pg of carbon released directly to the atmosphere annually through gas exchange as CO_2, which accounts for up to 50% of the carbon in inland waters[1,4–6]. The carbon turned over in streams and rivers is predominantly due to respiration, producing CO_2 as well as CH_4. The production of GHGs in freshwater environments results in surface waters which are often supersaturated with respect to the atmosphere[3,7–13], resulting in outgassing from streams and rivers[14]. Streams and rivers have recently been recognised as globally important with respect to carbon emissions, contributing 1.8 Pg CO_2-C yr^{-1} [3], and 26.8 Tg CH_4-C yr^{-1} [15] into the atmosphere. The flux of CH_4 is relatively small compared to the CO_2 flux, however, when considered as carbon equivalents it may offset over 25% of the terrestrial carbon sink, and CH_4 fluxes can be regionally significant[16–18]. Of disproportionate importance are small streams, which are estimated to contribute ~15% of the annual CO_2 flux from streams and rivers[3].

The majority of research into GHG production in streams and rivers has focused on surface water fluxes to the atmosphere[3,14,19,20]. However, stream sediments are 'hotspots' of nutrient spiralling and metabolic activity, with 40 to 90% of total stream metabolism resulting from hyporheic exchange[21], producing enhanced rates of carbon turnover[4,22–33].

Increased carbon turnover in the streambed leads to greater GHG concentrations in sediments than surface waters, with concentrations as high as 5 mmol CO_2 l^{-1} and 134 μmol CH_4 l^{-1} observed in streambeds[34,35]. Despite recent research indicating the global importance of carbon emissions from streams and rivers, as well as observations of elevated concentrations in porewaters relative to surface waters, the importance of streambed contributions to overall C emissions and drivers of enhanced concentrations in sediments remain insufficiently understood[1,2,4,6,36]. Developing this understanding is of increasing importance given projected changes in climate and land use, which are expected to increase CO_2 and CH_4 production[15,37–40].

CO_2 and CH_4 are end-products of respiration controlled by metabolism, residence time, temperature, substrate availability (e.g. DOC) and terminal electron acceptor availability (e.g. DO)[41–51]. Residence time and redox conditions are further controlled by sediment type, with sand sediments typically having greater resident times and anoxia than gravel sediments[43,52,53].

Sediment type also greatly affects CO_2 and CH_4 production, with fine sediments acting as a source of both CO_2 and CH_4[7,12,15,35,54], and coarse, gravel sediments acting as a source of CO_2 and a sink of CH_4[55]. CH_4 production in particular is heavily influenced by fine, OM-rich sediments[7,15,56,57], which are often present in streams of agricultural catchments[15]. Carbon cycling in agricultural streams is also greatly influenced by the quantity and quality of carbon entering the stream[58,59].

This study investigates streambed carbon cycling in an agriculturally-impacted catchment, focussing on concentrations of CO_2 and CH_4, and factors controlling their production. We hypothesise that the substantial anthropological influence on the study stream and other agricultural streams will result in large concentrations of CO_2 and CH_4 in the streambed. Furthermore, we aim to determine whether sediment type (sand versus gravel) and season (influenced by temperature and substrate availability), influence the CO_2 and CH_4 concentrations observed.

5.2 Materials and Methods

5.2.1 Study Site

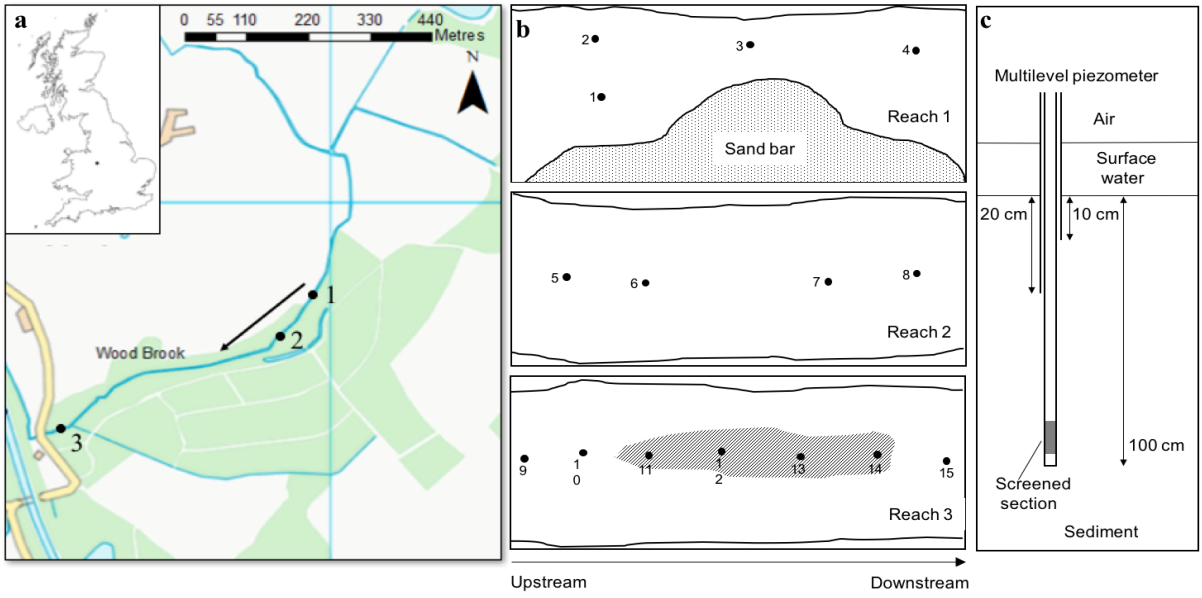

Figure 5.1a. The location of the Wood Brook within the UK and the location of the study reaches within the Wood Brook. Shown are the direction of the stream flow (black arrow), areas of woodland (green) and areas of fields (white), b. A diagram of the position of the piezometers within the three experimental reaches, and c. A diagram of the multilevel piezometers and diffusive equilibrium in thin-film gels used to sample the sediment porewaters.

The experiment was conducted in Wood Brook at BIFoR, Staffordshire, UK. Wood Brook is located in a mixed-use catchment where most of the area is arable land used for potatoes and winter wheat[60], with patches of deciduous woodland (Figure 5.1). The experiment focused on a 700 m reach of the Wood Brook, which flows through arable land before entering the study reach. The reach itself is located at the border between arable land and mature deciduous woodland, so that at the upstream end of the reach the stream is bordered by fields on one side and woodland on the other, before flowing into the woodland so that further downstream there is some woodland between the stream and the arable land. The regional groundwater aquifer is red Permo-Triassic sandstone on top of which are glacial till deposits (up to 10 m depth), overlain by sandy clay sediment between 0.15 and 0.6 m depth[60].

5.2.2 Experimental Setup

Water samples were collected seasonally from three distinct reaches within the main experimental reach (Figure 5.1a and b), in July 2016, October 2016, January 2017 and March 2017. Each reach had varying characteristics (Table 5.1) with the primary difference being that the sediments of reaches 1 and 2 were predominantly sand and those of reach 3 were predominantly gravel. The three reaches were spread throughout the experimental area so that the effect of land-use, from agricultural to woodland, on porewater chemistry and downstream transport was captured.

Table 5.1. Average key characteristics from each reach. Presented are the 3-dimensional flux of porewater through the streambed and the organic matter content of the sediment determined by loss on ignition.

Reach	q_{3D} (d^{-1})	OM Content (%)
1	42.4	2.9
2	35.4	1.4
3	80.5	0.9

5.2.2.1 Water Chemistry Sampling

Porewater samples were manually extracted at depths of 10 and 20 cm from multi-level piezometers installed into the streambed (Figure 5.1c). A surface water sample was also taken at each reach, during the period of piezometer sampling. Once collected, DO and temperature (YSI ProODO or EcoSense ODO200), and pH and electrical conductivity (Hanna HI98129) were immediately measured. Water samples were then filtered (0.45 then 0.22 μm Thames Resteck Nylon, ultrapure water-rinsed (18.2 MΩ)) into sterile centrifuge tubes (10% HCl-rinsed), and frozen until analysis.

5.2.2.2 Gas Sampling

Gas samples for analysis of GHG concentrations were generated in the field using a headspace equilibrium method. A 14 ml, ultrapure helium headspace was introduced to a 7 ml porewater sample, and shaken for 2 minutes to allow equilibration between gases in the porewater and the headspace. The headspace was then injected into a pre-evacuated exetainer and the gas sample was stored in the dark, at room temperature.

5.2.2.3 DOC Analysis

DOC concentrations were analysed on a Shimadzu Total Organic Carbon analyser (TOC-L CPH with ASI-L autosampler), with an accuracy and precision of 0.16 and ±0.45 mg l^{-1} for a 15 mg l^{-1} standard, respectively. The LOD was 0.5 mg l^{-1}.

5.2.2.4 Gas Analysis

The concentration of carbon dioxide and methane within the headspace gas samples were measured using a GC (Agilent 7890A) fitted with an FID for methane analysis and a thermal conductivity detector (TCD) for carbon dioxide analysis. The GC was used in splitless mode with a 250 μl sample loop, a 60°C oven temperature, a 250°C FID temperature and a 250°C TCD temperature. Helium was used as a carrier gas with a flow rate of 25 ml min^{-1}, and the FID was set up with a hydrogen flow of 30 ml min^{-1} and an air flow of 400 ml min^{-1}. A run time of two minutes was used, with methane and carbon dioxide eluted at 0.6 and 0.97

minutes, respectively. 1500 ppm standards of CO_2 gave an accuracy and precision of 275 and ±326 ppm, and 1000 ppm standards of CH_4 gave an accuracy and precision of 35 and ±11 ppm. The LOD was 0.5 mg l^{-1} and 0.5 μg l^{-1} for CO_2 and CH_4, respectively. The headspace concentration was converted to porewater concentration using Henry's constant[61,62].

5.2.2.5 $\delta^{13}C_{CO2}$ Analysis

$\delta^{13}C_{CO2}$ analysis was performed at the Life Sciences Mass Spectrometry Facility, Centre for Ecology and Hydrology, Lancaster, UK. $\delta^{13}C_{CO2}$ ratios were measured on a Preconcentrator (Isoprime Tracegas) coupled to an isotope ratio mass spectrometer (IRMS) (Isoprime, Elementar UK, Stockport). 60 to 600 μl (depending on sample concentration) of gas sample was injected into the Preconcentrator, and water was removed by a magnesium perchlorate chemical trap. The CO_2 was then cryogenically focussed before passing into the IRMS through an open split. A 500 ppm standard, calibrated against certified reference material CO_2-heavy (NIST number 8562), resulted in a precision ≥ ±0.12‰.

5.2.2.6 Statistical Inference

A linear mixed-effects model was fitted using the residual maximum likelihood in the nlme package in R, to determine the effect of reach and season on carbon cycling. To account for the repetition in sampling with time, the data were nested by season, and where the residuals did not fit the Gaussian assumption the data were shifted and transformed. The Akaike Information Criterion (AIC) was used to judge whether a model with (Equation 1) or without (Equation 2) the interaction between reach and season should be considered, with the model with the lowest AIC used.

$$y_{ijk} = \mu + \alpha_i + \beta_j + (\alpha\beta)_{ij} + \gamma_k + \varepsilon_{ijk}, \quad (1)$$

where y_{ijk} is the observation for reach i, season j and sample k; μ is the mean of y; α_i is the fixed effect for reach i; β_j is the fixed effect for season j; $(\alpha\beta)_{ij}$ is the interaction fixed

effect for reach i and season j; $\gamma_k \sim N(0, \sigma_\gamma^2)$ is the random event for the sample and $\varepsilon_{ijk} \sim N(0, \sigma^2)$ is the residual.

$$y_{ijk} = \mu + \alpha_i + \beta_j + \gamma_k + \varepsilon_{ijk}, \quad (2)$$

where y_{ijk} is the observation for reach i, season j and sample k; μ is the mean of y; α_i is the fixed effect for reach i; β_j is the fixed effect for season j; $\gamma_k \sim N(0, \sigma_\gamma^2)$ is the random event for the sample and $\varepsilon_{ijk} \sim N(0, \sigma^2)$ is the residual.

5.3 Results

5.3.1 DOC

DOC concentrations in the surface water were generally similar downstream, with a slight decrease observed in Spring and Autumn (Figure 5.2). The concentration of DOC was highest in Summer.

DOC concentrations did not vary greatly between reach, although concentrations in reach 2 were slightly higher than in reaches 1 and 3 in Autumn (Figure 5.2). Average DOC concentrations in the piezometers were season-dependent, with lowest concentrations found in Winter and Spring.

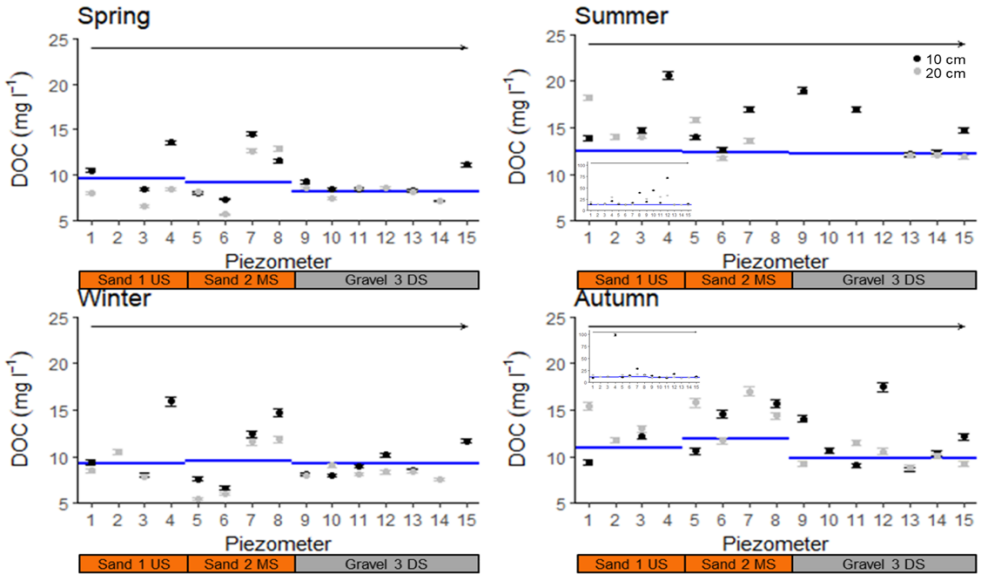

Figure 5.2. Porewater DOC concentrations at 10 (black) and 20 (grey) cm depth, with surface water concentrations for each reach shown with a blue line. The black arrow represents direction of surface flow from upstream to downstream.

5.3.2 Carbon Dioxide

CO_2 concentrations in the surface water were generally similar in reaches 1 and 2, which were greater than in reach 3 (Figure 5.3), with maximum concentrations observed in Winter. CO_2 concentrations were generally highest in reach 2 and lowest in reach 3, which was consistent across all seasons (Figure 5.3). There was little variation in CO_2 concentrations between seasons.

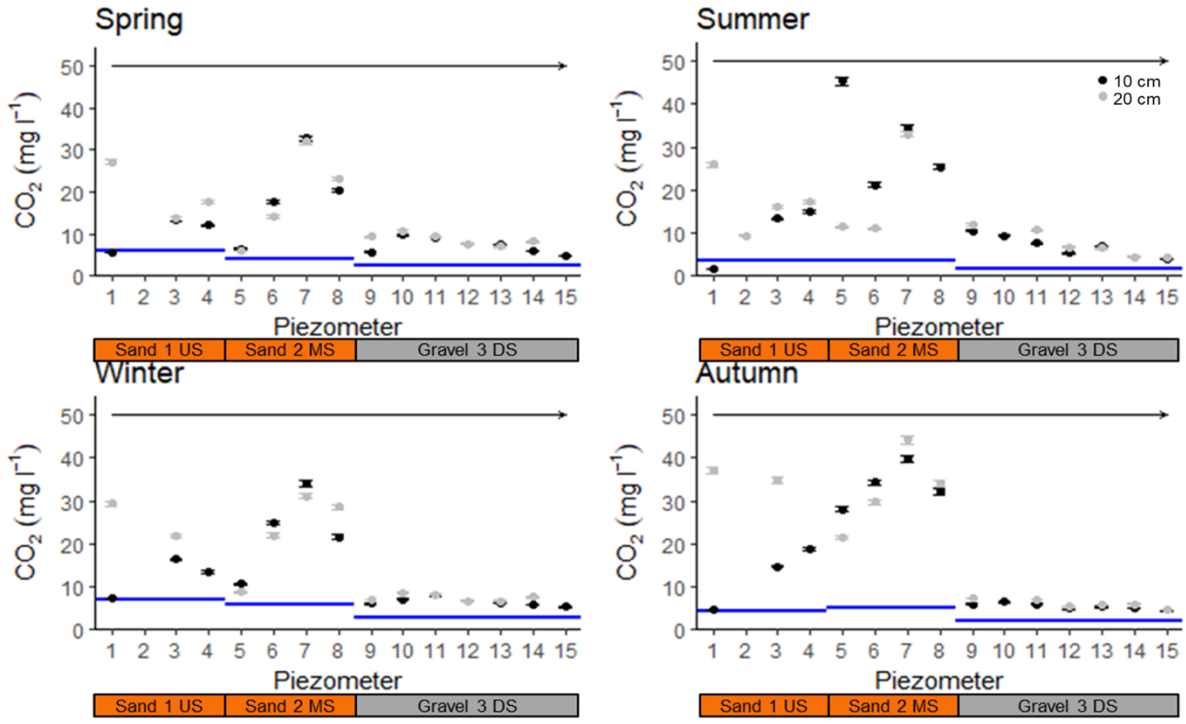

Figure 5.3. Porewater CO_2 concentrations at 10 (black) and 20 (grey) cm depth, with surface water concentrations for each reach shown with a blue line. The black arrow represents direction of surface flow from upstream to downstream.

5.3.3 Methane

CH_4 concentrations in the surface water were generally low in all seasons and reaches, and did not vary greatly between reach (Figure 5.4). Although similar, concentrations were generally greatest in Winter and Spring.

CH_4 concentrations were generally highest in reaches 1 and 2, and lowest in reach 3, which was consistent across all seasons (Figure 5.4). Variation in CH_4 concentrations between seasons was low.

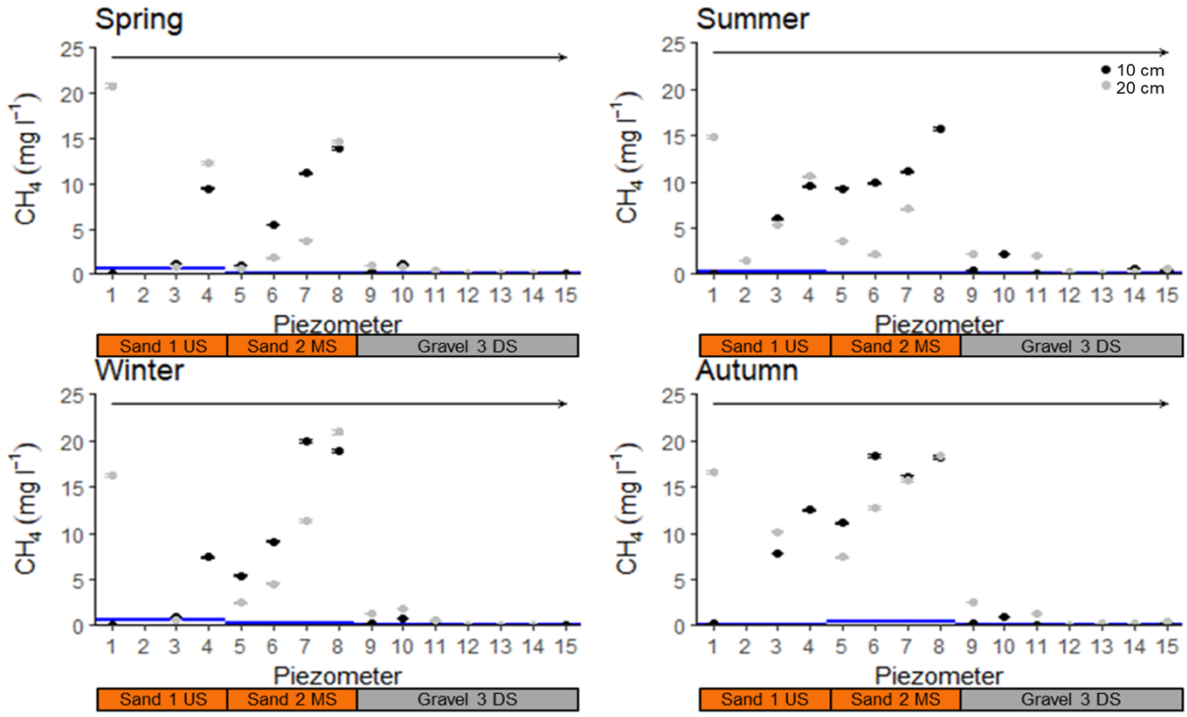

Figure 5.4. Porewater CH_4 concentrations at 10 (black) and 20 (grey) cm depth, with surface water concentrations for each reach shown with a blue line. The black arrow represents direction of surface flow from upstream to downstream.

5.3.4 CH_4:CO_2

The CH_4:CO_2 ratios in the surface water were generally low and generally decreased downstream (Figure 5.5). The variation in CH_4:CO_2 ratio throughout the year was heavily dependent on reach with the largest ratio observed in reach 1 in Spring, in reach 2 in Autumn and in reach 3 in Summer. The smallest ratios observed also varied between reaches, with the smallest ratio observed in reaches 1 and 3 in Autumn, and in reach 2 in Spring.

CH_4:CO_2 ratios in the piezometers were generally highest in reach 2, and lowest in reach 3, which was consistent across all seasons (Figure 5.5). CH_4:CO_2 ratios varied by season but this was not consistent between reaches.

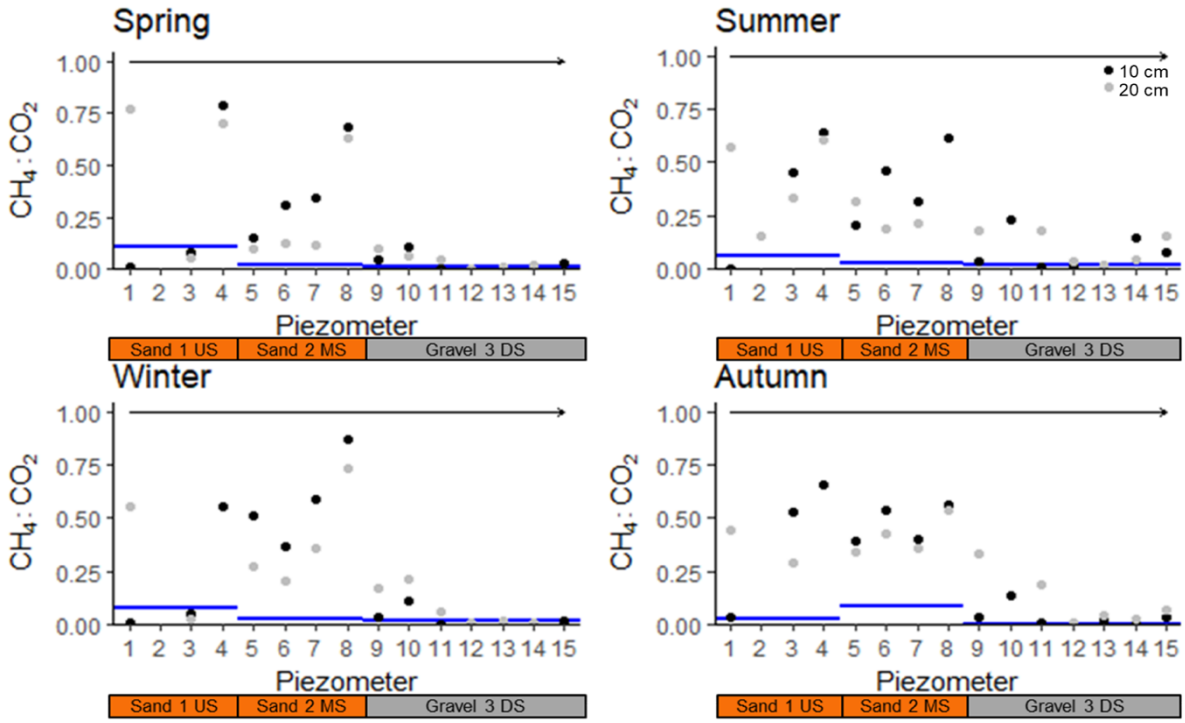

Figure 5.5. Porewater CH_4:CO_2 ratios at 10 (black) and 20 (grey) cm depth, with surface water ratios for each reach shown with a blue line. The black arrow represents direction of surface flow from upstream to downstream.

5.3.5 $\delta^{13}C_{CO2}$

$\delta^{13}C_{CO2}$ ratios in the surface water did not show a consistent pattern between reaches. Ratios were generally similar, and tended to decrease downstream (Figure 5.6). $\delta^{13}C_{CO2}$ ratios did not vary greatly throughout the year.

$\delta^{13}C_{CO2}$ ratios were generally highest in reach 2, and lowest in reach 3, which was consistent across all seasons (Figure 5.6). There was some variation in $\delta^{13}C_{CO2}$ ratios between seasons, however, this was reach-dependent.

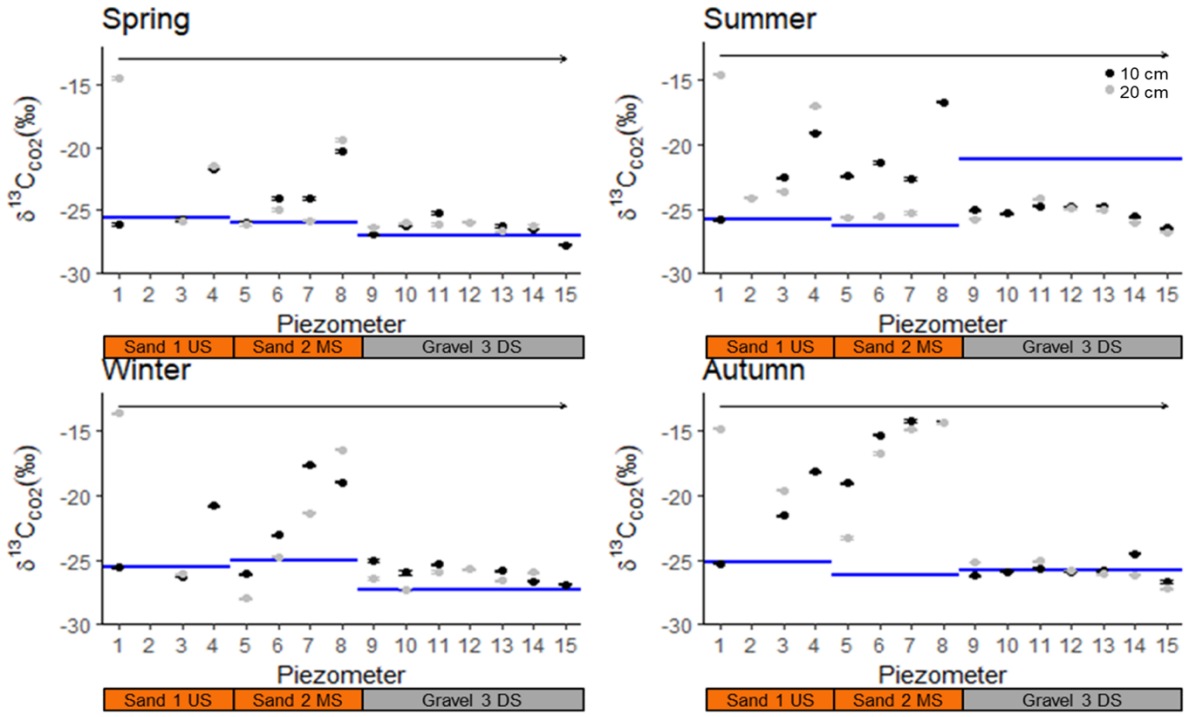

Figure 5.6. Porewater $\delta^{13}C_{CO2}$ ratios at 10 (black) and 20 (grey) cm depth, with surface water ratios for each reach shown with a blue line. The black arrow represents direction of surface flow from upstream to downstream.

5.3.6 DO

DO in the surface water was generally high with similar concentrations found in reaches 1 and 2, and largest concentrations found in reach 3, which was consistent across seasons (Figure 5.7). Variation in DO throughout the year was low, however, the lowest DO was observed in Autumn.

Clear trends in DO were not observed in the piezometers (Figure 5.7). All piezometers had DO concentrations below 50% saturation, except at 10 cm in piezometer 1, which had a similar DO concentration to the surface water of reach 1 in all seasons (between 77.7 and 88.3%), and at 10 cm in piezometer 9 in Spring and Winter. Variation in DO was relatively small in Summer, with % saturation slightly higher in reach 3 than reach 1.

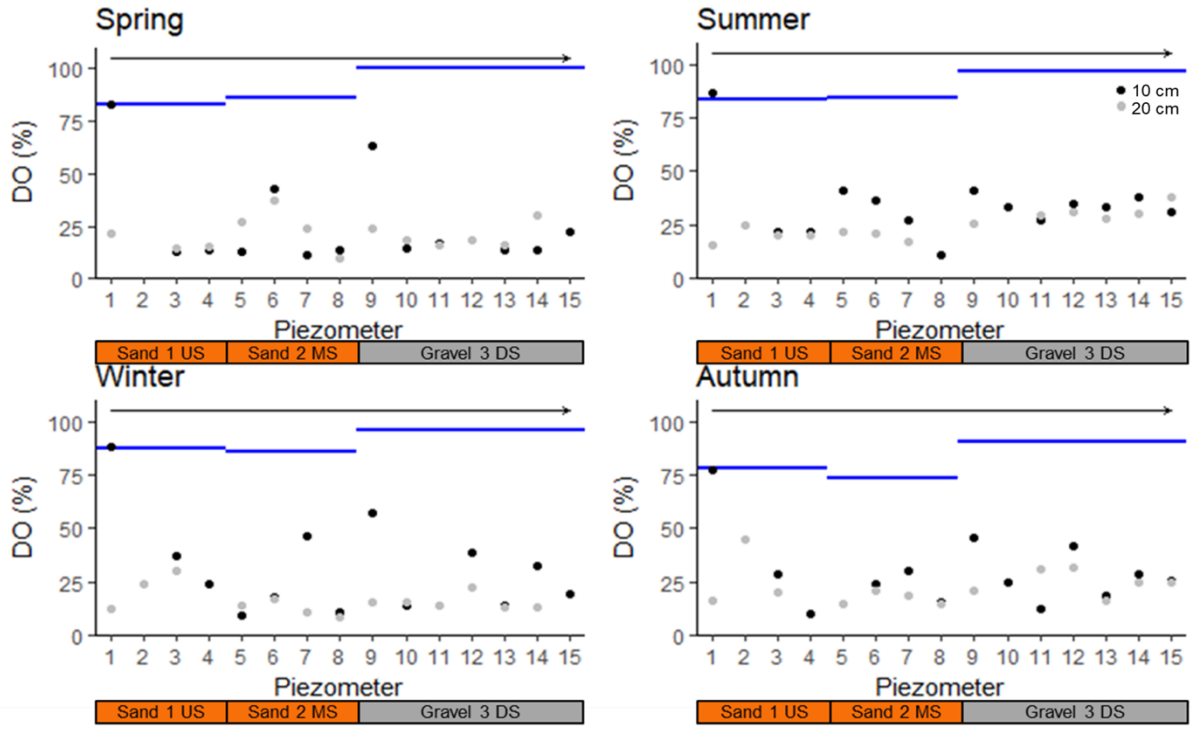

Figure 5.7. Porewater DO at 10 (black) and 20 (grey) cm depth, with surface water DO for each reach shown with a blue line. The black arrow represents direction of surface flow from upstream to downstream.

5.3.7 Temperature

Trends in temperature between the reaches varied greatly depending on season (Figure 5.8). Temperature varied throughout the year, with minimum temperatures found in Winter and maximum temperatures found in Summer.

Clear trends in temperatures in the piezometers were not observed between reaches and seasons (Figure 5.8). In general, temperatures in the piezometers reflected those in the surface water of the respective reach. However, in reach 2 in Winter, temperatures were greater in the piezometers, and in reach 3 temperatures were generally lower in the piezometers.

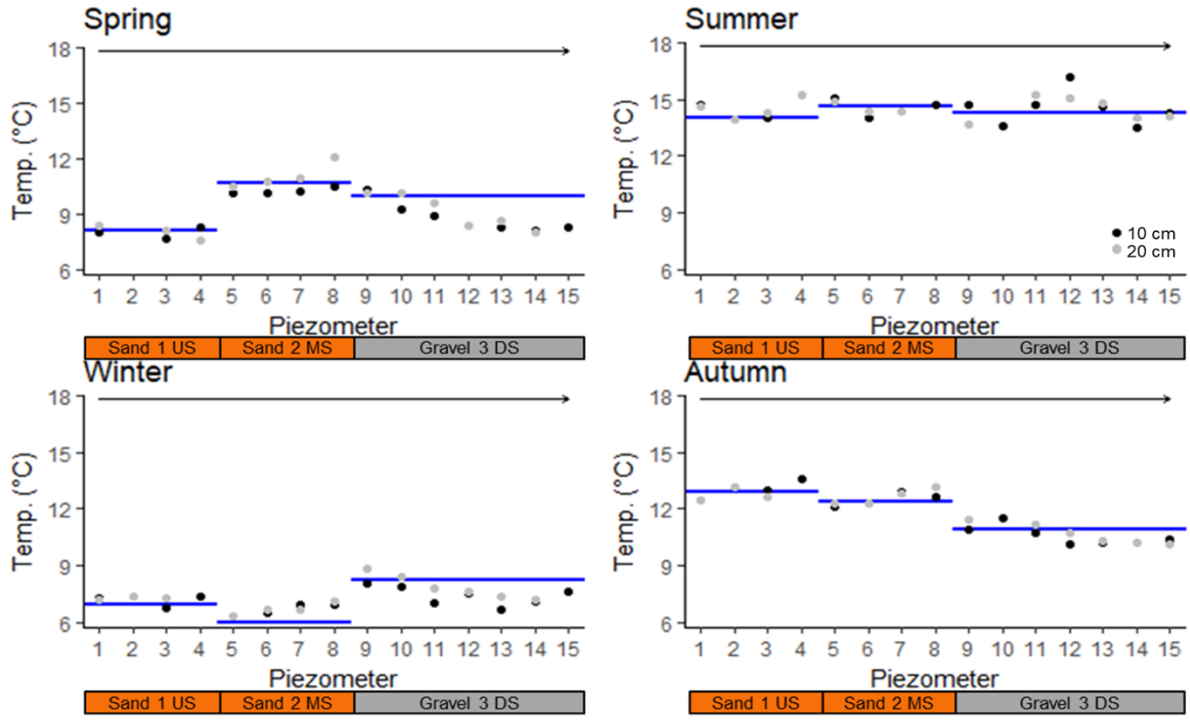

Figure 5.8. Porewater temperature at 10 (black) and 20 (grey) cm depth, with surface water temperatures for each reach shown with a blue line. The black arrow represents direction of surface flow from upstream to downstream.

5.4 Discussion

Surface water concentrations of DOC were relatively high compared to those typically found in agricultural and mixed-use catchments (0.38 to 4.64 mg C l^{-1} [52,56,63,64]), and showed little variation downstream, as observed previously[63]. However, there was a slight decrease from reaches 1 to 3 in Spring and Autumn. Highest DOC concentrations were found in the surface water in Summer and Autumn, which is likely due to C fixation within the stream[60,65]. CO_2 and CH_4 concentrations were generally greater than previous stream observations[7,34,66–70]. However, observed ranges for CO_2 were similar to those observed previously in a temperate peatland stream[69], and maximum CH_4 concentrations similar to those observed in an agricultural stream[70] and a stream influenced by wetlands and spring ponds[68]. CO_2 and CH_4 concentrations typically decreased downstream, likely due to decreases in in-stream productivity downstream, and atmospheric equilibration.

In Autumn, although concentrations decreased from reaches 1 to 3, reach 2 had a greater concentration than reach 2, which was also observed in the DOC data. This increase in C, and subsequent increase in CO_2 and CH_4 production, in reach 2 during Autumn is attributed to a large amount of leaf litter observed in this part of the stream. The highest CO_2 and CH_4 concentrations were found in Winter and Spring, which contradicted our predictions that the largest concentrations would be observed during periods of greatest microbial activity. The observations may be explained, however, by the increased solubility of gases in lower temperature water. CH_4:CO_2 ratios in the surface water were low, which was probably due to the oxidation of CH_4 to CO_2 within the water column.

DOC concentrations observed in the porewaters were consistently high across all reaches, ranging between 5.5±0.2 and 98.9±2.8 mg l^{-1}, with no significant difference between reach observed (p-value = 0.221, Table 5.2). The DOC concentrations observed were greater than those typically observed in agricultural streams (0.95-16.6 mg l^{-1})[34,46,52,71]. The DOC was high year-round, although there was a statistically significant (p-value = 0.000, Table 5.2) increase in DOC from lowest concentrations in Winter and Spring, to highest concentrations in Summer. Elevated concentrations in summer are likely due to an increase in C fixation by microbial communities within the stream during this time[60,65], and have been observed previously in gravel sediments [34]. These high carbon concentrations, coupled with the known increase in dissolved OM availability to microbes in agricultural landscapes[72,73], have the ability to maintain high rates of metabolism year-round, which may have large implications for nutrient spiralling, preventing any carbon limitation. This is particularly important in this agricultural catchment, and could prevent nitrate and ammonium from persisting within the stream.

Table 5.2. Results of the statistical analysis results from the linear mixed-effects modelling, significant p-values are shown in bold.

Parameter	Estimated Value	p-value
DOC		
Intercept	0.067	**0.000**
Reach	0.006	0.221
Season (Autumn-Spring)	0.035	**0.000**
Season (Autumn-Summer)	-0.022	**0.000**
Season (Autumn-Winter)	0.035	**0.000**
CO_2		
Intercept	-0.019	**0.445**
Reach	0.055	**0.000**
Season (Autumn-Spring)	0.000	0.956
Season (Autumn-Summer)	0.000	0.986
Season (Autumn-Winter)	-0.002	0.766
CH_4		
Intercept	2.048	**0.000**
Reach	-0.810	**0.000**
Season (Autumn-Spring)	-0.360	**0.000**
Season (Autumn-Summer)	0.051	0.498
Season (Autumn-Winter)	-0.231	**0.003**
$\delta^{13}C_{CO2}$		
Intercept	5.543	**0.000**
Reach	-0.555	**0.000**
Season (Autumn-Spring)	-1.070	**0.000**
Season (Autumn-Summer)	-0.756	**0.000**
Season (Autumn-Winter)	-0.886	**0.000**
Interaction Reach and Season (Autumn-Spring)	0.296	**0.000**
Interaction Reach and Season (Autumn-Summer)	0.238	**0.002**
Interaction Reach and Season (Autumn-Winter)	0.254	**0.001**

CO_2 and CH_4 concentrations were consistently elevated in the sediments compared to the surface water, which is consistent with previous observations[34,66]. The greatest concentrations of carbon dioxide, methane, ratios of CH_4:CO_2 and $\delta^{13}C_{CO2}$ ratios were co-located in the sand sediments of reach 2, with high concentrations and ratios also found in the sand sediments of reach 1. This resulted in statistically significant differences in CO_2, CH_4 and $\delta^{13}C_{CO2}$ between reaches (p-value = 0.000, 0.000 and 0.000, respectively, Table 5.2), and reflects increased residence times and areas of anoxia, which are typically associated with sand sediments[28,52,53], resulting in greater metabolic rates. Additionally, methane production is typically greater in fine, OM-rich sediments, explaining an increase in methane

concentrations in the sand sediments[7,15,56,57]. Low CH_4:CO_2 ratios were observed in reach 3, which may be due to oxidation of CH_4 to CO_2 in these generally oxygenated sediments, and that gravel sediments are usually sources of CO_2 but sinks of CH_4[55].

Carbon dioxide concentrations found in the porewaters of reach 1 were similar to previous observations of CO_2 in stream sediments, which ranged between 4.3 and 14.5 mg l^{-1} [34,74], however, maximum concentrations observed here were greater than these. The lowest of these previously observed values are from gravel sediments, suggesting sand sediments are characterized by higher concentrations. Previous work has shown that the contribution of gravel bar CO_2 to the atmosphere is significant[75], however, the low concentrations found in the gravel sediments here show that sand bedforms may be of greater importance. CO_2 concentrations in the porewaters of reach 2 were greater than those previously observed, with a maximum concentration of 45.4±1.0 mg l^{-1}. Larger CO_2 concentrations (231 mg l^{-1}) have been observed previously in the streambed[35], however these were observed in fine sediments trapped below macrophytes where substrate is plentiful.

The patterns in CH_4 concentrations were similar to those of the CO_2. The porewaters of reaches 1 and 2 had large ranges of CH_4 concentrations (4.1 μg l^{-1} to 20.8 mg l^{-1} and 600 μg l^{-1} and 21.0 mg l^{-1}, respectively), which have been observed previously in a gravel bar (8.7 μg l^{-1} to 11.8 mg l^{-1})[67]. The maximum concentration observed here, however, was much greater, probably due to residence times and anoxia typically being greater in sand than gravel sediments. Although the maximum concentrations were similar between reaches 1 and 2, concentrations in reach 2 were generally greater than in reach 1, and concentrations in both reaches were generally greater than those previously observed[7,34,66,70,74].

The observed carbon dioxide concentrations within the gravel sediments were similar to those seen previously in a gravel bar[34]. Here CO_2 ranged from 3.9 to 11.9 mg l^{-1}, virtually the same as those observed previously[34]. These values were not as low as those found in reach 1

and 2, which indicates that although gravel bars tend to have lower maximum concentrations of CO_2, they also have lower ranges than sand sediments. This may be due to more heterogeneity and pockets of anoxia within the sand sediments, which may lead to lower concentrations of CO_2 in certain areas.

Methane concentrations in the gravel sediments were relatively low and were similar to those observed previously in a gravel bar[34,66], with the maximum concentration observed here (2.5 mg CH_4 l^{-1}) similar to previous research (2.2 mg CH_4 l^{-1} [34]). However, these maximum concentrations were lower than previously observed gravel concentrations of 11.8 mg CH_4 l^{-1} [67]; this previous research indicates that a large range of methane concentrations should be expected in gravel sediments, with the lowest observed concentration only 8.7 μg CH_4 l^{-1} [67]. Surprisingly, given that fine, OM-rich sediments, ideal for methanogenesis, are typically found beneath vegetation[7,15,70,76], the CH_4 concentrations observed here in non-vegetated gravel sediments were similar, with a slightly greater maximum, to those observed in vegetated gravel sediments[7].

The seasonal variation of carbon dioxide and methane within the sediments was relatively small, with large concentrations observed throughout the year. The concentration of CO_2 did not vary significantly throughout the year (p-value > 0.445, Table 5.2), however, the concentration of CH_4 was significantly different between season (p-value < 0.003, Table 5.2). This contradicts previous work in a gravel bar, which has shown significant increases in carbon dioxide and methane concentrations during summer months (11.04±1.8 mg CO_2 l^{-1} and 302±71 μg CH_4 l^{-1} in Summer, and 4.3±0.27 mg CO_2 l^{-1} and 129±36 μg CH_4 l^{-1} in Winter)[34], as well as significant increases in CO_2 fluxes to the atmosphere in Summer[75]. To the authors knowledge there have been no other studies that measured concentrations of streambed CO_2 and CH_4 in Winter. Given the large concentrations found year-round in this study, further work is required to determine the concentrations of CO_2 and CH_4 in sediments

in all seasons in various systems, as well as the drivers controlling these. Here, temperature may have been controlling the low seasonal variation in CO_2 and CH_4 concentrations. Although temperature increased from 5-7°C in Winter to 14-17°C in Summer, this range was below the threshold of elevated temperature of 26°C, required to produce a substantial increase in sediment CO_2 and CH_4 production in sandstone streams.

Surface water $\delta^{13}C_{CO2}$ ratios, were typically consistent between reaches and seasons, implying the sources and processes affecting the carbon entering the stream were similar both spatially and temporally. Porewater $\delta^{13}C_{CO2}$ ratios, however, differed significantly between reaches (p-value = 0.000, Table 5.2), with the greatest ratios found in reach 2, and the smallest ratios found in reach 3. This suggests that streambed carbon processing was different between the reaches, with *in-situ* CO_2 production occurring. The positive, linear relationship between CO_2 concentration and $\delta^{13}C_{CO2}$ ratio (Figure 5.9) provides further evidence of *in-situ* CO_2 production; indicating that the $\delta^{13}C_{CO2}$ ratio becomes increasingly greater as more of the residual ^{13}C-enriched carbon source is incorporated.

The greatest *in-situ* CO_2 production likely occurred in reach 2, where CO_2 concentrations and $\delta^{13}C_{CO2}$ ratios were greatest, with the lowest *in-situ* CO_2 production occurring in reach 3 where the opposite was observed. The sediments of reach 1 also indicate substantial *in-situ* production (Figure 5.9). Our results therefore indicate that *in-situ* CO_2 production is greatest in sand than gravel sediments, although it should be noted that the source of carbon and its $\delta^{13}C_{CO2}$ ratio at this study site is unknown.

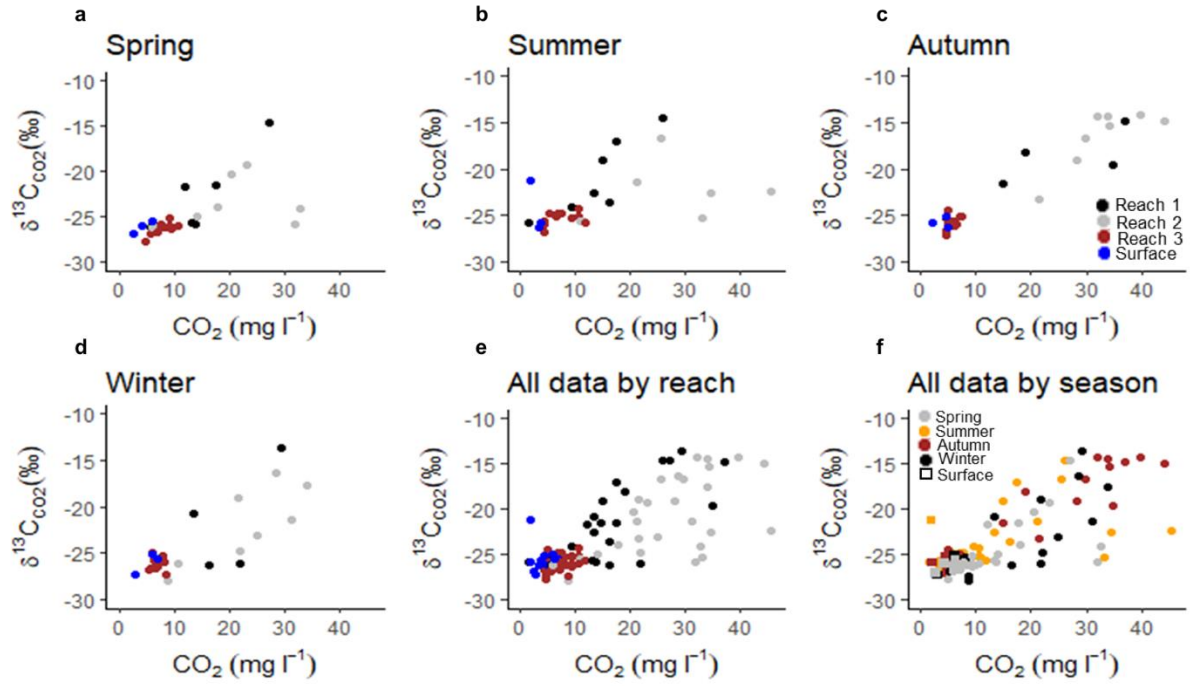

Figure 5.9. $\delta^{13}C_{CO2}$ plotted against CO_2 concentration for a. Spring separated by reach, b. Summer separated by reach, c. Autumn separated by reach, d. Winter separated by reach, e. All data separated by reach and f. All data separated by season.

Our results of high CO_2 and CH_4 concentrations in sand sediments of a small, non-vegetated, agricultural stream, which are systems known to contribute disproportionately to the annual C flux from streams and rivers[3], may indicate that C fluxes are currently underestimated. This may further explain estimations that small streams contribute disproportionately to the global CO_2 efflux from streams and rivers[3]. Bednařík et al., (2015)[67] determined that the contribution of the benthic flux of CH_4 from gravel sediments to overall CH_4 fluxes from the surface water were negligible (<1%). Our study, however, resulted in much larger concentrations and was conducted in sand sediments, where anoxia is generally greater, and where organic carbon was high, which has been associated with high methane ebullition[56]. Therefore, there may be a larger contribution of the benthic flux to overall CH_4 emissions here and further work is required to determine the contribution of benthic CH_4 from sand sediments. Additionally, further work is required to fully develop our understanding of the

contribution of the total benthic CO_2 and CH_4 flux to overall stream emissions, and the factors controlling CO_2 and CH_4 production within streambed sediments.

5.5 Conclusions

We found that carbon turnover and large CO_2 and CH_4 concentrations, were controlled by sediment type, with significantly greater carbon turnover observed in the sand than gravel sediments. This resulted in the largest *in-situ* CO_2 production and CH_4:CO_2 ratios observed in the sand sediments, indicating that CO_2 and CH_4 production was co-located, and relatively large concentrations of CH_4 were occurring in these typically anoxic environments. We found large concentrations of CO_2 and CH_4, and *in-situ* CO_2 production year-round, with no statistically significant seasonal influence observed on CO_2 concentrations, which has potential implications for annual carbon fluxes from streams and rivers to the atmosphere. Our results have wide repercussions for stream management approaches, particularly in small, agricultural streams where fine sediment and OM loading is typically high. They suggest that the reduction of sand sediments could reduce the carbon turnover within streambed sediments, and subsequently decrease the carbon flux from streams.

Further work to increase knowledge and understanding of carbon turnover and associated CO_2 and CH_4 production in streambed sediments, as well as the contribution of the benthic flux to the overall stream flux, is required. This is particularly important given that agricultural streams are a hotspot for fine sediment and OM loading[15,77], which are predicted to increase due to future land-use change[15], along with increased metabolic rates[39].

5.6 Acknowledgments

The authors would like to thank BIFoR for their support and use of the study site and Dr. Andy Stott at the NERC Life Sciences Mass Spectrometry Facility (LSMSF) for guidance and sample analysis. Additionally, we would like to thank Dr. Ben Marchant for his advice on the statistical analysis and Dr. Phillip Blaen for field and laboratory assistance. This work

was funded by NERC through a Central England NERC Training Alliance Studentship and grant NE/L004437/1. Additional funding was provided by the European Union through the H2020-MSCA-RISE-2016 project 734317, and the isotopic analysis of carbon dioxide was funded by the LSMSF (Grant number CEH_L102_05_2016).

5.7 References

1. Cole, J. J. *et al.* Plumbing the Global Carbon Cycle: Integrating Inland Waters into the Terrestrial Carbon Budget. *Ecosystems* **10,** 172–185 (2007).

2. Battin, T. J. *et al.* The boundless carbon cycle. *Nat. Geosci.* **2,** 598–600 (2009).

3. Raymond, P. a *et al.* Global carbon dioxide emissions from inland waters. *Nature* **503,** 355–359 (2013).

4. Trimmer, M. *et al.* River bed carbon and nitrogen cycling: state of play and some new directions. *Sci. Total Environ.* **434,** 143–58 (2012).

5. Tranvik, L. J. *et al.* Lakes and reservoirs as regulators of carbon cycling and climate. *Limnol. Oceanogr.* **54,** 2298–2314 (2009).

6. Striegl, R. G., Dornblaser, M. M., McDonald, C. P., Rover, J. R. & Stets, E. G. Carbon dioxide and methane emissions from the Yukon River system. *Global Biogeochem. Cycles* **26,** (2012).

7. Sanders, I. a. *et al.* Emission of methane from chalk streams has potential implications for agricultural practices. *Freshw. Biol.* **52,** 1176–1186 (2007).

8. Raymond, P. A., Caraco, N. F. & Cole, J. J. Carbon Dioxide Concentration and Atmospheric Flux in the Hudson River. *Estuaries* **20,** 381–390 (1997).

9. Frankignoulle, M. *et al.* Carbon Dioxide Emission from European Estuaries. *Science (80-.).* **282,** 434–436 (1998).

10. Kling, G. W., Kipphjtt, G. W. & Miller, M. C. Arctic Lakes and Streams as Gas Conduits to the Atmosphere: Implications for Tundra Carbon Budgets CO2. *Science (80-.).* **251,** 298–301 (1991).

11. Park, P. K., Gordon, L. I., Hager, S. W. & Cissell, M. C. Carbon Dioxide Partial Pressure in the Columbia River. *Science (80-.).* **166,** 867–868 (1969).

12. Crawford, J. T. & Stanley, E. H. Controls on methane concentrations and fluxes in streams draining human-dominated landscapes. *Ecol. Appl.* 15–1330.1 (2015). doi:10.1890/15-1330.1

13. Maurice, L., Rawlins, B. G., Farr, G., Bell, R. & Gooddy, D. C. The influence of flow and bed slope on gas transfer in steep streams and their implications for evasion of CO_2. *J. Geophys. Res. Biogeosciences* (2017). doi:10.1002/2017JG004045

14. Richey, J. E., Melack, J. M., Aufdenkampe, A. K., Ballester, V. M. & Hess, L. L. Outgassing from Amazonian rivers and wetlands as a large tropical source of atmospheric CO2. *Nature* **416,** 617–620 (2002).

15. Stanley, E. H. *et al.* The ecology of methane in streams and rivers: Patterns, controls, and global significance. *Ecol. Monogr.* **86,** 146–171 (2016).

16. Panneer Selvam, B., Natchimuthu, S., Arunachalam, L. & Bastviken, D. Methane and carbon dioxide emissions from inland waters in India - implications for large scale greenhouse gas balances. *Glob. Chang. Biol.* **20,** 3397–3407 (2014).

17. Crawford, J. T. *et al.* CO2 and CH4 emissions from streams in a lake-rich landscape: Patterns, controls, and regional significance. *Glob. Chang. Biol.* **20,** 3408–22 (2014).

18. Bastviken, D. *et al.* Freshwater methane emissions offset the continental carbon sink. *Science.* **331,** 50 (2011).

19. Hotchkiss, E. R. *et al.* Sources of and processes controlling CO2 emissions change with the size of streams and rivers. *Nat. Geosci.* **8,** 696–699 (2015).

20. De Fátima F. L. Rasera, M. *et al.* Estimating the surface area of small rivers in the

southwestern amazon and their role in CO2 outgassing. *Earth Interact.* **12,** 1–16 (2008).

21. Battin, T. J., Kaplan, L. a, Newbold, J. D. & Hendricks, S. P. A mixing model analysis of stream solute dynamicsand the contribution of a hyporheic zone to ecosystemfunction. *Freshw. Biol.* **48,** 995–1014 (2003).

22. McClain, M. E. *et al.* Biogeochemical Hot Spots and Hot Moments at the Interface of Terrestrial and Aquatic Ecosystems. *Ecosystems* **6,** 301–312 (2003).

23. Lautz, L. K. & Fanelli, R. M. Seasonal biogeochemical hotspots in the streambed around restoration structures. *Biogeochemistry* **91,** 85–104 (2008).

24. Krause, S., Tecklenburg, C., Munz, M. & Naden, E. Streambed nitrogen cycling beyond the hyporheic zone: Flow controls on horizontal patterns and depth distribution of nitrate and dissolved oxygen in the upwelling groundwater of a lowland river. *J. Geophys. Res. Biogeosciences* **118,** 54–67 (2013).

25. Jones, J. B. & Holmes, R. M. Surface-subsurface interactions in stream ecosystems. *Trends Ecol. Evol.* **11,** 239–242 (1996).

26. Krause, S. *et al.* Inter-disciplinary perspectives on processes in the hyporheic zone. **499,** 481–499 (2011).

27. Seitzinger, S. *et al.* Denitrification across landscaes and waterscapes: a synthesis. *Ecol. Appl.* **16,** 2064–2090 (2006).

28. Boulton, A. J., Findlay, S., Marmonier, P., Stanley, E. H. & Valett, H. M. The Functional Significance of the Hyporheic Zone in Streams and Rivers. *Annu. Rev. Ecol. Syst.* **29,** 59–81 (1998).

29. Krause, S., Louise Heathwaite, a., Binley, A. & Keenan, P. Nitrate concentration

changes at the groundwater-surface water interface of a small Cumbrian river. *Hydrol. Process.* **23,** 2195–2211 (2009).

30. Hlaváčová, E., Rulík, M., Čáp, L. & Mach, V. Greenhouse gas (CO2, CH4, N2O) emissions to the atmosphere from a small lowland stream in Czech Republic. *Arch. für Hydrobiol.* **165,** 339–353 (2006).

31. Findlay, S. Importance of surface-subsurface exchange in stream ecosystems: The hyporheic zone. *Limnol. Oceanogr.* **40,** 159–164 (1995).

32. Boano, F., Revelli, R. & Ridolfi, L. Effect of streamflow stochasticity on bedform-driven hyporheic exchange. *Adv. Water Resour.* (2010). doi:10.1016/j.advwatres.2010.03.005

33. Houghton, R. A. The worldwide extent of land-use change. *Bioscience* **44,** (1994).

34. Hlaváčová, E., Rulík, M. & Čáp, L. Anaerobic microbial metabolism in hyporheic sediment of a gravel bar in a small lowland stream. *River Res. Appl.* **21,** 1003–1011 (2005).

35. Trimmer, M., Sanders, I. A. & Heppell, C. M. Carbon and nitrogen cycling in a vegetated lowland chalk river impacted by sediment. **2238,** 2225–2238 (2009).

36. Yvon-Durocher, G., Montoya, J. M., Woodward, G., Jones, J. I. & Trimmer, M. Warming increases the proportion of primary production emitted as methane from freshwater mesocosms. *Glob. Chang. Biol.* **17,** 1225–1234 (2011).

37. Orr, H. G. *et al.* Detecting changing river temperatures in England and Wales. *Hydrol. Process.* **29,** 752–766 (2015).

38. Kaushal, S. S. *et al.* Rising stream and river temperatures in the United States. *Front. Ecol. Environ.* **8,** 461–466 (2010).

39. Venkiteswaran, J. J., Rosamond, M. S. & Schiff, S. L. Nonlinear response of riverine N2O fluxes to oxygen and temperature. *Environ. Sci. Technol.* **48,** 1566–1573 (2014).

40. Acuña, V., Wolf, A., Uehlinger, U. & Tockner, K. Temperature dependence of stream benthic respiration in an Alpine river network under global warming. *Freshw. Biol.* **53,** 2076–2088 (2008).

41. Fischer, H., Kloep, F., Wilzcek, S. & Pusch, M. T. A river's liver - Microbial processes within the hyporheic zone of a large lowland river. *Biogeochemistry* **76,** 349–371 (2005).

42. Hedin, L. O. *et al.* Thermodynamic Constraints on Nitrogen Transformations and Other Biogeochemical Processes at Soil-Stream Interfaces. *Ecology* **79,** 684–703 (1998).

43. Boulton, A., Findlay, S. & Marmonier, P. The functional significance of the hyporheic zone in streams and rivers. *Annu. Rev. Ecol. Syst.* 59–81 (1998). doi:10.1146/annurev.ecolsys.29.1.59

44. Stanford, J. A. & Ward, J. V. An ecosystem perspective of alluvial rivers: Connectivity and the hyporheic corridor. *J. North Am. Benthol. Soc.* **12,** 48–60 (1993).

45. Brunke, M. & Gonser, T. The ecological significance of exchange processes between rivers and groundwater. *Freshw. Biol.* **37,** 1–33 (1997).

46. Zarnetske, J. P., Haggerty, R., Wondzell, S. M. & Baker, M. a. Dynamics of nitrate production and removal as a function of residence time in the hyporheic zone. *J. Geophys. Res.* **116,** G01025 (2011).

47. Gomez-Velez, J. D., Krause, S. & Wilson, J. L. Effect of low-permeability layers on spatial patterns of hyporheic exchange and groundwater upwelling. *Water Resour. Res.*

(2014). doi:10.1002/2013WR015054

48. Marzadri, A., Tonina, D. & Bellin, A. Quantifying the importance of daily stream water temperature fluctuations on the hyporheic thermal regime: Implication for dissolved oxygen dynamics. *J. Hydrol.* (2013). doi:10.1016/j.jhydrol.2013.10.030

49. Mulholland, P. J. *et al.* Stream denitrification across biomes and its response to anthropogenic nitrate loading. *Nature* **452,** 202–205 (2008).

50. Deforet, T. *et al.* Do parafluvial zones have an impact in regulating river pollution? Spatial and temporal dynamics of nutrients, carbon, and bacteria in a large gravel bar of the Doubs River (France). *Hydrobiologia* (2009). doi:10.1007/s10750-008-9661-0

51. Bardini, L., Boano, F., Cardenas, M. B., Revelli, R. & Ridolfi, L. Nutrient cycling in bedform induced hyporheic zones. *Geochim. Cosmochim. Acta* (2012). doi:10.1016/j.gca.2012.01.025

52. Lansdown, K. *et al.* The interplay between transport and reaction rates as controls on nitrate attenuation in permeable, streambed sediments. *J. Geophys. Res. G Biogeosciences* **120,** 1093–1109 (2015).

53. Baker, M. A., Dahm, C. N. & Valett, H. M. in *Streams and Ground Waters* (eds. Jones, J. B. & Mulholland, P. J.) 259–283 (Elsevier, 2000). doi:10.1016/B978-0-12-389845-6.50012-0

54. Jones, J. B. & Mulholland, P. J. Influence of drainage basin topography and elevation on carbon dioxide and methane supersaturation of stream water. *Biogeochemistry* **40,** 57–72 (1998).

55. Trimmer, M., Maanoja, S., Hildrew, A. G., Pretty, J. L. & Grey, J. Potential carbon fixation via methane oxidation in well-oxygenated riverbed gravels. **55,** 560–568

(2010).

56. Baulch, H. M., Dillon, P. J., Maranger, R. & Schiff, S. L. Diffusive and ebullitive transport of methane and nitrous oxide from streams: Are bubble-mediated fluxes important? *J. Geophys. Res.* **116,** G04028 (2011).

57. Sawakuchi, H. O. *et al.* Methane emissions from Amazonian Rivers and their contribution to the global methane budget. *Glob. Chang. Biol.* **20,** 2829–2840 (2014).

58. Graeber, D., Gelbrecht, J., Pusch, M. T., Anlanger, C. & von Schiller, D. Agriculture has changed the amount and composition of dissolved organic matter in Central European headwater streams. *Sci. Total Environ.* **438,** 435–446 (2012).

59. Stanley, E. H., Powers, S. M., Lottig, N. R., Buffam, I. & Crawford, J. T. Contemporary changes in dissolved organic carbon (DOC) in human-dominated rivers: Is there a role for DOC management? *Freshw. Biol.* **57,** 26–42 (2012).

60. Blaen, P. J. *et al.* High-frequency monitoring of catchment nutrient exports reveals highly variable storm event responses and dynamic source zone activation. *J. Geophys. Res. Biogeosciences* 1–17 (2017). doi:10.1002/2017JG003904

61. Hudson, F. Sample Preparation and Calculations for Dissolved Gas Analysis in Water Samples Using a GC Headspace Equilibration Technique. 1–14 (2004). doi:10.1111/j.1365-2133.2004.v151_is68_disclaimer.x

62. Wilhelm, E., Battino, R. & Wilcock, R. J. Low-Pressure Solubility of Gases in Liquid Water. *Chem. Rev.* **77,** 219–262 (1977).

63. Casas-Ruiz, J. P. *et al.* A tale of pipes and reactors: Controls on the in-stream dynamics of dissolved organic matter in rivers. *Limnol. Oceanogr.* (2017). doi:10.1002/lno.10471

64. Jarvie, H. P. *et al.* Within-river nutrient processing in Chalk streams: The Pang and Lambourn, UK. *J. Hydrol.* **330,** 101–125 (2006).

65. Jaffé, R. *et al.* Spatial and temporal variations in DOM composition in ecosystems: The importance of long-term monitoring of optical properties. *J. Geophys. Res. Biogeosciences* **113,** 1–15 (2008).

66. Rulik, M., Cap, L. & Hlavacova, E. Methane in the Hyporheic Zone of a Small Lowland Stream (Sitka , Czech Republic). **30,** 359–366 (2000).

67. Bednařík, A., Čáp, L., Maier, V. & Rulík, M. Contribution of Methane Benthic and Atmospheric Fluxes of an Experimental Area (Sitka Stream). *CLEAN - Soil, Air, Water* **43,** 1136–1142 (2015).

68. Crawford, J. T. *et al.* Spatial heterogeneity of within-stream methane concentrations. *J. Geophys. Res. Biogeosciences* **122,** 1036–1048 (2017).

69. Hope, D., Palmer, S. M., Billett, M. F. & Dawson, J. J. C. Carbon dioxide and methane evasion from a temperate peatland stream. *Limnol. Oceanogr.* **46,** 847–857 (2001).

70. Wilcock, R. J. & Sorrell, B. K. Emissions of Greenhouse Gases CH4 and N2O from Low-gradient Streams in Agriculturally Developed Catchments. *Water. Air. Soil Pollut.* **188,** 155–170 (2008).

71. Ullah, S. *et al.* Influence of emergent vegetation on nitrate cycling in sediments of a groundwater-fed river. *Biogeochemistry* **118,** 121–134 (2014).

72. Wilson, H. F. & Xenopoulos, M. A. Effects of agricultural land use on the composition of fluvial dissolved organic matter. *Nat. Geosci.* **2,** 37–41 (2009).

73. Williams, C. J., Yamashita, Y., Wilson, H. F., Jaffe, R. & Xenopoulos, M. A. Unraveling the role of land use and microbial activity in shaping dissolved organic

matter characteristics in stream ecosystems. *Limnol. Oceanogr.* **55,** 1159–1171 (2010).

74. Schindler, J. E. & Krabbenhoft, D. P. The hyporheic zone as a source of dissolved organic carbon and carbon gases to a temperate forested stream. 157–174 (1998).

75. Boodoo, K. S., Trauth, N., Schmidt, C., Schelker, J. & Battin, T. J. Gravel bars are sites of increased CO2 outgassing in stream corridors. *Sci. Rep.* **7,** 1–9 (2017).

76. Heffernan, J. B., Sponseller, R. A. & Fisher, S. G. Consequences of a biogeomorphic regime shift for the hyporheic zone of a Sonoran Desert stream. *Freshw. Biol.* **53,** 1954–1968 (2008).

77. Wood, P. J. & Armitage, P. D. Biological Effects of Fine Sediment in the Lotic Environment. *Environ. Manage.* **21,** 203–217 (2007).

Chapter 6: Sediment type and season as factors controlling nutrient cycling in agricultural streams. Part II Nitrogen

Sophie A. Comer-Warner[1], Daren C. Gooddy[2], Liam Glover[3], Aishling Percival[3,4], Sami Ullah[1,3], Nick Kettridge[1], Sarah K. Wexler[5], Jan Kaiser[5] and Stefan Krause[1]

1. School of Geography, Earth and Environmental Sciences, University of Birmingham, Edgbaston, Birmingham B15 2TT, UK

2. British Geological Survey (BGS), Maclean Building, Wallingford, Oxfordshire OX10 8BB, UK

3. School of Geography, Geology and the Environment, University of Keele, Keele, Newcastle ST5 5BG, UK

4. School of Chemical and Pharmaceutical Sciences, Dublin Institute of Technology, Kevin Street, Dublin, D08 X622, Ireland

5. Centre for Ocean and Atmospheric Sciences, School of Environmental Sciences, University of East Anglia, Norwich Research Park, Norwich NR4 7TJ, UK

6.1 Introduction

Large inputs of nutrients, such as nitrate and ammonium, transported to freshwater ecosystems either directly or through subsurface flows, are a major issue in agricultural catchments[1]. This is due to high nitrogen concentrations often leading to eutrophication, causing a reduction in oxygen content, water quality, and adequate stream habitats[1–4]. Regulating surface water nitrate and ammonium concentrations in these environments is, therefore, of upmost importance to the overall health of these ecosystems.

Within streams and rivers, sediments have been identified as hotspots of biogeochemical reactivity[5–8], due to observations of increased residence time and substrate availability within these environments[9–13]. Sediments, therefore, tend to have large rates of nutrient attenuation,

leading to reductions in nitrate concentrations and subsequent improvements in surface water quality, ecosystem services and ecosystem health[14–16].

Although agricultural catchments often have large inputs of nutrients, they have also been identified as areas able to support dissimilatory reduction of nitrate to N_2 gas, mainly through denitrification[17–20]. Denitrification is a key process in nitrate removal in stream sediments, as denitrification rates are usually elevated in the streambed relative to the surface water[21]. Streambed denitrification is controlled by substrate availability, C quality, redox conditions, temperature, enzyme activity and pH[22–29], which are often influenced by sediment type. Additionally, recent work has shown that sediment residence times are a key control on denitrification, with short residence times unable to support substantial nitrate reduction, and long residence times resulting in complete denitrification and associated water quality improvements[21]. While denitrification is a permanent removal mechanism for the removal of reactive nitrogen, this process also produces the GHG N_2O.

Denitrification is a multistep reaction and N_2O may be produced when the process is incomplete[21,30,31], with the reduction of N_2O via denitrification the only substantial pathway for the biological removal of N_2O[32]. When nitrate concentrations are high, the relative amount of N_2O produced by denitrification increases[33], which may lead to high concentrations of N_2O in aquatic ecosystems[17–20]. Agricultural catchments, therefore, are hotspots of anthropogenic N_2O emissions[34–36]. N_2O is also produced as a by-product of nitrification or dissimilative nitrate reduction to ammonium[37–39], the latter being of minor magnitude compared to nitrification and denitrification. Although denitrification is known to be the predominant source of N_2O in soils and hyporheic sediments[40–42], recent research found ammonium oxidation was the major producer of N_2O in estuarine sediments[43]. Further investigation, therefore, is required to explain the processes and environmental drivers controlling N_2O production in sediments. Recent work addressing these research questions

determined that intermediate residence times lead to partial denitrification, resulting in a reduction in nitrate concentration and increase in water quality, but producing N_2O[21,44]. For example, an optimal residence time of 9 hours for N_2O production was determined in experiments conducted in sand dunes[21].

Production of N_2O is crucial to understand given that it is a GHG approximately 298 times more potent than CO_2 on a mole per mole basis[45], with a large ozone-depleting potential compared to other anthropogenic substances[46], in the 21st Century. Current estimates of N_2O emissions from rivers predict ranges from 0.1 to 0.68 Tg N_2O-N yr^{-1} [47,48], depending on whether anthropogenic emissions are included, with the highest estimate equal to approximately 10% of global anthropogenic emissions[48]. Given the potential of streambeds to be a significant source of global N_2O[48–50], and that the factors controlling N_2O production in stream sediments remain poorly understood[21], research into streambed N_2O production is crucial.

Characterising the key processes of streambed denitrification and N_2O production through the investigation of substrate, environmental and physical controls enables further understanding of key drivers. Fluorescein diacetate (FDA) hydrolysis and extracellular phenol oxidase activity provide information on substrate controls on microbial activity, and C and N uptake. FDA hydrolysis includes the activity of proteases, lipases and esterases in soils and sediments, which represents microbial-mediated organic carbon turnover and decomposition rates, through the secretion of these extra-cellular enzymes. Sediment type can have a large influence on the quality and quantity of organic C, and thus FDA can be used as a surrogate of total microbial activity and organic C decomposition to understand biogeochemical reactivity[51]. This is particularly important in hyporheic sediments, where enzyme activity is poorly studied. Extracellular phenol oxidase activity is used to indicate the microbial decomposition of aromatic phenolic compounds, for the procurement of carbon and nutrients,

particularly N[52]. This assay predominantly captures the activity of tyrosinase, monophenol oxidase and laccase enzymes, where phenolic compounds are oxidized using O_2 as a terminal electron acceptor. Hence, combining the information gained from enzyme assays with *in-situ* observations of nitrogen cycling in the streambed, should provide a powerful tool to address unresolved research questions.

Here we investigate denitrification in a small, agricultural stream, where denitrification and subsequent N_2O emissions may be disproportionately important due to increased nutrient uptake and processing rates in small streams[53]. We approach this through the determination of enzyme activity, denitrification potentials and *in-situ* porewater concentrations. We determine whether sediment type, specifically sand versus gravel sediments, supports differing rates of denitrification given the contrast in residence times and aerobic conditions typically observed in these sediments[9,19,54]. Additionally, we consider whether there is a seasonal trend in denitrification and nutrient and N_2O concentrations, associated with annual variations in nitrogen and carbon inputs, and streambed temperatures.

6.2 Materials and Methods

6.2.1 Study Site

Experiments were conducted in the Wood Brook (BIFoR, Staffordshire, UK), which is situated within a mixed-use catchment. The catchment is dominated by arable fields, predominantly used to grow potatoes and winter wheat[55], with the rest of the catchment area comprised of young and mature deciduous woodland (Figure 6.1a). The catchment geology is red Permo-Triassic sandstone overlain by up to 10 m of glacial till deposits, which in turn are overlain by 0.15 to 0.6 m of sandy clay sediment[55].

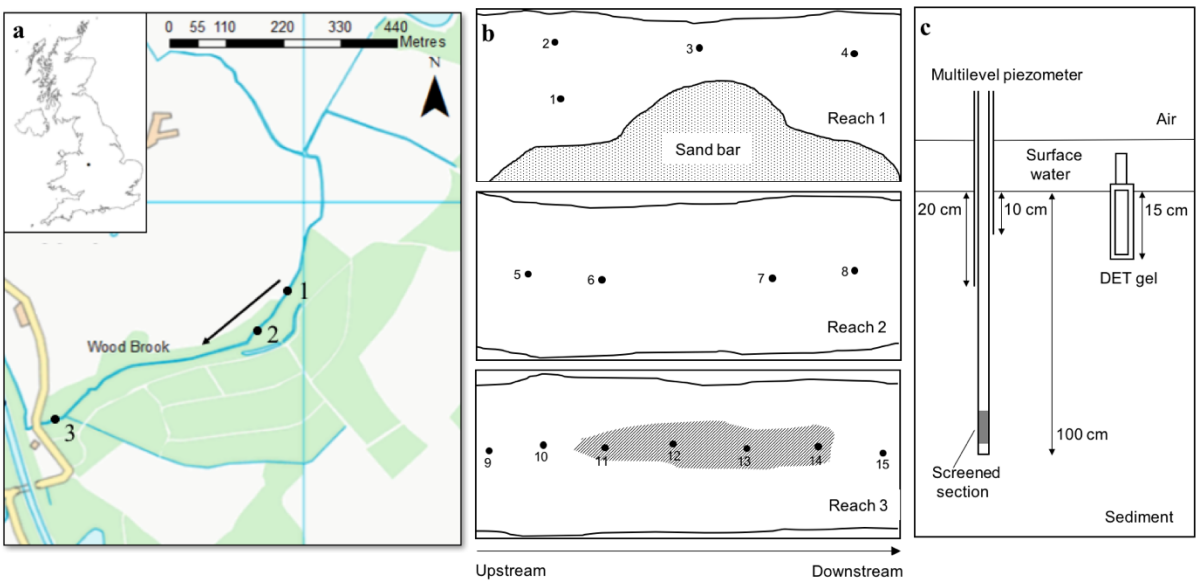

Figure 6.1a. The location of the Wood Brook within the UK and the location of the study reaches within the Wood Brook. Shown are the direction of the stream flow (black arrow), areas of woodland (green) and areas of fields (white), b. A diagram of the locations of the piezometers within each reach, and c. A diagram of the two sampling techniques used: multilevel piezometers sampled at 10 and 20 cm depth and diffusive equilibrium in thin-film gels.

The experiment was conducted within a 700 m reach of the Wood Brook, downstream of an agricultural catchment dominated by arable and grass ley systems, where the stream flows just within a patch of mature deciduous woodland (Figure 6.1a). This resulted in the upstream end of the reach directly bordering the arable fields on one side, with the stream being separated from the fields by a narrow strip of woodland further downstream. Within the experimental reach, three smaller reaches were identified (Figure 6.1a), with sand sediments in reaches 1 and 2, and gravel sediments in reach 3. Further reach characteristics can be found in Table 6.1.

Table 6.1. Average key characteristics from each reach. Presented are the dissolved oxygen, temperature, dissolved organic carbon, 3-dimensional flux of porewater through the streambed and the organic matter content of the sediment determined by loss on ignition.

Reach	DO (% Sat.)	Temperature (°C)	DOC (mg l^{-1})	q_{3D} (d^{-1})	OM Content (%)
1	31.5	10.8	16.1	42.4	2.9
2	20.9	11.0	13.2	35.4	1.4
3	25.9	10.5	13.2	80.5	0.9

6.2.2 Laboratory Incubation Experiments

6.2.2.1 Sediment Collection and Storage

Sediments were collected during June 2015 from two locations within the streambed, representative of the sand and gravel sediments found in the experimental reaches. Sediment samples were collected between 0 and 10 cm depth using an AMS slide hammer (5 cm dia.) and a trowel. Five pseudo-replicates of each sample were collected at each site. Sediment samples were homogenised and sieved (2 mm) within 36 hours of collection, and stored cold.

6.2.2.2 OM Analysis

Sediment subsamples were dried, crushed and sieved (2 mm), and approximately 10g of sediment was weighed into ceramic crucibles. Samples were placed into a furnace at 550°C for a minimum of 3 hours and then reweighed. The OM content was determined by the difference in sediment weight before and after combustion.

6.2.2.3 FDA Hydrolysis Activity

1g of homogenised air-dried sediment was weighed into 125 ml Erlenmeyer flasks, and 50 ml of 1 M tris-hydroxymethyl-aminomethane (THAM) buffer and 0.5 ml of FDA substrate were added to each flask. A blank sample of 1 M THAM buffer and FDA substrate with no sediment, and a control sample of sediment with 1 M THAM buffer and 0.5 ml of acetone, but no FDA substrate, were also prepared. The flasks were then mixed, stoppered and incubated at 37°C for 3 hours. After which, the flasks were removed from the incubator and 2 ml of acetone was added to each flask to prevent further FDA hydrolysis. FDA substrate was added to the control and mixed thoroughly. Samples were then filtered (Whatman No.2) and the absorbance at 490 nm was measured on a spectrophotometer (Varian Cary UV-Vis).

6.2.2.4 Phenol Oxidase activity

0.5 g of dried soil was weighed into four 15 ml centrifuge tubes (three replicates with one non-substrate control). 3 ml of deionised water was added and the tubes were gently mixed on a shaker for 10 minutes, after which, 2 ml of 10 mM dihydroxy phenylalanine (L-DOPA) was added to each replicate. The tubes were shaken on a platform shaker (100 rpm) for 30 minutes at 25°C. After 30 minutes, the tubes were centrifuged for 15 minutes, at 4000 rpm at 25°C, to terminate the reaction. The slurry was then filtered (GF/C filter paper) and the absorbance of the end colorimetric product, dopachrome, was determined at 475 nm on a spectrophotometer (Varian Cary). The phenol oxidase activity is reported here in μmol of dopachrome formed g^{-1} soil hr^{-1} [56].

6.2.2.5 Denitrification potential

10g of field-moist sediment was placed into 100 ml glass serum bottles. The bottles were wrapped in foil, to simulate dark conditions within the streambed, and then covered in parafilm and stored cold for less than 24 hours. The bottles were removed from the refrigerator prior to the incubation experiments to allow the samples to reach room temperature. 20 ml of the relevant stock solution (ultrapure water for the control incubations, 30 mg NO_3^- l^{-1} solution for the nitrate-spiked incubations, 40 mg C (glucose) l^{-1} solution for the carbon-spiked incubations or a 30 mg NO_3^- l^{-1}, 40 mg C l^{-1} solution for the mixed substrate incubations) was added to each bottle. The spiking with nitrate and glucose was to evaluate if denitrification was nitrate and/or C limited under induced anoxic conditions. Following addition of the substrates, the bottles were capped with a gas tight rubber septa and then flushed with oxygen-free Ar gas for 30 minutes to induce anoxic conditions and 10% of the headspace was replaced with pure acetylene gas to prevent the conversion of N_2O to N_2[57]. Incubations were performed at 22°C on a reciprocating shaker at 400 rpm, and 7 ml gas samples were taken from the headspace at 0, 3 and 6 hours and injected into 5.6 ml pre-

evacuated exetainers. The headspace volume and pressure was maintained throughout the experiment by replacing the removed gas with a 10:1 argon:acetylene mixture after each sampling time.

6.2.2.6 Statistical Inference

The responses between the sand and gravel sediments for each incubation experiment were tested for significant differences using a Welch's Two Sample t-test or the non-parametric equivalent (Wilcoxon Rank Sum Test) where the assumptions of normality and equal variance were violated.

The effect of reach and season on nitrogen cycling was inferred using a linear mixed-effects model fitted using the residual maximum likelihood in the nlme package in R. The data were nested by season to account for the sampling repetition in time and were shifted and transformed where the residuals did not fit the Gaussian assumption. The model was fitted both with (Equation 1) and without (Equation 2) the interaction between reach and season.

$$y_{ijk} = \mu + \alpha_i + \beta_j + (\alpha\beta)_{ij} + \gamma_k + \varepsilon_{ijk}, \quad (1)$$

where y_{ijk} is the observation for reach i, season j and sample k; μ is the mean of y; α_i is the fixed effect for reach i; β_j is the fixed effect for season j; $(\alpha\beta)_{ij}$ is the interaction fixed effect for reach i and season j; $\gamma_k \sim N(0, \sigma_\gamma^2)$ is the random event for the sample and $\varepsilon_{ijk} \sim N(0, \sigma^2)$ is the residual.

$$y_{ijk} = \mu + \alpha_i + \beta_j + \gamma_k + \varepsilon_{ijk}, \quad (2)$$

where y_{ijk} is the observation for reach i, season j and sample k; μ is the mean of y; α_i is the fixed effect for reach i; β_j is the fixed effect for season j; $\gamma_k \sim N(0, \sigma_\gamma^2)$ is the random event for the sample and $\varepsilon_{ijk} \sim N(0, \sigma^2)$ is the residual.

The Akaike Information Criterion (AIC) was used to compare the models and the model with the lowest AIC was used.

6.2.3 Field Experiments

6.2.3.1 Water Sampling

Porewater samples were collected manually at 10 and 20 cm depth from multilevel piezometers installed into the streambed at three locations (Figure 6.1), in July 2016, October 2016, January 2017 and March 2017. A surface water sample was taken in each reach at the same time as porewater sampling. The pH (Hanna HI98129), electrical conductivity (Hanna HI98129), DO (YSI ProODO or EcoSense ODO200) and temperature (YSI ProODO or EcoSense ODO200) of the samples were measured immediately. Water samples were then filtered (0.45 and 0.22 μm Thames Resteck nylon) into sterile centrifuge tubes and frozen until analysis.

DET gels were co-located with the piezometers in reaches 1 and 2, and were deployed at least 72 hours prior to sampling to allow equilibration of the natural conditions and the DET gel with the surrounding porewater[58]. DET gels were removed at the time of porewater sampling and sliced at 2.5 cm within 25 minutes. Gel slices were then placed into sterile centrifuge tubes and cooled until processing.

6.2.3.2 Gas Sampling

A headspace equilibrium method was used to create gas samples from the porewaters. 7 ml of water sample was shaken vigorously for two minutes with 14 ml of ultrapure helium. The headspace was then collected in a pre-evacuated exetainer (12 ml) and stored at room temperature, in the dark, until analysis.

6.2.3.3 Processing of DET gels

DET gels were weighed and multiplied by the assumed water content of the saturated gel (95%), to determine the volume of water in each gel slice. 5 ml of ultrapure water (18.2 MΩ) was then added to each gel and the gels were shaken for 24 hours on ice, on a reciprocating

shaker to back-equilibrate the solute from the gel. The resulting solution was then frozen until analysis.

6.2.3.4 Ammonium, Nitrate and Nitrite Analysis

Nutrient concentrations in the surface water, porewater and gel samples were analysed on a continuous flow analyser (Skalar San++), and standards of 0.58, 1.00 and 1.00 mg N L^{-1} were ran for Ammonium, Nitrate and Nitrite, respectively. These resulted in an accuracy and precision of 0.03 and ±0.05 mg NH_4^+-N l^{-1}, 0.06 and ±0.05 mg NO_3^--N l^{-1}, and 0.02 and ±0.005 mg NO_2^--N l^{-1}, respectively. The LOD was 0.05, 0.02 and 0.02 mg N l^{-1}, for Ammonium, Nitrate and Nitrite, respectively.

6.2.3.5 Gas Sample Analysis

N_2O concentrations within the gas samples of both the incubation and field experiments were measured using a GC (Agilent 7890A) fitted with a micro electron capture detector (μECD). Laboratory and July field samples were analysed using a 1 ml sample loop in splitless mode, with an oven temperature of 60ºC, and an ECD temperature of 350ºC. A make-up gas of argon and methane was used with a flow rate of 2 ml min^{-1}, and a run time of 9 minutes was used, with N_2O eluted at 7 minutes. The LOD was 0.08 ppm, and a 6.2 ppm standard resulted in an accuracy of 0.1 ppm and a precision of ±0.2 ppm. All other field samples were analysed on a GC-ECD in splitless mode with a 250 μl sample loop, an oven temperature of 30ºC and an ECD temperature of 300ºC. A makeup gas of N_2 with a flow rate of 30 ml s^{-1} was used, with a run time of 5 minutes resulting in N_2O eluting at 3 minutes. The LOD was 0.01 μg l^{-1}, and a standard of 9.71 ppm resulted in an accuracy of 0.10 ppm and a precision of ±1.75 ppm. Henry's constant was used to determine the porewater concentration for all field samples[59,60].

6.2.3.6 $\delta^{15}N_{NO3^-}$ and $\delta^{18}O_{NO3^-}$ Analysis

The nitrate isotope analysis was performed at the Analytical Facilities, University of East Anglia using the denitrifier method[61,62]. Isotope analysis was performed by converting NO_3^- within the sample to N_2O using denitrifying bacteria, the isotopic signature of the N_2O was then measured, with a measurement limit of 2 μM NO_3^-. The long-term measurement precision was ±0.3 and ±0.4‰ and the accuracy was 0.0 and 0.0‰ for $\delta^{15}N_{NO3^-}$ and $\delta^{18}O_{NO3^-}$, respectively. International isotope reference materials IAEA-NO_3^-, USGS-34, and USGS-35 were used as standards and resulted in $\delta^{15}N_{NO3^-}$ ratios of +4.69, -1.88 and +3.83‰, respectively, with a measurement precision of ±0.14, ±0.11 and ±0.19‰, and $\delta^{18}O_{NO3^-}$ ratios of +25.61, -28.17 and 57.09‰, respectively, with a measurement precision of ±0.19, ±0.37 and ±0.59‰.

6.3 Results

6.3.1 Influence of sediment type on microbial activity and denitrification potential

FDA hydrolysis, a proxy for total microbial activity, was greater in the sand (1.35 mg fluorescein kg^{-1} soil hr^{-1}) than gravel (0.36 mg fluorescein kg^{-1} soil hr^{-1}) sediments (Figure 6.2a), whereas phenol oxidation, a proxy for the uptake of recalcitrant phenolic organic compounds, was greater in the gravel (2.76 μmol dopachrome g^{-1} soil hr^{-1}) than in the sand (1.70 μmol dopachrome g^{-1} soil hr^{-1}) sediments (Figure 6.2b).

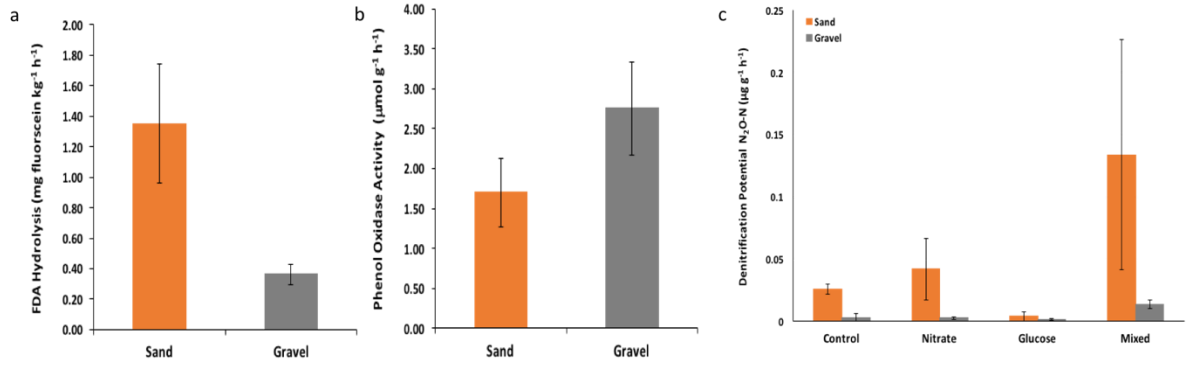

Figure 6.2a. The total microbial activity in sand and gravel sediments, expressed in mg fluorescein kg^{-1} h^{-1}, b. Phenol oxidation activity in sand and gravel sediments, expressed in

μmol g^{-1} h^{-1}, and c. The denitrification potential of sand and gravel sediments under various conditions, expressed in μg N_2O-N g^{-1} h^{-1}.

Potential rates of denitrification were greater in the sand than the gravel across all treatments (Figure 6.2c). The control experiments, indicative of conditions within the streambed, resulted in denitrification potentials which were almost 10 times greater in the sand than the gravel sediments (0.026±0.004 N_2O-N μg g^{-1} h^{-1} for sand and 0.003±0.003 N_2O-N μg g^{-1} h^{-1} for gravel). Denitrification potentials in the sand sediments of the nitrate-spiked samples increased to 0.042±0.025 N_2O-N μg g^{-1} h^{-1}, however, in the gravel sediments, the denitrification potential showed no increase over that of the control (0.003±0.001 N_2O-N μg g^{-1} h^{-1}). Addition of C did not result in larger denitrification potentials in both sediment types (0.004±0.004 N_2O-N μg g^{-1} hr^{-1} for sand and 0.001±0.001 N_2O-N μg g^{-1} hr^{-1} for gravel). The mixed substrate experiment, indicative of ideal denitrification conditions with reference to electron donor and acceptor availability, resulted in larger denitrification potentials within the sand sediment (0.134±0.092 N_2O-N μg g^{-1} hr^{-1}), which were 10 times greater than within the gravel sediments (0.0134±0.003 N_2O-N μg g^{-1} hr^{-1}).

6.3.2 Influence of reach (sediment type) and season on nitrogen cycling

6.3.2.1 Ammonium

Ammonium concentrations in the surface water were low and decreased downstream in Winter and Spring (Figure 6.3), with lowest concentrations found in Autumn.

Porewater ammonium concentrations were greatest in reaches 1 and 2, which was consistent across all seasons (Figure 6.3). Ammonium concentrations were highest in Autumn, especially in reach 2, and were lowest in Winter and Spring.

Ammonium concentrations within the DET gels generally increased with depth, and this was most pronounced in gels 1 and 4 (Figure 6.4). There was considerable variation in profiles between seasons and locations.

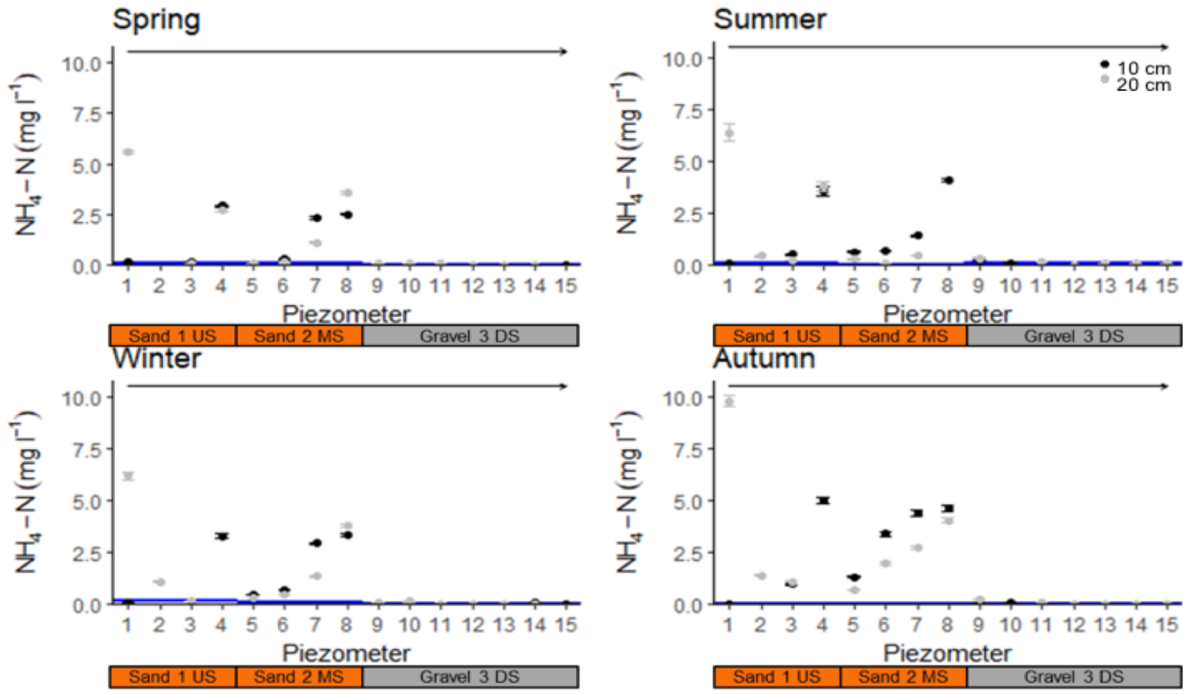

Figure 6.3. Porewater NH_4^+-N concentrations at 10 (black) and 20 (grey) cm depth, with surface water concentrations for each reach shown with a blue line. The black arrow represents direction of surface flow from upstream to downstream.

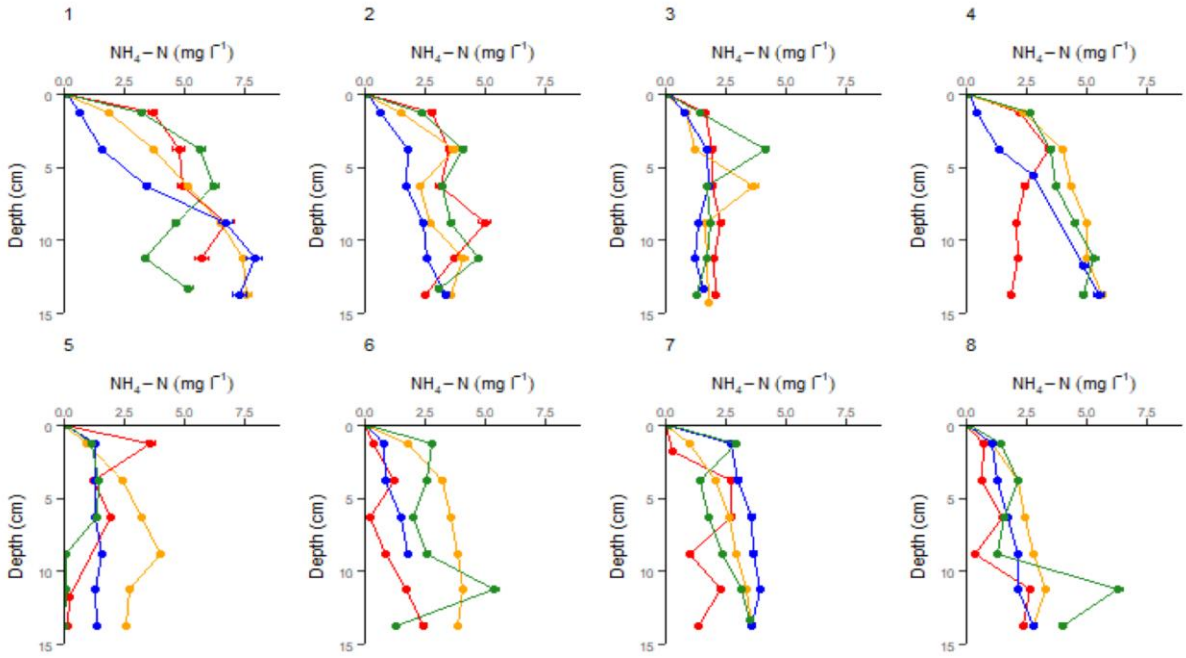

Figure 6.4. Vertical porewater NH_4^+-N concentrations in DET gels colocated with piezometers 1-8.

6.3.2.2 Nitrate

NO_3^- concentrations in the surface water generally showed little variation between reaches, however, they decreased downstream in Spring (Figure 6.5), with maximum concentrations observed in Winter and Spring.

Porewater nitrate concentrations were generally highest in reaches 1 and 3, and lowest in reach 2, which was consistent across all seasons (Figure 6.5). Variation in nitrate concentrations between seasons was low.

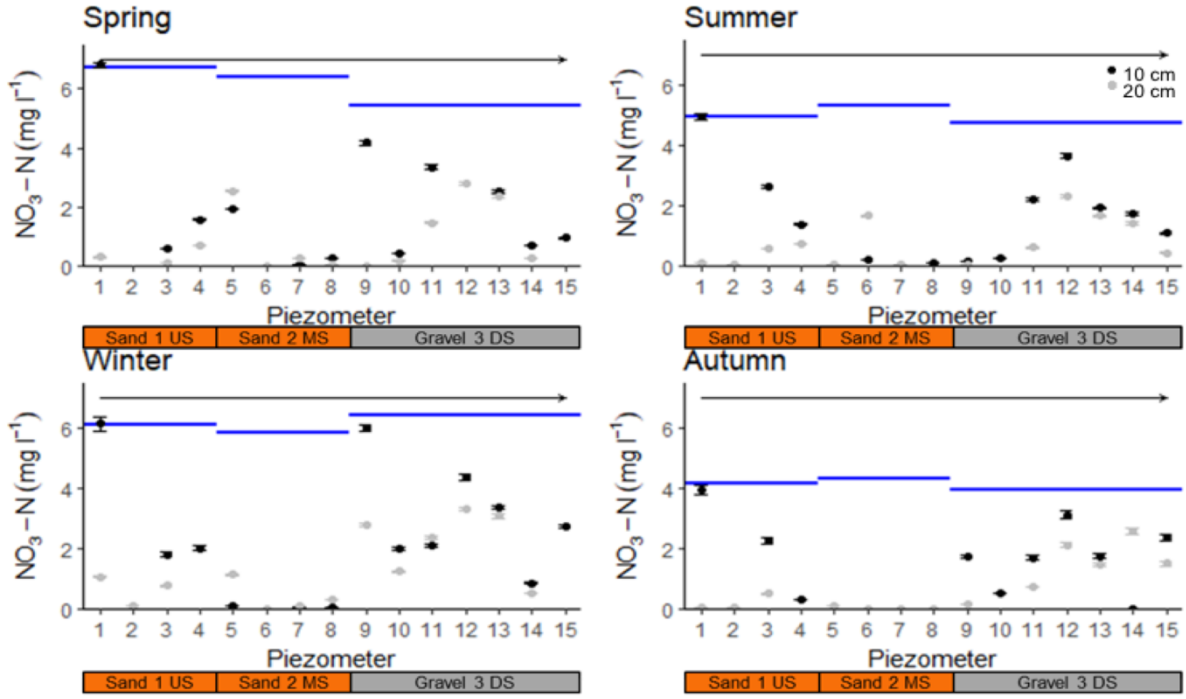

Figure 6.5. Porewater NO_3^--N concentrations at 10 (black) and 20 (grey) cm depth, with surface water concentrations for each reach shown with a blue line. The black arrow represents direction of surface flow from upstream to downstream.

Nitrate concentrations within the DET gels decreased with depth, so that concentrations were similar between locations and seasons below 5 cm (Figure 6.6). Concentrations above 5 cm

in gels 1-4 were generally greatest in Winter and lowest in Autumn. When comparing gels in reaches 1 and 2, there appeared to be less variation with depth in reach 2, especially in the top 5 cm.

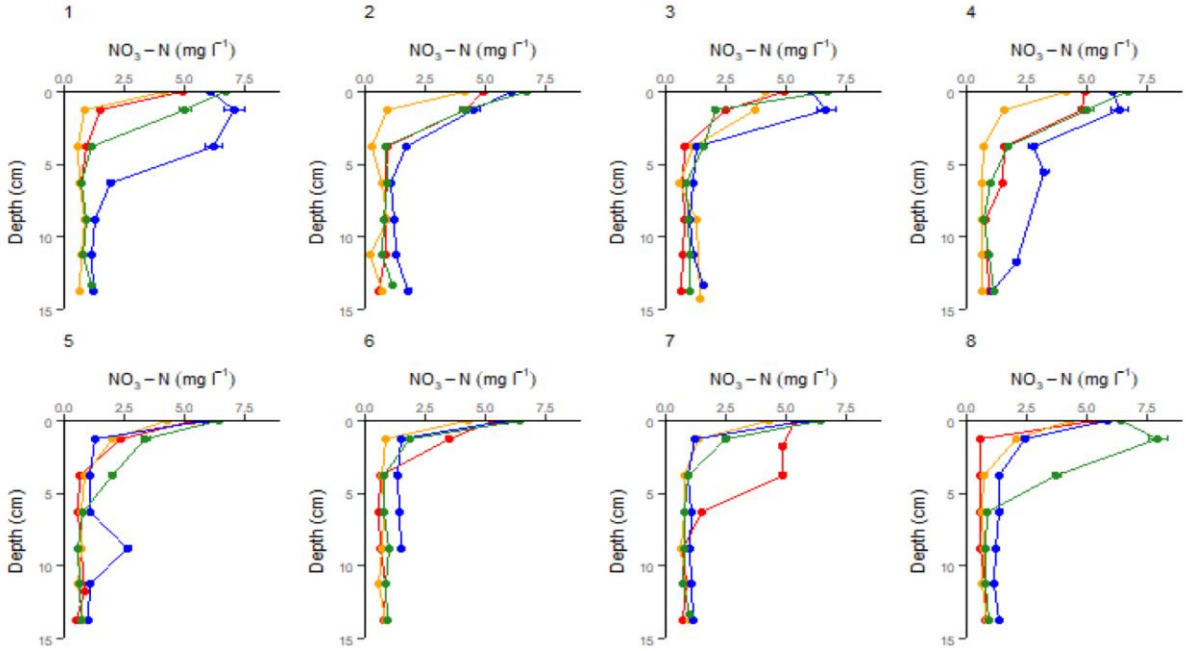

Figure 6.6. Vertical porewater NO_3^--N concentrations in DET gels colocated with piezometers 1-8.

6.3.2.3 Nitrite

NO_2^- concentrations in the surface water decreased downstream in Summer and increased downstream in Winter (Figure 6.7), with maximum concentrations observed in Spring in all reaches.

Porewater nitrite concentrations were greatest in reach 3, with low concentrations found in both reaches 1 and 2, which was consistent across all seasons (Figure 6.7). Nitrite concentrations varied greatly between seasons in reach 3, with concentrations highest in Summer and Autumn.

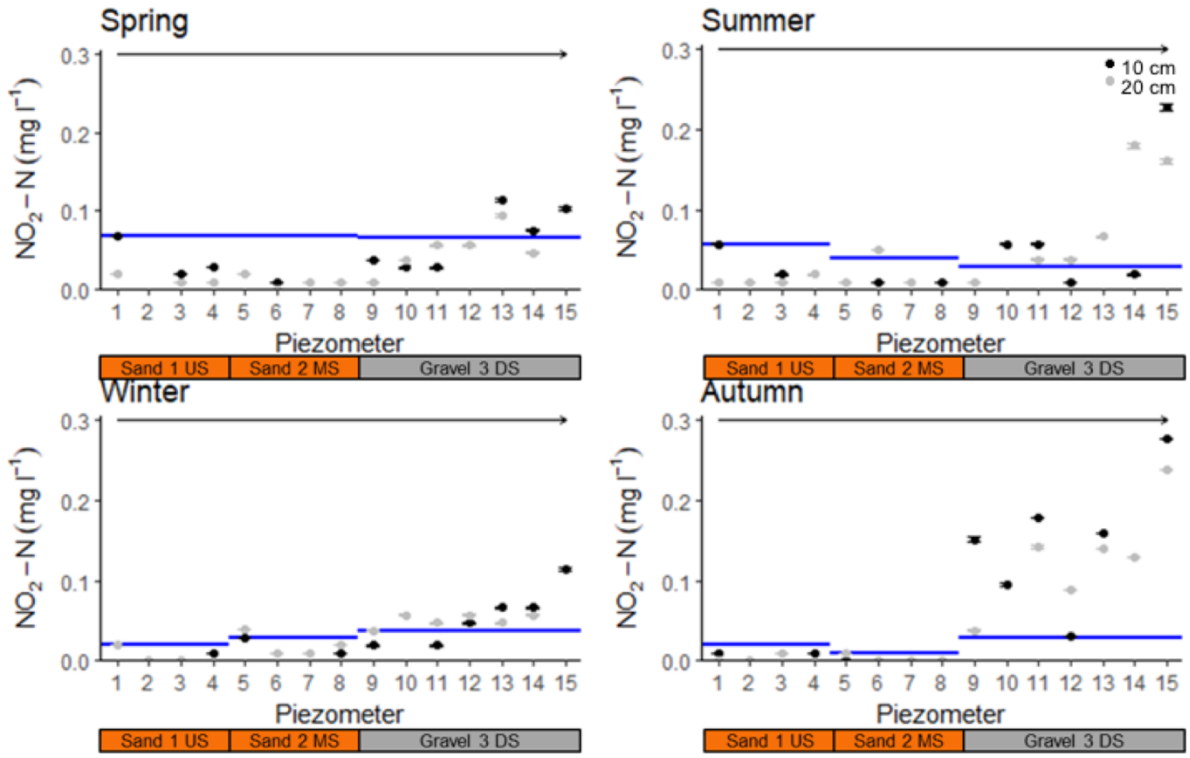

Figure 6.7. Porewater NO_2^--N concentrations at 10 (black) and 20 (grey) cm depth, with surface water concentrations for each reach shown with a blue line. The black arrow represents direction of surface flow from upstream to downstream.

6.3.2.4 Nitrous Oxide

N_2O concentrations in the surface water were generally similar in reaches 1 and 2, and lower in reach 3 (Figure 6.8), with maximum concentrations observed in Winter and minimum concentrations observed in Summer.

Porewater N_2O concentrations were greatest in reaches 1 and 3, with concentrations in Autumn elevated in reach 3 compared to reach 1 (Figure 6.8). N_2O concentrations did not vary greatly throughout the year in reaches 1 and 2, but were elevated in Autumn in reach 3.

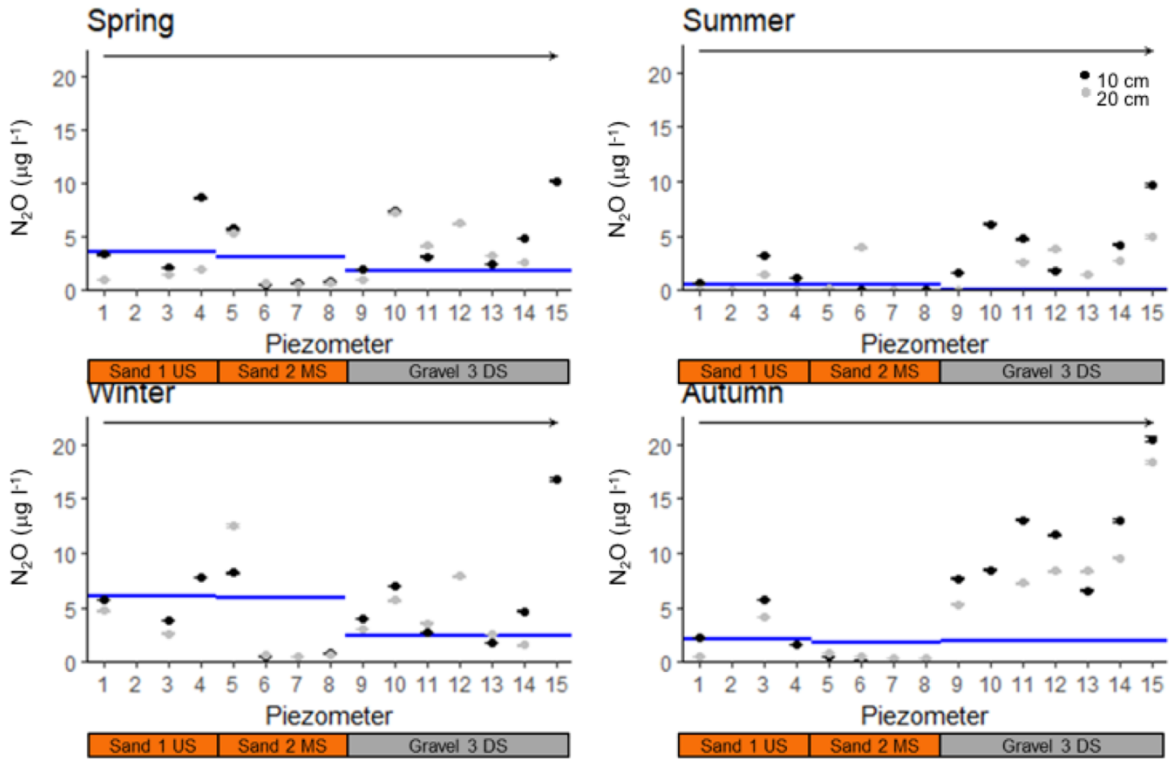

Figure 6.8. Porewater N_2O concentrations at 10 (black) and 20 (grey) cm depth, with surface water concentrations for each reach shown with a blue line. The black arrow represents direction of surface flow from upstream to downstream.

6.3.2.5 $\delta^{15}N_{NO3^-+NO2^-}$

$\delta^{15}N_{NO3^-+NO2^-}$ ratios in the surface water were similar in all reaches, and did not vary greatly throughout the year (Figure 6.9).

Porewater $\delta^{15}N_{NO3^-+NO2^-}$ ratios were generally highest in reach 3, which was consistent across all seasons, but less pronounced in Winter (Figure 6.9). In reach 3, ratios varied greatly with season, with lowest ratios found in Winter.

6.3.2.6 $\delta^{18}O_{NO3^-+NO2^-}$

$\delta^{18}O_{NO3^-+NO2^-}$ ratios in the surface water were similar in all reaches except reach 1 in Autumn, and did not vary greatly throughout the year (Figure 6.10).

Patterns in porewater $\delta^{18}O_{NO3^-+NO2^-}$ ratios were not very pronounced but were generally lowest in reach 1 and highest in reach 3 (Figure 6.10). $\delta^{18}O_{NO3^-+NO2^-}$ ratios did not vary greatly with season.

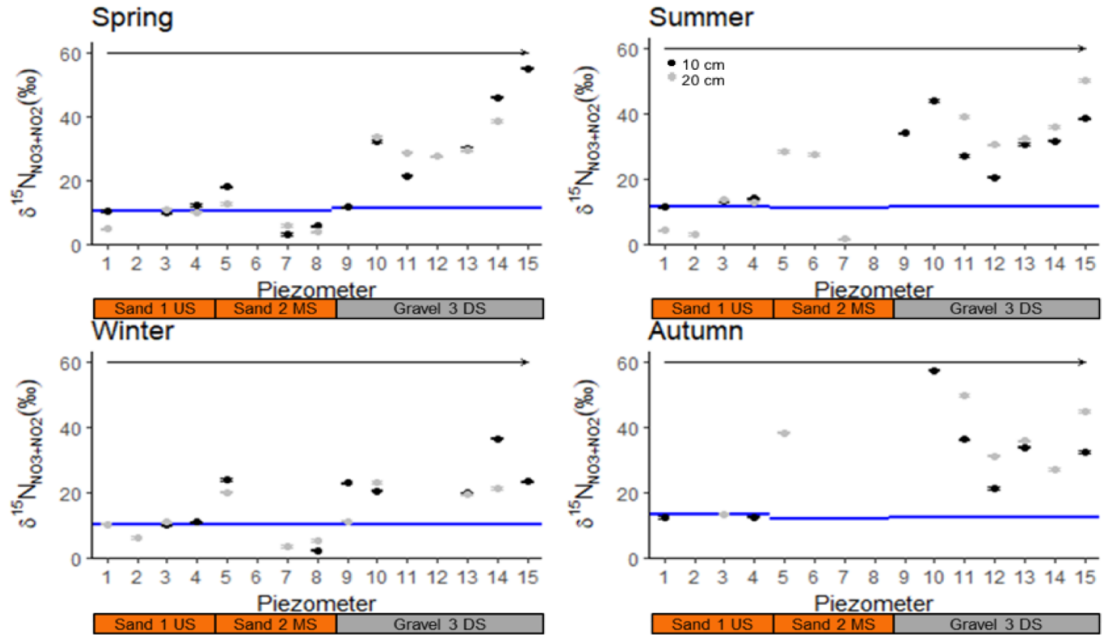

Figure 6.9. Porewater $\delta^{15}N_{NO3^-+NO2^-}$ ratios at 10 (black) and 20 (grey) cm depth, with surface water concentrations for each reach shown with a blue line. The black arrow represents direction of surface flow from upstream to downstream.

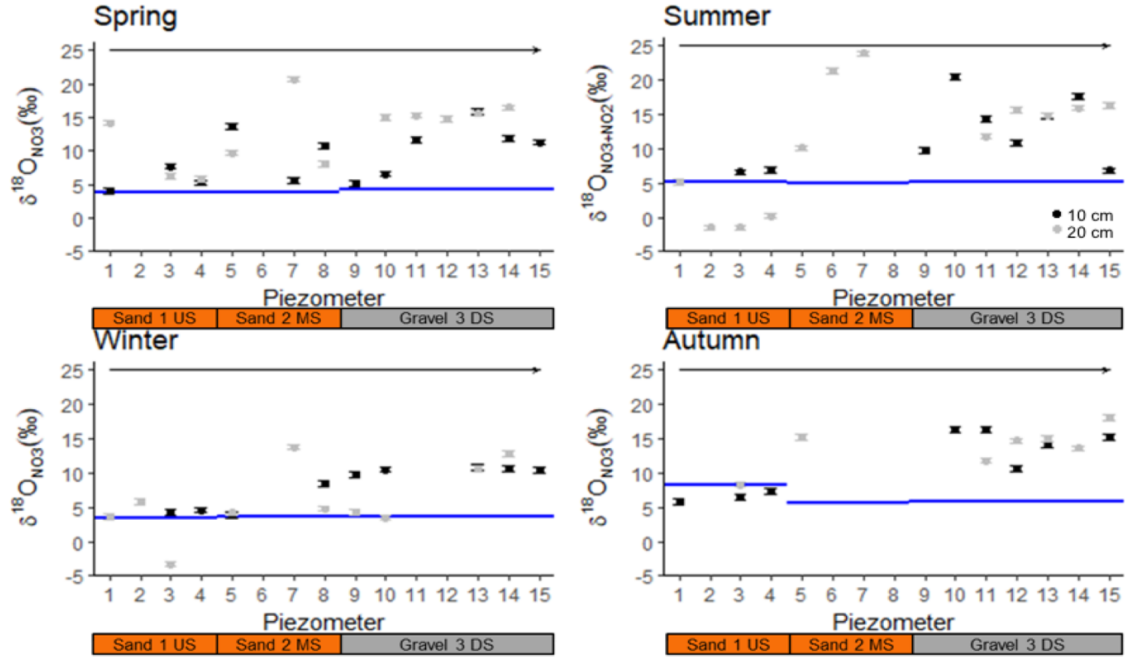

Figure 6.10. Porewater $\delta^{18}O_{NO3^-+NO2^-}$ ratios at 10 (black) and 20 (grey) cm depth, with surface water concentrations for each reach shown with a blue line. The black arrow represents direction of surface flow from upstream to downstream.

6.3.2.7 Carbon:Nitrogen

The C:N ratios in the surface water were low and did not vary greatly between reaches or season (Figure 6.11). C:N ratios in the porewaters of the piezometers were below 40.2, except at 10 cm in piezometer 14 during Autumn, where the C:N ratio was 404.8 (Figure 6.11). C:N ratios were generally highest in reach 2, and lowest in reach 3, which was consistent across all seasons but more pronounced in Autumn and Winter. C:N ratios showed little variation between seasons in reaches 1 and 3, whereas there was greater variation in reach 2.

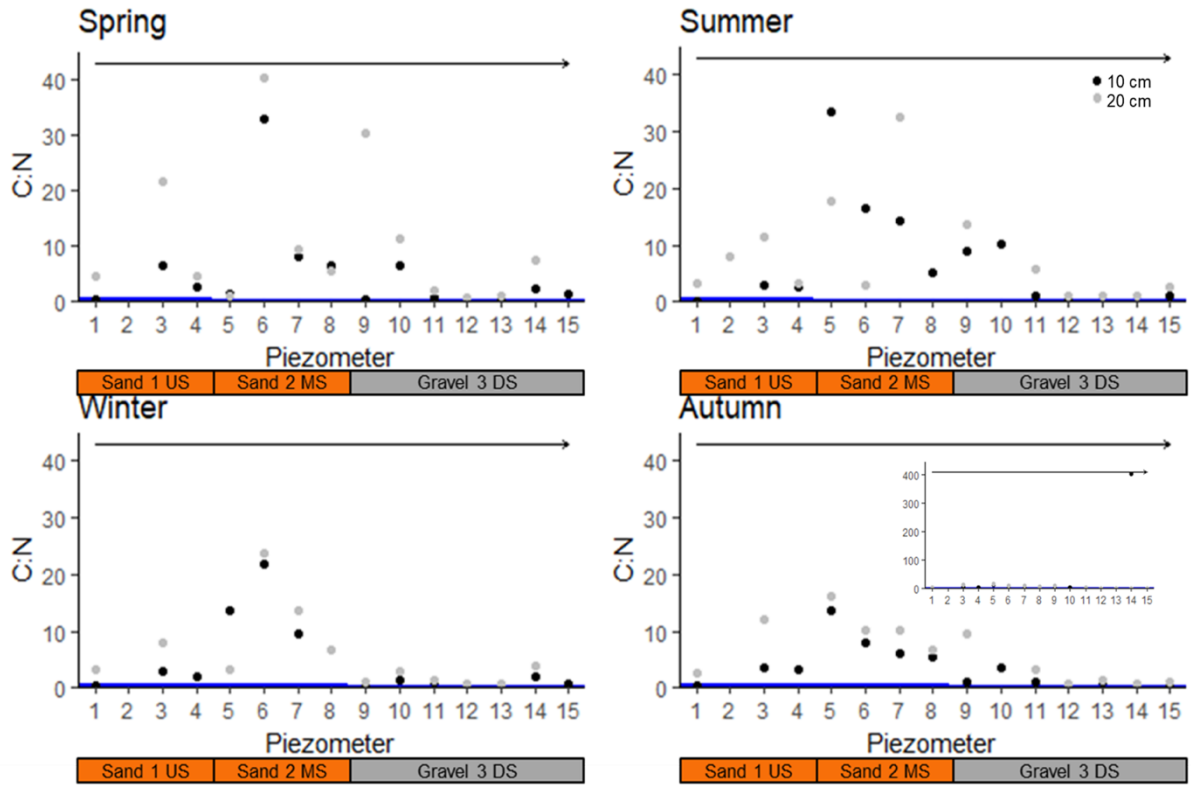

Figure 6.11. Porewater C:N ratios at 10 (black) and 20 (grey) cm depth, with surface water ratios for each reach shown with a blue line. The black arrow represents direction of surface flow from upstream to downstream.

6.4 Discussion

6.4.1 Influence of sediment type on microbial activity and denitrification potential

The greatest extracellular enzyme activity was not observed in the same sediment type for both assays. Extracellular FDA hydrolysis activity was significantly greater (p-value = 0.004, Table 6.2) in the sand sediments, whereas, extracellular phenol oxidase activity was significantly greater (p-value = 0.032, Table 6.2) in the gravel sediments. This indicates that the quantity and quality of C differed between the two sediment types, with the C quality and quantity greatest in the sand sediments. The FDA hydrolysis activity also suggests that organic carbon turnover and decomposition rates were greatest in the sand sediments, resulting in the sand sediments being characterised by greater total microbial activity than the gravel sediments[51]. The gravel sediments, however, were characterised by greater rates of microbial decomposition of aromatic phenolic compounds than the sand sediments. This indicates that the C utilised by microbes was more aromatic, and therefore less bioavailable, in the gravel than the sand sediments. The uptake of aromatic phenolic compounds provides microbes with nutrients, as well as C, and particularly indicates the mining of organic N where N availability is low[52]. This was contradictory to the *in-situ* data, where nitrate concentrations were relatively high in the gravel sediments.

Table 6.2. Details of the statistical analysis performed for the laboratory incubation experiments comparing responses in the sand and gravel sediments. Significant p-values are shown in bold and d.f. is the degrees of freedom.

Experiment (sand v gravel)	Test	p-value	d.f.
Denitrification Potential: Control	Wilcoxon Rank Sum Test	**0.036**	-
Denitrification Potential: NO_3	Wilcoxon Rank Sum Test	**0.008**	-
Denitrification Potential: Carbon	Welch Two Sample t-test	0.193	4.353
Denitrification Potential: Mixed	Wilcoxon Rank Sum Test	**0.008**	-
Fluorescein Diacetate Assay	Welch Two Sample t-test	**0.004**	4.237
Phenol Oxidation Assay	Wilcoxon Rank Sum Test	**0.032**	-

The denitrification potential was greater in the sand than the gravel sediments under all treatment conditions, with the control experiments (where no additional substrate was added) indicating that *in-situ* denitrification was significantly greater in the sand than gravel sediments (p-value = 0.036, Table 6.2). The nitrate-spiked incubations resulted in a large increase in denitrification potential in the sand sediments, but no response in the gravel sediments, when compared to the controls, resulting in significantly different denitrification potentials (p-value = 0.008, Table 6.2). This showed that denitrification was nitrate limited in the sand sediments only, as has been observed previously at <2 mg NO_3^--N l^{-1} [63], again suggesting that *in-situ* denitrification was greatest in this sediment type, and likely almost to completion. The large increase in denitrification potential observed in the nitrate- and carbon-spiked experiments suggests that, under optimal conditions, the microbial communities within both sediment types were able to attenuate more nitrate than is currently denitrified in the stream. This resulted in denitrification potentials within sand sediments 10 times those in gravel sediments, which were significantly greater (p-value = 0.008, Table 6.2), again confirming that sand sediments are able to support greater rates of microbial respiration and denitrification.

Surprisingly, given that carbon may limit microbial denitrification in the HZ[64,65], the carbon-spiked experiments did not result in enhanced denitrification potentials, resulting in no significant difference between the two sediment types (p-value = 0.193, Table 6.2). This suggests the limitation of denitrification by other factors, which in this case was nitrate, given that the denitrification potentials were enhanced in the nitrate-spiked experiments.

The greatest total microbial activity and denitrification potentials, therefore, were found in the sand sediments representative of reaches 1 and 2, where residence times and anoxic conditions were expected to be greatest[19,54,66]. This indicates that microbial respiration and nitrate attenuation is greater in sand than gravel sediments. The uptake of more recalcitrant

carbon, such as aromatic compounds, was greatest in the gravel sediments. This suggests that the microbial community within the gravel sediments of reach 3 were adapted to less bioavailable carbon.

6.4.2 Influence of reach (sediment type) and season on nitrogen cycling

NH_4^+ concentrations in the surface water were low or similar to NH_4^+ concentrations found previously in streams of agricultural catchments[1,12,67–69]. Porewater NH_4^+ concentrations were highest in reach 2 and lowest in reach 3, resulting in much larger concentrations in the sand sediments of reach 2 than are typically found in agricultural streams[1,12,68]. Concentrations similar to those observed here, however, have been reported previously[68]. The persistence of such large NH_4^+ values year-round is likely due to leaching from the large amount of leaf litter entering the stream in reach 2, which could be buried in the sediments. This is also indicated by the enhanced NH_4^+ concentrations in the streambed relative to the surface water in reaches 1 and 2, indicating that these sand sediments are a source of NH_4^+. NH_4^+ concentrations in the porewaters of reach 3 were very low, which is likely due to increased nitrification in these typically well-oxygenated gravel sediments.

Concentrations of NO_3^- within the surface water were large compared to those generally observed in agricultural streams[1,12,19,67–70], however, greater concentrations have been observed[71]. Porewater concentrations, however, were typically similar to or lower than those observed previously. The low concentrations found within reach 2 were similar to those found previously in a gravel bar[12], whereas the larger concentrations found in reaches 1 and 3 were similar or slightly lower than those found in both vegetated and unvegetated sediments[1,19,68,70]. Surface water NO_3^- concentrations were greater than in the porewaters of all reaches, indicating that the streambed here was acting as a nitrate sink year-round, and suggesting denitrification occurred within the sediments. There was a seasonality to the nitrate concentrations observed, which were greater in Winter and Spring, when microbial

activity is expected to be lowest[6], with this seasonal pattern most pronounced in the surface waters.

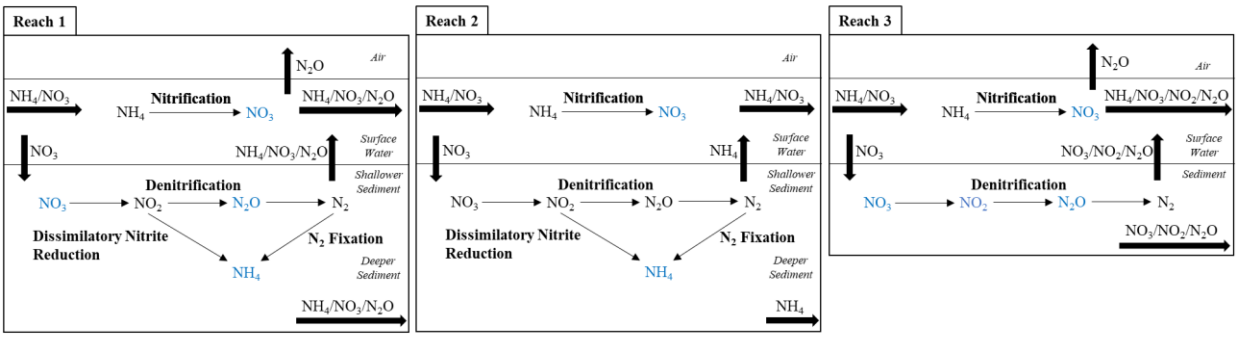

Figure 6.12. A conceptual figure of the processes occurring in the surface water and porewaters of the three study reaches. Nitrogen species are shown in blue where they occurred at high concentrations, processes are represented by 'thin' arrows and labelled in bold, and transportation is represented by 'thick' arrows.

The porewaters of the three study reaches were characterised by varying concentrations of nitrogen species, resulting in differing degrees of denitrification (Figure 6.12). Relatively large concentrations of nitrate in the porewaters of reaches 1 and 3 were initially unexpected, given predictions that denitrification would be greater in the sand sediments of reaches 1 and 2, than the gravel sediments of reach 3. This prediction was due to typically enhanced residence times and anoxia in sand than gravel sediments[66,19,54], and greater denitrification potentials observed in the sand sediments. The spatial pattern, however, can be explained by nutrient spiralling through the sand sediments of large inputs of nitrogen from the agricultural land upstream of the study site, leading to a reduction in nitrate between reaches 1 and 2. The low denitrification potential of the gravel sediments of reach 3, coupled with increased nitrogen inputs downstream of reach 2 (e.g. leaf litter and run-off), produced large nitrate concentrations able to persist within the gravel sediments. This resulted in nitrate concentrations being significantly different between reaches (p-value = 0.009, Table 6.3).

Table 6.3. Results of the statistical analysis results from the linear mixed-effects modelling, significant p-values are shown in bold.

Parameter	Estimated Value	p-value
NH_4		
Intercept	-5.798	**0.000**
Reach	4.338	**0.000**
Season (Autumn-Spring)	4.198	**0.000**
Season (Autumn-Summer)	3.958	**0.000**
Season (Autumn-Winter)	2.742	**0.009**
Interaction Reach and Season (Autumn-Spring)	-1.643	**0.000**
Interaction Reach and Season (Autumn-Summer)	-2.093	**0.000**
Interaction Reach and Season (Autumn-Winter)	-1.227	**0.005**
NO_3		
Intercept	0.094	0.724
Reach	0.300	**0.009**
Season (Autumn-Spring)	0.128	0.248
Season (Autumn-Summer)	0.037	0.730
Season (Autumn-Winter)	0.318	**0.004**
NO_2		
Intercept	13.695	**0.000**
Reach	-2.828	**0.000**
Season (Autumn-Spring)	-3.241	**0.000**
Season (Autumn-Summer)	-3.206	**0.000**
Season (Autumn-Winter)	-2.413	**0.006**
Interaction Reach and Season (Autumn-Spring)	1.636	**0.000**
Interaction Reach and Season (Autumn-Summer)	1.604	**0.000**
Interaction Reach and Season (Autumn-Winter)	1.286	**0.001**
N_2O		
Intercept	-0.575	0.274
Reach	1.168	**0.000**
Season (Autumn-Spring)	1.517	**0.003**
Season (Autumn-Summer)	0.534	0.277
Season (Autumn-Winter)	2.088	**0.000**
Interaction Reach and Season (Autumn-Spring)	-0.813	**0.000**
Interaction Reach and Season (Autumn-Summer)	-0.608	**0.003**
Interaction Reach and Season (Autumn-Winter)	-0.979	**0.000**
$\delta^{15}N_{NO3}$		
Intercept	-0.678	0.925
Reach	12.448	**0.000**
Season (Autumn-Spring)	-7.449	0.324
Season (Autumn-Summer)	-3.399	0.647
Season (Autumn-Winter)	3.068	0.686
Interaction Reach and Season (Autumn-Spring)	0.100	0.973
Interaction Reach and Season (Autumn-Summer)	0.057	0.984
Interaction Reach and Season (Autumn-Winter)	-6.358	**0.040**
$\delta^{18}O_{NO3}$		
Intercept	1.140	**0.000**
Reach	0.088	**0.000**
Season (Autumn-Spring)	-0.022	0.472
Season (Autumn-Summer)	-0.042	0.179
Season (Autumn-Winter)	-0.119	**0.001**

Nitrate concentrations within the sand sediments of reach 2 were very low (<2.56 mg NO_3^--N l^{-1}), suggesting rates of denitrification within these sand sediments were high leading to

almost complete NO_3^--depletion. This reflects the nitrate limitation on denitrification potentials that we observed within the sand sediments in the laboratory experiments. Further evidence for denitrification within the sediments of reaches 1 and 2 was observed in the vertical profiles of NO_3^- within the DET gels, which showed large decreases in nitrate at depths greater than 5 cm. This indicates that surface water nitrate was attenuated within 5 cm of the surface water-sediment interface, supporting the presence of denitrification in reaches 1 and 2. The decrease in nitrate with depth in the gels, was coupled with an increase in ammonium with depth, which supports previous findings that the majority of biogeochemical activity and nutrient cycling occurs within the top few centimetres of the streambed[72–74]. This decrease in NO_3^- with depth was also reflected in the piezometers where concentrations were generally greater at 10 cm than 20 cm.

Evidence of denitrification, as well as the extent of completion, was also found by considering concentrations of nitrogen species (NO_2^- and N_2O) that are intermediate products of denitrification[30]. NO_2^- concentrations were relatively low within the sand sediments of reaches 1 and 2, indicating that denitrification was more complete in the sand than gravel sediments, and NO_2^- concentrations were significantly different between reaches (p-value = 0.000, Table 6.3). The relatively large NO_2^- concentrations observed in the gravel sediments could result from incomplete denitrification or nitrification; given that we do not have any information on nitrification rates, the process resulting in these high NO_2^- concentrations cannot be determined. The sediments of reaches 1 and 2 generally had lower concentrations of NO_2^- than in the surface water, and therefore, were acting as a nitrite sink, whereas concentrations within the sediments of reach 3 were often greater than within the surface water, therefore, primarily acting as a NO_2^- source in Summer, Autumn and Winter. This was linked to the large seasonality in NO_2^- concentrations within the sediments of reach 3, which was not observed within reaches 1 and 2, with NO_2^- concentrations lowest in Winter and

Spring, presumably reflecting the expected lower reactivity's, and greater observed NO_3^- concentrations, during these times. The spike in NO_2^- concentrations in Autumn in reach 3 may also be linked to the increase in NH_4^+ inputs into reach 2 during this time.

Evidence for partial denitrification in reach 3 was also observed in the N_2O data, where relatively large concentrations of N_2O were observed, with N_2O concentrations significantly different between reaches (p-value = 0.000, Table 6.3). This is consistent with the relatively low microbial activity and denitrification potential determined in the gravel sediments, indicating that partial denitrification was expected. These high N_2O concentrations in the gravel sediments support previous research which found increased N_2O production associated with high nitrate concentrations and low organic carbon reactivity[21]. The concentrations of N_2O in reach 1 were similar to those in reach 3 during Winter, indicating that denitrification was only partially complete in those sediments at that time. The concentrations of N_2O within the porewaters of reach 2 were generally low, providing further evidence of complete denitrification within the sand sediments of this reach. This finding is further substantiated by the greater denitrification potential of the sand sediments. Similar to NO_2^- concentrations, there was a large seasonal variation in N_2O concentrations in reach 3, where N_2O was greatest in Autumn, again reflecting an increase in substrate due to leaf fall and a subsequent increase in denitrification. This was contradictory to previous research, which did not find any significant difference in seasonal N_2O concentrations in streambed gravel sediments[75]. In the surface water, N_2O concentrations were greatest in the Winter and Spring, which did not correlate with the nitrate data, however, this could be due to an increase in N_2O saturation concentration at lower stream water temperatures[76].

Large values of $\delta^{15}N_{NO3^-+NO2^-}$ and $\delta^{18}O_{NO3^-+NO2^-}$, indicative of denitrification[77] due to isotopic fractionation, were found in the porewater and gel samples of all reaches, and supported the evidence for denitrification observed in the concentration data. Contrary to the concentration

data, however, the largest $\delta^{15}N_{NO3^-+NO2^-}$ and $\delta^{18}O_{NO3^-+NO2^-}$ ratios were found in the gravel sediments of reach 3, which were significantly larger than those in reaches 1 and 2 (p-value = 0.000 and 0.000, respectively, Table 6.3), suggesting that rates of denitrification were greatest in these sediments.

The larger $\delta^{15}N$:$\delta^{18}O$ ratios observed in reach 3 may be due to source rather than process influence, however, $\delta^{15}N_{NO3^-+NO2^-}$ and $\delta^{18}O_{NO3^-+NO2^-}$ ratios in the surface water were consistently similar between reaches and seasons, except in reach 1 in Autumn, which had a slightly higher $\delta^{18}O_{NO3^-+NO2^-}$ ratio. This suggests that the source of nitrate and the processes affecting nitrate concentrations were not significantly different in the surface water between reach and season. Therefore, most processes affecting nitrate concentration likely occurred within the sediments. It is possible that the gravel sediments of reach 3, which were typically characterised by greater subsurface fluxes (Table 6.1), received a different subsurface input of enriched nitrate, which was already enriched in $\delta^{15}N_{NO3^-+NO2^-}$ and $\delta^{18}O_{NO3^-+NO2^-}$. Furthermore, average isotopic ratios for each reach and the gel samples did have $\delta^{15}N$:$\delta^{18}O$ ratios indicative of denitrification (Figure 6.13), despite values being greatest in reach 3, providing further evidence of denitrification in all reaches of the streambed of the Wood Brook. Although, it should be noted that these diagrams are based on global data and so it is necessary to fully characterise the isotopic values of local sources to accurately interpret source and process information.

Additionally, the denitrifying method used in the isotopic analysis measures $\delta^{15}N_{NO3^-+NO2^-}$ and $\delta^{18}O_{NO3^-+NO2^-}$ in both nitrate and nitrite[61,62], therefore, samples in which the ratio of NO_2^-:NO_3^- was high may be influenced by $\delta^{15}N_{NO2^-}$. Samples with a ratio greater than 5% accounted for many of the extreme values of $\delta^{15}N_{NO3^-+NO2^-}$ observed, and although the remaining samples still resulted in higher $\delta^{15}N_{NO3^-+NO2^-}$ ratios in the porewaters of reach 3, the difference between the sand and gravel sediments was greatly reduced.

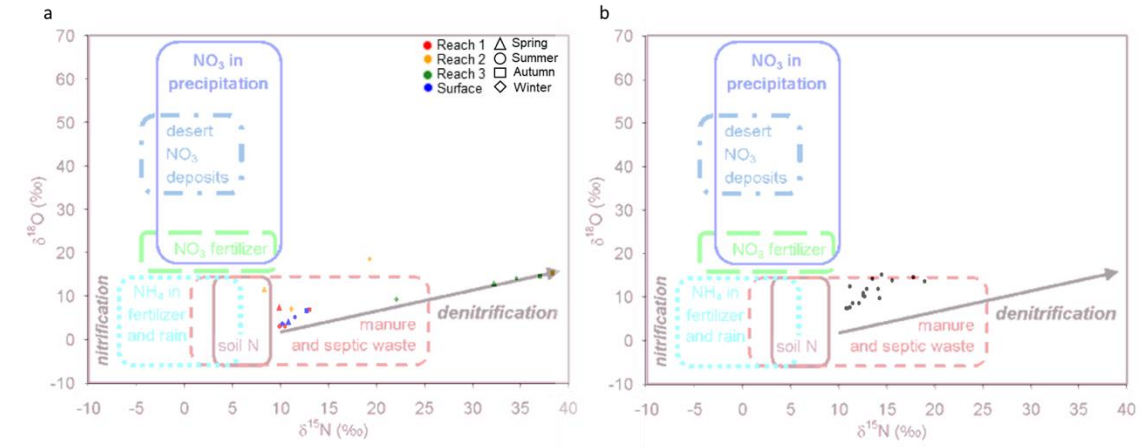

Figure 6.13a. Average porewater isotopic ratios per reach from the multilevel piezometers, as well as surface water isotopic ratios, plotted onto 'Kendall diagrams' of typical global isotopic ratios of sources and processes[30], and b. Porewater isotopic ratios from the DET gels plotted onto 'Kendall diagrams' of typical global isotopic ratios of sources and processes[30].

The high NO_3^- and low NO_2^- and N_2O concentrations observed in Winter and Spring suggest that denitrification was lowest during these seasons, with the seasonal influence statistically significant for all species (p-value = 0.004, <0.006 and <0.003, respectively, Table 6.3). High NO_2^- and N_2O concentrations observed in reach 3 in Autumn, indicated large rates of denitrification in the gravel sediments during that time. This increase in denitrification from Winter to Autumn was also evidenced in the $\delta^{15}N_{NO3^-+NO2^-}$ and $\delta^{18}O_{NO3^-+NO2^-}$ ratios, which increased significantly (p-value = 0.040 and 0.001, respectively, Table 6.3) from Winter to Autumn and was particularly clear in the gravel sediments of reach 3. This seasonality is likely due to increased biogeochemical activity as temperatures increase in Summer[6], and nitrogen inputs increase in Autumn.

The concentration data indicates that denitrification was greatest in the sand sediments of reach 2, where nitrate was almost completely depleted, and NO_2^- and N_2O concentrations were low. This was also suggested by the largest average porewater $\delta^{15}N_{NO3^-+NO2^-}$ and

$\delta^{18}O_{NO3^-+NO2^-}$ ratios, which occurred in reach 2 in Autumn (Figure 6.13). Partial denitrification was most prevalent in the gravel sediments of reach 3, where NO_3^-, NO_2^- and N_2O concentrations were all high. This reflects the results of our incubation experiments in which the sand sediments were characterised by greater rates of microbial activity and denitrification potential than the gravel sediments, and was expected given the greater residence times and anoxic zones associated with sand sediments[19,54,66]. Our results indicate that nitrate reduction is greatest in sand sediments, but that production of the GHG, N_2O, is greatest in gravel sediments.

6.4.2.1 Streambed N_2O Concentrations

Unlike with the other major GHGs, CO_2 and CH_4[75], streambed concentrations of N_2O were not consistently elevated over surface water concentrations in all reaches. In reach 3, this was observed and the concentration of N_2O was greater in the sediment than the surface water, suggesting these gravel sediments may be a source of N_2O into the stream, and subsequently, the atmosphere. This is consistent with previous research, which found significant N_2O production associated with intermediate residence times[21], that are often found in gravel sediments. However, in the sand sediments of reaches 1 and 2, N_2O concentrations were consistently lower than those in the stream, indicating that the sand sediments were not a source of N_2O to the stream. This observation of lower N_2O production in sand (typically low in DO) vs gravel (typically higher in DO) sediments contradicts previous research, which found low oxygen concentration was the primary control on N_2O production, exhibiting threshold responses[76]. Although surface water N_2O concentrations observed here were similar to many previous observations in agricultural streams and rivers[69,75,78–80], many previous observations were much greater[81–83]. This, therefore, indicates that the importance of N_2O production from small, agricultural streams, may be overestimated, or other factors may be more important.

6.5 Summary

Denitrification was strongly controlled by sediment type, with sand sediments characterised by greater rates of denitrification than gravel sediments. This resulted in partial denitrification, and associated high concentrations of N_2O, in the gravel sediments. Our results, therefore, indicate that nitrate reduction is greatest in sand sediments, however, production of the GHG, N_2O, is greatest in gravel sediments.

Additionally, season also controlled denitrification, with rates increasing from Winter to Autumn. Our results have important consequences for management strategies, suggesting that increases in sand sediments may improve water quality within agricultural streams, without compromising efforts to reduce anthropogenic GHG fluxes into the atmosphere.

Further work to fully constrain the drivers of denitrification and N_2O production within streambed sediments, and subsequent contributions to atmospheric fluxes, is required. This is especially crucial given the estimated importance of agricultural streams and rivers in the global N_2O cycle, and predictions that N_2O fluxes will increase in the future due to increased nutrient loading and temperature, and changes in land use[76].

6.6 Acknowledgments

The authors would like to thank BIFoR for their support and use of the study site, Dr. Ben Marchant for his advice on the statistical analysis and Dr. Phillip Blaen for field and laboratory assistance. We would also like to thank NERC for their financial support through a Central England NERC Training Alliance Studentship and the grant NE/L004437/1, as well as the European Union who provided funding via the H2020-MSCA-RISE-2016 project 734317.

6.7 References

1. Krause, S., Louise Heathwaite, a., Binley, A. & Keenan, P. Nitrate concentration changes at the groundwater-surface water interface of a small Cumbrian river. *Hydrol. Process.* **23,** 2195–2211 (2009).

2. McMahon, P. B. & Böhlke, J. K. Denitrification and mixing in a stream-aquifer system: Effects on nitrate loading to surface water. *J. Hydrol.* **186,** 105–128 (1996).

3. Brunke, M. & Gonser, T. The ecological significance of exchange processes between rivers and groundwater. *Freshw. Biol.* **37,** 1–33 (1997).

4. Sophocleous, M. Interactions between groundwater and surface water: The state of the science. *Hydrogeol. J.* **10,** 52–67 (2002).

5. Krause, S., Tecklenburg, C., Munz, M. & Naden, E. Streambed nitrogen cycling beyond the hyporheic zone: Flow controls on horizontal patterns and depth distribution of nitrate and dissolved oxygen in the upwelling groundwater of a lowland river. *J. Geophys. Res. Biogeosciences* **118,** 54–67 (2013).

6. Lautz, L. K. & Fanelli, R. M. Seasonal biogeochemical hotspots in the streambed around restoration structures. *Biogeochemistry* **91,** 85–104 (2008).

7. McClain, M. E. *et al.* Biogeochemical Hot Spots and Hot Moments at the Interface of Terrestrial and Aquatic Ecosystems. *Ecosystems* **6,** 301–312 (2003).

8. Trimmer, M. *et al.* River bed carbon and nitrogen cycling: state of play and some new directions. *Sci. Total Environ.* **434,** 143–58 (2012).

9. Boulton, A., Findlay, S. & Marmonier, P. The functional significance of the hyporheic zone in streams and rivers. *Annu. Rev. Ecol. Syst.* 59–81 (1998). doi:10.1146/annurev.ecolsys.29.1.59

10. Grimm, N. B. & Fisher, S. G. Exchange between interstitial and surface water: Implications for stream metabolism and nutrient cycling. *Hydrobiologia* **111,** 219–228 (1984).

11. Pinay, G., O'Keefe, T. ., Edwards, R. . & Naiman, R. . Nitrate removal in the hyporheic zone of a salmon river in Alaska. *River Res. Appl.* **25,** 367–375 (2009).

12. Zarnetske, J. P., Haggerty, R., Wondzell, S. M. & Baker, M. a. Dynamics of nitrate production and removal as a function of residence time in the hyporheic zone. *J. Geophys. Res.* **116,** G01025 (2011).

13. Mulholland, P. J. *et al.* Nitrogen Cycling in a Forest Stream Determined by a 15N Tracer Addition. *Ecol. Monogr.* **70,** 471–493 (2000).

14. Duff, J. H. & Triska, F. J. in *Streams and Ground Waters* (eds. Jones, J. & Mulholland, P. J.) 197–220 (Elsevier Inc., 2000). doi:10.1016/B978-0-12-389845-6.50009-0

15. Rivett, M. O., Buss, S. R., Morgan, P., Smith, J. W. N. & Bemment, C. D. Nitrate attenuation in groundwater: A review of biogeochemical controlling processes. *Water Res.* **42,** 4215–4232 (2008).

16. Wang, L. *et al.* Prediction of the arrival of peak nitrate concentrations at the water table at the regional scale in Great Britain. *Hydrol. Process.* **26,** 226–239 (2012).

17. Duff, J. H., Tesoriero, A. J., Richardson, W. B., Strauss, E. A. & Munn, M. D. Whole-Stream Response to Nitrate Loading in Three Streams Draining Agricultural Landscapes. *J. Environ. Qual.* **37,** 1133 (2008).

18. Groffman, P. M., Gold, A. J. & Addy, K. Nitrous oxide production in riparian zones and its importance to national emission inventories. *Chemosph. - Glob. Chang. Sci.* **2,**

291–299 (2000).

19. Lansdown, K. *et al.* The interplay between transport and reaction rates as controls on nitrate attenuation in permeable, streambed sediments. *J. Geophys. Res. G Biogeosciences* **120,** 1093–1109 (2015).

20. Stelzer, R. S., Bartsch, L. A., Richardson, W. B. & Strauss, E. A. The dark side of the hyporheic zone: Depth profiles of nitrogen and its processing in stream sediments. *Freshw. Biol.* **56,** 2021–2033 (2011).

21. Quick, A. M. *et al.* Controls on nitrous oxide emissions from the hyporheic zones of streams. *Environ. Sci. Technol.* (2016). doi:10.1021/acs.est.6b02680

22. Bonin, P., Tamburini, C. & Michotey, V. Determination of the bacterial processes which are sources of nitrous oxide production in marine samples. *Water Res.* **36,** 722–732 (2002).

23. Senbayram, M., Chen, R., Budai, A., Bakken, L. & Dittert, K. N2O emission and the N2O/(N2O+N2) product ratio of denitrification as controlled by available carbon substrates and nitrate concentrations. *Agric. Ecosyst. Environ.* **147,** 4–12 (2012).

24. Codispoti, L. A. Interesting Times for Marine N2O. *Science (80-.).* **327,** 1339–1340 (2010).

25. Bakken, L. R., Bergaust, L., Liu, B. & Frostegard, A. Regulation of denitrification at the cellular level: a clue to the understanding of N2O emissions from soils. *Philos. Trans. R. Soc. B Biol. Sci.* **367,** 1226–1234 (2012).

26. Silvennoinen, H., Liikanen, A., Torssonen, J., Stange, C. F. & Martikainen, P. J. Denitrification and N2O effluxes in the Bothnian Bay (northern Baltic Sea) river sediments as affected by temperature under different oxygen concentrations.

Biogeochemistry **88,** 63–72 (2008).

27. Silvennoinen, H., Liikanen, A., Torssonen, J., Florian Stange, C. & Martikainen, P. J. Denitrification and nitrous oxide effluxes in boreal, eutrophic river sediments under increasing nitrate load: A laboratory microcosm study. *Biogeochemistry* **91,** 105–116 (2008).

28. Findlay, S. Importance of surface-subsurface exchange in stream ecosystems: The hyporheic zone. *Limnol. Oceanogr.* **40,** 159–164 (1995).

29. Kaplan, L. a. & Newbold, J. D. in *Streams and Ground Waters* (eds. Jones, J. B. & Mulholland, P. J.) 237–253 (Elsevier Inc., 2000). doi:10.1890/0012-9623(2008)89[19:DOC]2.0.CO;2

30. Kendall, C. in *Isotope Tracers in Catchment Hydrology* (eds. C. Kendall and J.J. McDonnell) 519–576 (Elsevier, 1998).

31. Firestone, M. K. & Davidson, E. A. in *Exchange of Trace Gases between Terrestrial Ecosystems and the Atmosphere* (eds. Andreae, M. & Schimel, D.) 7–21 (John Wiley and Sons, 1989).

32. García-Ruiz, R., Pattinson, S. N. & Whitton, B. A. Nitrous oxide production in the river Swale-Ouse, North-East England. *Water Res.* **33,** 1231–1237 (1999).

33. Frasier, R., Ullah, S. & Moore, T. R. Nitrous Oxide consumption potentials of well-drained forest soils in Southern Québec, Canada. *Geomicrobiol. J.* **27,** 53–60 (2010).

34. Davidson, E. A. The contribution of manure and fertilizer nitrogen to atmospheric nitrous oxide since 1860. *Nat. Geosci.* **2,** 659–662 (2009).

35. McMahon, P. B. & Dennehy, K. F. N2O emissions from a nitrogen-enriched river. *Environ. Sci. Technol.* **33,** 21–25 (1999).

36. Park, S. *et al.* Trends and seasonal cycles in the isotopic composition of nitrous oxide since 1940. *Nat. Geosci.* **5,** 261–265 (2012).

37. Usui, T., Koike, I. & Ogura, N. N2O production, nitrification and denitrification in an estuarine sediment. *Estuar. Coast. Shelf Sci.* **52,** 769–781 (2001).

38. Stevens, R. J. & Laughlin, R. J. Measurement of nitrous oxide and di-nitrogen emissions from agricultural soils. *Nutr. Cycl. Agroecosystems* **52,** 131–139 (1998).

39. Wrage, N., Velthof, G. L., Van Beusichem, M. L. & Oenema, O. Role of nitrifier denitrification in the production of nitrous oxide. *Soil Biol. Biochem.* **33,** 1723–1732 (2001).

40. Lansdown, K. *et al.* Characterization of the key pathways of dissimilatory nitrate reduction and their response to complex organic substrates in hyporheic sediments. *Limnol. Oceanogr.* **57,** 387–400 (2012).

41. Bollmann, A. & Conrad, R. Influence of O2availability on NO and N2O release by nitrification and denitrification in soils. *Glob. Chang. Biol.* **4,** 387–396 (1998).

42. Davidson, E. A. in *Microbial production and consumption of greenhouse gases: methane, nitrogen oxides, and halomethanes* (eds. Rogers, J. E. & Whitman, W. B.) 219–235 (American Society for Microbiology, 1991).

43. Barnes, J. & Upstill-Goddard, R. C. The denitrification paradox: The role of O2 in sediment N2O production. *Estuar. Coast. Shelf Sci.* **200,** 270–276 (2018).

44. Burgin, A. J., Lazar, J. G., Groffman, P. M., Gold, A. J. & Kellogg, D. Q. Balancing nitrogen retention ecosystem services and greenhouse gas disservices at the landscape scale. *Ecol. Eng.* **56,** 26–35 (2013).

45. Forster, P. *et al.* in *Climate Change 2007: The Physical Science Basis. Contribution of*

Working Group I to the Fourth Assessment Report of the Intergovernmental Panel on Climate Change (eds. Solomon, S. et al.) (Cambridge University Press, 2007). doi:10.1103/PhysRevB.77.220407

46. Ravishankara, A. R., Daniel, J. S. & Portmann, R. W. Nitrous Oxide (N 2 O): The Dominant Ozone-Depleting Substance Emitted in the 21st Century. **123,** 2007–2010 (2009).

47. Anderson, B. *et al. Methane and Nitrous Oxide Emissions from Natural Sources*. (Office of Atmospheric Programs, US EPA, EPA 430-R-10-001, 2010).

48. Beaulieu, J. J. *et al.* Nitrous oxide emission from denitrification in stream and river networks. *Proc. Natl. Acad. Sci.* **108,** 214–219 (2011).

49. Mosier, A., Kroeze, C., Nevison, C., Oenema, O. & Seitzinger, S. Closing the global N 2 O budget : nitrous oxide emissions through the agricultural nitrogen cycle inventory methodology. *Nutr. Cycl. Agroecosystems* **52,** 225–248 (1998).

50. Mulholland, P. J. *et al.* Stream denitrification across biomes and its response to anthropogenic nitrate loading. *Nature* **452,** 202–205 (2008).

51. Sinsabaugh, R. L. & Findlay, S. Microbial production, enzyme activity, and carbon turnover in surface sediments of the Hudson River estuary. *Microb. Ecol. An Int. J.* **30,** 127–141 (1995).

52. Sinsabaugh, R. L. Phenol oxidase, peroxidase and organic matter dynamics of soil. *Soil Biol. Biochem.* **42,** 391–404 (2010).

53. Alexander, R. B., Smith, R. A. & Schwarz, G. E. Effect of stream channel size on the delivery of nitrogen to the Gulf of Mexico. *Nature* **403,** 758–761 (2000).

54. Baker, M. A., Dahm, C. N. & Valett, H. M. in *Streams and Ground Waters* (eds.

Jones, J. B. & Mulholland, P. J.) 259–283 (Elsevier, 2000). doi:10.1016/B978-0-12-389845-6.50012-0

55. Blaen, P. J. *et al.* High-frequency monitoring of catchment nutrient exports reveals highly variable storm event responses and dynamic source zone activation. *J. Geophys. Res. Biogeosciences* 1–17 (2017). doi:10.1002/2017JG003904

56. Toberman, H. *et al.* Summer drought effects upon soil and litter extracellular phenol oxidase activity and soluble carbon release in an upland Calluna heathland. *Soil Biol. Biochem.* **40,** 1519–1532 (2008).

57. Sgouridis, F. & Ullah, S. Denitrification potential of organic, forest and grassland soils in the Ribble-Wyre and Conwy River catchments, UK. *Environ. Sci. Process. Impacts* **16,** 1551–1562 (2014).

58. Ullah, S. *et al.* In situ measurement of redox sensitive solutes at high spatial resolution in a riverbed using Diffusive Equilibrium in Thin Films (DET). *Ecol. Eng.* **49,** 18–26 (2012).

59. Hudson, F. Sample Preparation and Calculations for Dissolved Gas Analysis in Water Samples Using a GC Headspace Equilibration Technique. 1–14 (2004). doi:10.1111/j.1365-2133.2004.v151_is68_disclaimer.x

60. Wilhelm, E., Battino, R. & Wilcock, R. J. Low-Pressure Solubility of Gases in Liquid Water. *Chem. Rev.* **77,** 219–262 (1977).

61. Casciotti, K. L., Sigman, D. M., Hastings, M. G., Bohlke, J. K. & Hilkert, A. Measurement of the oxygen isotopic composition of nitrate in seawater and freshwater using the dentirifier method. *Anal. Chem.* **74,** 4905–4912. (2002).

62. Sigman, D. M. *et al.* A Bacterial Method for the Nitrogen Isotopic Analysis of Nitrate

in Seawater and Freshwater. *Anal* **73,** 4145–4153 (2001).

63. Schipper, L. & Vojvodić-Vuković, M. Nitrate Removal from Groundwater Using a Denitrification Wall Amended with Sawdust: Field Trial. *J. Environ. Qual.* **27,** 664 (1998).

64. Zarnetske, J. P., Haggerty, R., Wondzell, S. M. & Baker, M. a. Labile dissolved organic carbon supply limits hyporheic denitrification. *J. Geophys. Res.* **116,** G04036 (2011).

65. Baker, M. A., Dahm, C. N. & Valett, H. M. Acetate retention and metabolism in the hyporheic zone of a mountain stream. *Limnol. Oceanogr.* **44,** 1530–1539 (1999).

66. Boulton, A. J., Findlay, S., Marmonier, P., Stanley, E. H. & Valett, H. M. The Functional Significance of the Hyporheic Zone in Streams and Rivers. *Annu. Rev. Ecol. Syst.* **29,** 59–81 (1998).

67. Baulch, H. M., Dillon, P. J., Maranger, R. & Schiff, S. L. Diffusive and ebullitive transport of methane and nitrous oxide from streams: Are bubble-mediated fluxes important? *J. Geophys. Res.* **116,** G04028 (2011).

68. Lansdown, K. *et al.* Fine-scale in situ measurement of riverbed nitrate production and consumption in an armored permeable riverbed. *Environ. Sci. Technol.* **48,** 4425–34 (2014).

69. Outram, F. N. & Hiscock, K. M. Indirect nitrous oxide emissions from surface water bodies in a lowland arable catchment: A significant contribution to agricultural greenhouse gas budgets? *Environ. Sci. Technol.* **46,** 8156–8163 (2012).

70. Ullah, S. *et al.* Influence of emergent vegetation on nitrate cycling in sediments of a groundwater-fed river. *Biogeochemistry* **118,** 121–134 (2014).

71. Lazar, J. G. *et al.* Instream large wood: Denitrification hotspots with low N2O production. *J. Am. Water Resour. Assoc.* **50,** 615–625 (2014).

72. Knapp, J. L. A. *et al.* Tracer-based characterization of hyporheic exchange and benthic biolayers in streams. *Water Resour. Res.* **53,** 1575–1594 (2017).

73. O'Connor, B. L. & Harvey, J. W. Scaling hyporheic exchange and its influence on biogeochemical reactions in aquatic ecosystems. *Water Resour. Res.* **44,** 1–17 (2008).

74. Battin, T. J., Kaplan, L. A., Newbold, J. D. & Hansen, C. M. E. Contributions of microbial biofilms to ecosystem processes in stream mesocosms. *Nature* **426,** 439–442 (2003).

75. Hlaváčová, E., Rulík, M. & Čáp, L. Anaerobic microbial metabolism in hyporheic sediment of a gravel bar in a small lowland stream. *River Res. Appl.* **21,** 1003–1011 (2005).

76. Venkiteswaran, J. J., Rosamond, M. S. & Schiff, S. L. Nonlinear response of riverine N_2O fluxes to oxygen and temperature. *Environ. Sci. Technol.* **48,** 1566–1573 (2014).

77. Amberger, A. & Schmidt, H.-L. Naturliche Isotopengehalte von Nitrat als Indikatoren fur dessen Herkunft. *Geochim. Cosmochim. Acta* **51,** 2699–2705 (1987).

78. Hlaváčová, E., Rulík, M., Čáp, L. & Mach, V. Greenhouse gas (CO2, CH4, N2O) emissions to the atmosphere from a small lowland stream in Czech Republic. *Arch. für Hydrobiol.* **165,** 339–353 (2006).

79. Clough, T. J., Bertram, J. E., Sherlock, R. R., Leonard, R. L. & Nowicki, B. L. Comparison of measured and EF5-r-derived N2O fluxes from a spring-fed river. *Glob. Chang. Biol.* **12,** 352–363 (2006).

80. Cole, J. J. & Caraco, N. F. Carbon in catchments: Connecting terrestrial carbon losses

with aquatic metabolism. *Mar. Freshw. Res.* **52,** 101–110 (2001).

81. Hama-Aziz, Z. Q., Hiscock, K. M. & Cooper, R. J. Dissolved nitrous oxide (N2O) dynamics in agricultural field drains and headwater streams in an intensive arable catchment. *Hydrol. Process.* **31,** 1371–1381 (2017).

82. Wilcock, R. J. & Sorrell, B. K. Emissions of Greenhouse Gases CH4 and N2O from Low-gradient Streams in Agriculturally Developed Catchments. *Water. Air. Soil Pollut.* **188,** 155–170 (2008).

83. Audet, J., Wallin, M. B., Kyllmar, K., Andersson, S. & Bishop, K. Nitrous oxide emissions from streams in a Swedish agricultural catchment. *Agric. Ecosyst. Environ.* **236,** 295–303 (2017).

Chapter 7: Conclusions and Future Outlook

7.1 Conclusions

The work presented here aimed to investigate knowledge gaps in streambed carbon and nitrogen cycling, focussing on a lack of adequate sampling techniques as well as investigating controls on biogeochemical processes. The first aim of addressing a paucity of sampling methodologies and standard sampling protocols across disciplines was successfully addressed. This was achieved through the development of a novel high-resolution methodology capable of sampling nitrate concentration and isotopic data at a vertical resolution up to 1 cm in the upper 15 cm of the streambed, and through a combined review and comparison study of available techniques.

Laboratory experiments confirmed that nitrate isotopes did not fractionate on diffusion into or out of DET gels during sampling or subsequent back-equilibration, with $\delta^{15}N_{NO3^-}$ and $\delta^{18}O_{NO3^-}$ ratios independent of nitrate concentration and equilibrium time. Results from an initial field application demonstrated the potential of this methodology, allowing profiles of porewater nitrate concentration and isotopic data to be determined at a vertical resolution not previously achievable. The field application also demonstrated the power of this methodology to prevent incorrect interpretation of biogeochemical processes resulting from consideration of concentration data alone. This methodology, therefore, adds to the technologies available for streambed sampling, enabling increased understanding of key mechanistic processes at the sediment-water interface in freshwater environments.

Nitrate and ammonium profiles obtained from three biogeochemical streambed sampling techniques (multilevel minipiezometers, USGS Minipoint samplers and DET gel samplers) were compared and resulted in statistically different ammonium concentrations between all three samplers. This variation is suggested to arise from the differences between active and passive samplers, and the varying depth-resolution between USGS Minipoint samplers and

multilevel minipiezometers. These differences in nutrient concentrations, as well as the review of available sampling methodologies examined here, should allow research questions to be answered more effectively, using the most appropriate methodology based on its performance, temporal and spatial resolution, and advantages and limitations.

The advance of targeted sampling methodologies and standard sampling protocols is crucial to the success of interdisciplinary research focused on streambed biogeochemical processes. Samplers able to achieve a high spatial resolution in the upper few centimetres of the streambed, where the majority of biogeochemical activity occurs, allow key processes to be identified and examined. Samplers with a coarser resolution, but able to sample at larger depths, however, remain a valuable tool for the investigation of larger scale processes and the influences of groundwater at greater depths.

The second aim to explore environmental controls on streambed carbon and nitrogen cycling, and associated GHG production, was successfully addressed. This was achieved by advancing knowledge on the variation of the thermal sensitivity of streambed carbon emissions with sediment properties, and the influence of sediment type and season on streambed biogeochemical cycling in an agricultural stream.

Laboratory incubation experiments showed that the thermal sensitivity of streambed CO_2 and CH_4 emissions was heavily dependent on streambed geology and sedimentology, with substrate, OM content and geological origin causing large variations in the magnitude of the carbon flux. This indicates that local variation in sediment properties has a key influence on streambed carbon emissions, with emissions exhibiting non-linearity and threshold responses to temperature, which varied between sediment type and geological origin. This has wide implications for predicting future carbon emissions from streams and rivers, with streambed heterogeneity necessary to consider. It is also, therefore, necessary to consider streambed production when estimating carbon fluxes from freshwater ecosystems, with projected

changes in climate and land-use likely to have a great effect on future carbon fluxes from streams and rivers.

Further to the influence of sedimentology on carbon emissions observed during laboratory incubation experiments, sediment type exhibited a large control over *in-situ* streambed CO_2 and CH_4 concentrations. Carbon turnover and subsequent concentrations of CO_2 and CH_4 were greater in sand than gravel sediments, with the largest *in-situ* CO_2 production occurring in the sand sediments. Despite temperature having a large control on CO_2 and CH_4 emissions, season produced little variation in streambed CO_2 and CH_4 concentrations, with an insignificant effect on CO_2 observed. This resulted in large concentrations of CO_2 and CH_4 year-round, which could have wide implications for estimates of annual carbon fluxes from small, agricultural streams. Our results suggest that management of agricultural streams to reduce sediment loading of fine, OM-rich sediments, which often occurs in these environments, and to reduce sand sediment within streams, could reduce the carbon flux from streams and rivers.

Sediment type also exhibited a strong control on nitrogen cycling within the streambed, with sand sediments characterised by greater potential rates of denitrification and total microbial activity than gravel sediments. Gravel sediments, however, were characterised by greater uptake of phenolic compounds for mining of carbon and nitrogen. This resulted in *in-situ* sand sediments with lower concentrations of NO_3^-, NO_2^- and N_2O than gravel sediments, resulting in partial denitrification and associated large concentrations of N_2O observed in the gravel sediments. Our results indicate, therefore, that nitrate attenuation is greatest in sand sediments, leading to improvements in water quality, with N_2O production greatest in gravel sediments. Additionally, denitrification varied with season, with greatest denitrification observed in summer and autumn. Our results have large implications for management

strategies, suggesting sand sediments should be utilised to improve water quality through nutrient reduction, without increasing the release of the GHG, N_2O, into the atmosphere. Temperature, sedimentology, geology and season were found to be key drivers of streambed carbon and nitrogen cycling, and associated GHG production. The sediment itself played a large role in biogeochemical reactivity within porewaters, with variations in substrate, sediment type and OM-content resulting in differing rates of cycling and GHG production. The observation of high CO_2 and CH_4 in sand sediments, but high N_2O in gravel sediments, indicates that managing streambeds to reduce GHG emissions is complex, as reducing sand sediments would potentially reduce carbon emissions while increasing nitrogen emissions. Small, agricultural streams, characterised by excess nutrient loading and fine, OM-rich sediment, were confirmed to support large rates of nitrogen and carbon cycling, and large concentrations of GHGs. This is of particular importance given that these environments are common throughout large areas of the world, and that temperatures, nutrient loadings and fine, OM-rich sediment loadings are expected to increase under future climate and land-use scenarios[1,2].

7.2 Future Outlook

The work presented here addressed the aims of the research and moved towards closing some of the gaps in available sampling methodologies and understanding of drivers of streambed carbon and nitrogen cycling. However, due to the broad knowledge gap targeted here, additional work remains necessary to further improve available sampling technologies and to constrain drivers of streambed biogeochemical cycling.

The study of streambed biogeochemistry has been hampered by a paucity of sufficient sampling technologies[3–7], however, several advancements have been made recently. These include the use of mini-drivepoint samplers[8–10], DET gels[11–14] and multilevel minipiezometers[15]. As more sampling methodologies, such as the DET-isotope method

developed here, and standard protocols emerge, the technical difficulties associated with research into streambed biogeochemistry should be overcome. Further work is required, therefore, to focus on ensuring sufficient sampling techniques are available, which are able to address a variety of research questions at multiple spatial and temporal scales within the streambed. For example, the DET-isotope method developed here may be suitable for brackish and marine systems, and could present itself as a valuable tool for use in these ecosystems, however, the effect of high concentrations of interfering ions will first need to be assessed.

A large amount of previous research has been conducted focussing on streambed carbon and nitrogen cycling, however, it is only recently that the role of streams and rivers as globally important contributors to GHG emissions has been recognised[2,16–24]. These observations, combined with streambeds known to be hotspots of biogeochemical reactivity[25–28] and observations of high GHG concentrations within them[21–23,29,30], have resulted in an uptake of interest in drivers of streambed GHG production and its contribution to total stream GHG emissions. Further work to determine the key drivers of streambed nutrient attenuation and GHG production is required, and in particular the simultaneous investigation of multiple controlling factors is necessary to fully understand biogeochemical processes occurring in the streambed. Determining key drivers of nutrient attenuation and GHG production is crucial to enable streams and rivers to be managed to maximise the efficiency of nutrient removal from the system without increasing GHG emissions to the atmosphere. Additional insight into the effect of sand versus gravel sediments on nutrient attenuation and GHG emissions is important to further the work presented here, given that the results indicate that sand sediments increase CO_2 and CH_4, but reduce N_2O emissions. This also highlights the necessity to study multiple biogeochemical cycles simultaneously, which should include the integration of the phosphorus cycle as well. Furthermore, the use of stable isotopes as tracers

to determine the varying biogeochemical pathways which are present in sand versus gravel sediments, and their relative importance may provide further insight into why there are differences in biogeochemical cycling between these sediment types. For example, pathways of N_2O production via denitrification, anaerobic ammonium oxidation and dissimilatory nitrate reduction to ammonia, and which are most important can have large implications for whether nitrogen is lost from the system or retained.

A crucial area for future research is to determine the relative importance of streambed GHG production to total stream and river emissions of GHGs. Important to ascertain is both the proportion of GHG produced *in-situ* versus that transported laterally or vertically into the streambed, and the relative contribution of the benthic GHG flux to overall GHG emissions across the surface water-atmosphere interface. This will enable a more complete understanding of streambed biogeochemistry to be gained, including whether streambeds may sequester carbon through the production of CO_2 and CH_4, which is not released into the overlying water column. Any proportion of the GHG found in streambeds which is transported in from the surrounding landscape, may also be sequestered here in the same way. Further research into physical conditions affecting benthic emissions of GHGs are, therefore, also crucial to determine, which could be used in more effective management strategies designed to reduce nutrient pollution as well as GHG emissions in streams and rivers. Increased understanding of drivers of streambed nutrient attenuation and GHG production should also be considered in the context of future climate change and land-use change, which may produce positive or negative feedbacks on drivers, and, therefore, affect stream management.

7.3 References

1. Venkiteswaran, J. J., Rosamond, M. S. & Schiff, S. L. Nonlinear response of riverine N2O fluxes to oxygen and temperature. *Environ. Sci. Technol.* **48,** 1566–1573 (2014).

2. Stanley, E. H. *et al.* The ecology of methane in streams and rivers: Patterns, controls, and global significance. *Ecol. Monogr.* **86,** 146–171 (2016).

3. Krause, S. *et al.* Inter-disciplinary perspectives on processes in the hyporheic zone. **499,** 481–499 (2011).

4. Boano, F. *et al.* Hyporheic flow and transport processes: Mechanisms, models, and bioghemical implications. *Rev. Geophys.* 1–77 (2014). doi:10.1002/2012RG000417.Received

5. Hannah, D. M., Sadler, J. P. & Wood, P. J. Hydroecology and ecohydrology: a potential route forward? *Hydrol. Process.* **21,** 3385–3390 (2007).

6. Krause, S., Louise Heathwaite, a., Binley, A. & Keenan, P. Nitrate concentration changes at the groundwater-surface water interface of a small Cumbrian river. *Hydrol. Process.* **23,** 2195–2211 (2009).

7. Krause, S., Hannah, D. M. & Fleckenstein, J. H. Hyporeheic hydrology: interactions at the groundwater-surface water interface. *Hydrol. Process.* **23,** 2103–2107 (2009).

8. Duff, J. H. *et al.* A mini drivepoint sampler for measuring pore water solute concentrations in the hyporheic zone of sand-bottom streams. *Limnol. Ocean.* **43,** 1378–1383 (1998).

9. Harvey, J. W. & Fuller, C. C. Effect of enhanced manganese oxidation in the hyporheic zone on basin-scale geochemical mass balance. *Water Resour. Res.* **34,** 623 (1998).

10. Sanders, I. A. & Trimmer, M. In situ application of the 15NO3- isotope pairing technique to measure denitrification in sediments at the surface water-groundwater interface. *Limnol. Oceanogr. Methods* **4,** 142–152 (2006).

11. Metzger, E. *et al.* Simultaneous Nitrite/Nitrate Imagery at Millimeter Scale through the Water–Sediment Interface. *Environ. Sci. Technol.* acs.est.6b00187 (2016). doi:10.1021/acs.est.6b00187

12. Kessler, A. J., Glud, R. N., Cardenas, M. B. & Cook, P. L. M. Transport Zonation Limits Coupled Nitrification-Denitri fi cation in Permeable Sediments. (2013).

13. Roberts, K. L., Kessler, A. J., Grace, M. R. & Cook, P. L. M. Increased rates of dissimilatory nitrate reduction to ammonium (DNRA) under oxic conditions in a periodically hypoxic estuary. *Geochim. Cosmochim. Acta* **133,** 313–324 (2014).

14. Krom, M. ., Davison, P., Zhang, H. & Davison, W. High-resolution pore-water sampling with a gel sampler. (1994).

15. Rivett, M. *et al.* Cost-effective mini drive-point piezometers and multilevel samplers for monitoring the hyporheic zone. *Q.J.Eng.Geol.Hydrogeol.* **41,** 49–60 (2008).

16. Raymond, P. a *et al.* Global carbon dioxide emissions from inland waters. *Nature* **503,** 355–359 (2013).

17. Cole, J. J. *et al.* Plumbing the Global Carbon Cycle: Integrating Inland Waters into the Terrestrial Carbon Budget. *Ecosystems* **10,** 172–185 (2007).

18. Tranvik, L. J. *et al.* Lakes and reservoirs as regulators of carbon cycling and climate. *Limnol. Oceanogr.* **54,** 2298–2314 (2009).

19. Richey, J. E., Melack, J. M., Aufdenkampe, A. K., Ballester, V. M. & Hess, L. L. Outgassing from Amazonian rivers and wetlands as a large tropical source of

atmospheric CO2. *Nature* **416,** 617–620 (2002).

20. Anderson, B. *et al. Methane and Nitrous Oxide Emissions from Natural Sources*. (Office of Atmospheric Programs, US EPA, EPA 430-R-10-001, 2010).

21. Beaulieu, J. J. *et al.* Nitrous oxide emission from denitrification in stream and river networks. *Proc. Natl. Acad. Sci.* **108,** 214–219 (2011).

22. Mosier, A., Kroeze, C., Nevison, C., Oenema, O. & Seitzinger, S. Closing the global N 2 O budget : nitrous oxide emissions through the agricultural nitrogen cycle inventory methodology. *Nutr. Cycl. Agroecosystems* **52,** 225–248 (1998).

23. Mulholland, P. J. *et al.* Stream denitrification across biomes and its response to anthropogenic nitrate loading. *Nature* **452,** 202–205 (2008).

24. Trimmer, M. *et al.* River bed carbon and nitrogen cycling: state of play and some new directions. *Sci. Total Environ.* **434,** 143–58 (2012).

25. McClain, M. E. *et al.* Biogeochemical Hot Spots and Hot Moments at the Interface of Terrestrial and Aquatic Ecosystems. *Ecosystems* **6,** 301–312 (2003).

26. Lautz, L. K. & Fanelli, R. M. Seasonal biogeochemical hotspots in the streambed around restoration structures. *Biogeochemistry* **91,** 85–104 (2008).

27. Krause, S., Tecklenburg, C., Munz, M. & Naden, E. Streambed nitrogen cycling beyond the hyporheic zone: Flow controls on horizontal patterns and depth distribution of nitrate and dissolved oxygen in the upwelling groundwater of a lowland river. *J. Geophys. Res. Biogeosciences* **118,** 54–67 (2013).

28. Krause, S., Boano, F., Cuthbert, M. O., Fleckenstein, J. H. & Lewandowski, J. Understanding process dynamics at aquifer-surface water interfaces: An introduction to the special section on new modeling approaches and novel experimental

technologies. *Water Resour. Res.* **50,** 1847–1855 (2014).

29. Hlaváčová, E., Rulík, M. & Čáp, L. Anaerobic microbial metabolism in hyporheic sediment of a gravel bar in a small lowland stream. *River Res. Appl.* **21,** 1003–1011 (2005).

30. Trimmer, M., Sanders, I. A. & Heppell, C. M. Carbon and nitrogen cycling in a vegetated lowland chalk river impacted by sediment. **2238,** 2225–2238 (2009).